Examensarbete vid Institutionen för geovetenskaper
ISSN 1650-6553 Nr XXX

Adding the Weather Research and Forecast model (WRF) as a Models-3 Community Multiscale Air Quality (CMAQ) modelling system driver, and analysing the forecasted ozone and nitrogen dioxide concentrations during a four-day period in May 2006.

Sara Johansson

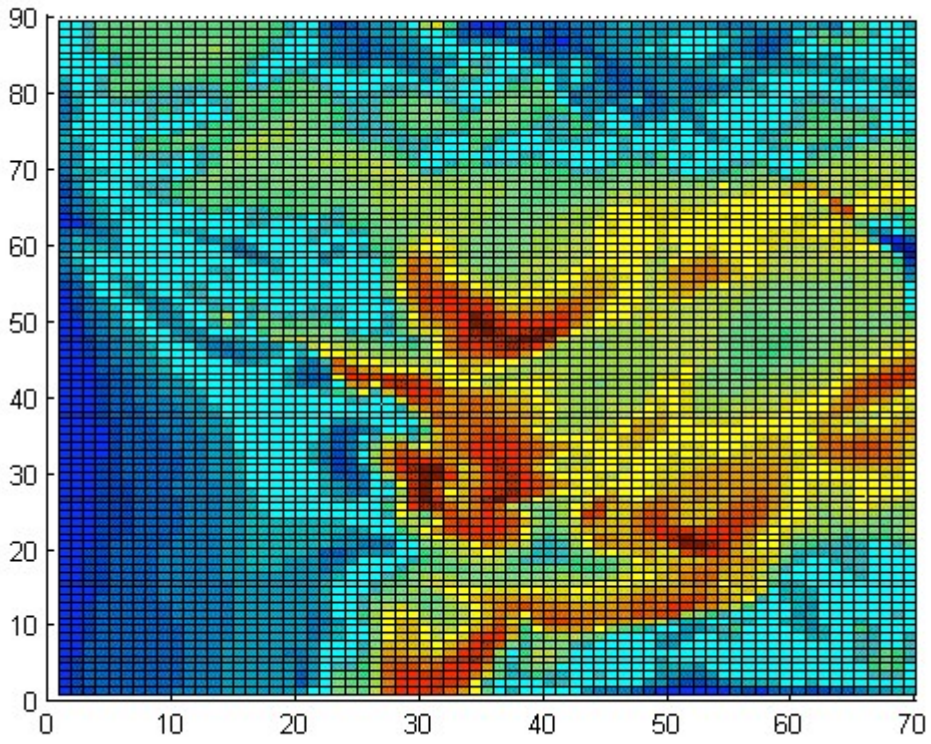

Ozone concentration 18/5 15.00

Abstract

Air quality forecasts are of great value since several pollutants in our environment are harmful not only for humans, but also vegetation, animals, and materials. Air quality forecasts helps preventing e.g. illness, global warming, bad crop yields, and acidification of forests and lakes. This since these forecasts makes people aware of the presence and the quantity of pollutants and gives them a chance to protect themselves, their business and the Earth.
Many different air quality models are in daily use all over the world, providing citizens with forecasts of air quality and warnings of unhealthy air quality if recommended highest concentrations are exceeded.

This study focuses on the topic to use the WRF model (Weather research and Forecasting model) as a driver of the air quality model; CMAQ (models-3 Community Multiscale Air Quality model), and to produce forecasts for the southwestern Canada, more exactly the region British Columbia. Furthermore, the concentrations of ozone and nitrogen dioxide in the air are analyzed and compared with observed data during a four-day period in May, 2006. The area of study were the analysis is located is the Lower Fraser Valley, a fertile valley surrounded by mountain chains, it is stretching from the Pacific coast and eastwards towards the Rocky Mountains. This valley hosts more than 2 million people and it is west Canada's fastest growing region. The valley holds a big city, Vancouver, several suburbs, numerous industries and a widespread agricultural production.

The analyzed four-day period in May holds a high-pressure synoptic situation with local variations, which together are favorable for high concentrations of pollutants as ozone and nitrogen dioxide. The created WRF/CMAQ model constellation forecasts an acceptable magnitude of nitrogen dioxide but the daily variations are not recreated properly by the model. The WRF/CMAQ model forecasts the daily variation of ozone in a satisfying way, but the forecasted concentrations are overestimated by between 20 and 30 ppb throughout the study.
Factors that could contribute to the elevated ozone concentrations are investigated and it comes to light that the forecasting model WRF is not generating fully reliable meteorological values to produce a correct air quality forecast. As the WRF model usually is a good forecasting model, the short spin-up time for the model could be a probable cause for its insufficient performance.

Sammanfattning
Prognoser över luftkvaliteten är mycket värdefulla då flera luft föroreningar i vår närmiljö är skadliga, inte bara för människor utan även för växtligheten, djur och olika material. Luftkvalitetsprognoser hjälper till att förebygga bl.a. sjukdomar, global uppvärmning, dåliga skördar, och försurning av skog och vattendrag. Detta eftersom dessa prognoser gör människan mer medveten om närvaron av luftföroreningar och i vilken mängd de finns, så att människan ges en chans att vidta skyddsåtgärder för att skydda sig själv, sitt eventuella levebröd, och Jorden.
Många olika luftkvalitetsmodeller används dagligdags över hela världen och förser invånare med prognoser för luftkvaliteten och varningar om koncentrationerna av föroreningar överstiger rekommenderade värden.

Den här studien fokuserar på att driva luftkvalitetsmodellen CMAQ (Models-3 Community Multiscale Air Quality model) med prognosmodellen WRF (Weather reasearch and Forecasting model), och därefter producera luftkvalitetsprognoser för sydvästra Kanada,

närmare bestämt regionen British Columbia. Därefter analyseras ozon- och kvävedioxidhalterna i luften mot observerade data under en fyra dagars period i maj, 2006. Studieområdet för analysen koncentreras till området Lower Fraser Valley, en bördig dalgång omgiven av bergskedjor vilken sträcker sig från Stilla havskusten och österut mot klippiga bergen. I denna dalgång bor mer än 2 miljoner människor och det är västra Kanadas snabbast växande region. Dalen rymmer en storstad, Vancouver, flera förorter, många industrier och även stora jordbruksområden.

Den fyra dagars period i maj som analyseras bjuder på ett högtrycksbetonat synoptiskt väderläge med lokala variationer som tillsammans är gynnsamma för att uppmäta höga koncentrationer av luftföroreningar som ozon och kvävedioxid. Den skapade WRF/CMAQ modellen prognostiserar godtagbar magnitud hos kvävedioxid men den dagliga variationen återskapas inte av modellen. Modellen prognostiserar den dagliga variationen av ozon koncentration på ett tillfredsställande sätt, men storleksmässigt ligger koncentrationerna en faktor 20-30ppb för högt rakt av under hela studien.
Kringliggande faktorer som kan påverka koncentrationen ozon studeras närmare och det framkommer att den meteorologiska prognosmodellen WRF inte genererar fullt tillförlitliga värden för en rättvisande luftkvalitetsprognos. Då WRF modellen är en vanligtvis bra prognosmodell kan den korta spin-up tiden för modellen vara en trolig orsak till dess otillräckliga prestation.

Contents

1 Introduction

The quality of the air we breathe is of great concern for most people; pollutants in unhealthy quantities can for example cause severe health issues, destroy crops and enhance global warming. Air quality models is needed to forecast the concentrations of harmful pollutants in our environment, with their help we can protect ourselves, our animals, our business and the Earth from serious damage.
Today, there are several air quality forecasts in operational use all over the world, providing citizens with forecasts, and warnings are carried out by the weather bureaus when the pollutants are reaching unhealthy concentrations.

The University of British Columbia (UBC) is one of the world leading in research in air quality ensemble forecasting, where Luca Delle Monache started the research by adding the forecasting models MM5 and MC2 to CMAQ and analyse the forecasts [Delle Monache et al. 2006]. Both MM5/CMAQ and MC2/CMAQ with resolution 4 and 12 kilometres are now in operational use at UBC. To expand this ensemble, the next step is to add the newer forecasting model WRF to this ensemble, and this is the main goal with this master thesis.

A new ensemble member is created, using the forecasting model WRF (Weather research and Forecasting Model) as meteorological input to the models-3 CMAQ (Community Multiscale Air Quality) model.
The air quality data from the WRF/CMAQ model is then evaluated by comparison with observed concentrations of NO_2 and O_3 data that are collected by the Greater Vancouver Regional District in five different places in the Lower Fraser Valley during a four-day episode in May, 2006.

The basic concept for ensemble forecasts is that since the atmosphere exhibits a chaotic behaviour, you need to predict the predictability of the forecasts to determine how reliable a certain forecast is.
The atmosphere is a dynamical system described by mathematical equations. By integrating these equations you can predict the evolution of the atmosphere's state, under the condition that you know the initial stage of development. The initial state in this case, is the observed state and can often not be determined precisely. Some of the dynamical systems show a divergent behaviour when integrated, which means that two close but different initial state conditions creates two eventually divergent solutions.
It was in the early 1960´s that Lorentz [1963] studied the behaviour of such systems, called chaotic systems, and emerged that since the equations describing the atmospheres dynamic structure are coupled and might involve non-linear terms, numerical solutions are very sensitive to the initial values of the dependent variables, describing the present state of the system. Regardless of the difference between two solutions in their initial state, the two solutions will eventually differ from each other. This implies that, for such a system of equations, there is an upper limit in time after which one solution is no longer acceptable.

The ensemble technique in numerical weather prediction (NWP) is widespread, using the fact that different models perform better in different situations. Combining several models into an ensemble has been found to provide better accuracy than any single numerical model run. Since there are similar code complexities and constraints to air quality models as for NWP models, the ensemble technique can potentially yield similar benefits to air-quality modelling, Different air quality models can be better for different air-pollution episodes, also in ways that cannot always be anticipated.

The main goal for this master thesis is as said, the creation of a new ensemble member, WRF/CMAQ to the already existing ensemble in operational use at UBC. The task is therefore to add WRF forecast data to the air quality model CMAQ by using different pre-processors to handle the input meteorology, the emissions, the influence of the sun, and the initial and boundary conditions. The air quality output during four days in May, 2006 is then compared to observed data from the Emergency Weather Net and analysed. The synoptic and mesoscale situation in the area of study is also investigated.

As an introduction, some basic facts about the air pollutants ozone and nitrogen dioxide are presented. The research area and the weather patterns typical for the region are also included in chapter 2. In the 3rd chapter, the air quality modelling system used and developed for this study is presented, and the 4th chapter presents the input meteorology forecast model used, the Weather Research and Forecasting model, WRF.
The statistics used to evaluate the output from the air quality modelling system, hereby called the WRF/CMAQ, is described in chapter 5. Chapter 6 contains information about the data that has been evaluated in the study; the observed data, the forecasted data, and synoptic weather data. The results, analysis, discussion and the conclusions are presented in chapter 7 and 8, and suggestions on topics for future work in chapter 9.

2 Air pollution

2.1 Ozone, O_3

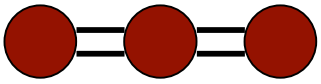

Fig 2.1: The ozone molecule

Ozone is a reactive oxidant gas naturally produced in the atmosphere, and the ozone molecule contains of three oxygen atoms, thereby denoted O_3.
Ozone resides both in the stratosphere and in the troposphere; the stratospheric ozone absorbs ultraviolet radiation emitted by the sun, and thus protects the life on earth from this harmful radiation. But, as mentioned, ozone also exists in the troposphere, near the Earth's surface. The tropospheric ozone is harmful to humans, animals and vegetation and is thus of great concern to research, which shows that the amount ozone in the troposphere is increasing due to human activity.

About 90% of the ozone is stratospheric and resides in what we call the "ozone layer", their abundance here are up to 12.000 ozone molecules for every billion air molecules i.e. 12.000 parts per billion (ppb). The remaining 10% is the tropospheric ozone, with a typical range of 20-100 ppb. The highest surface values of ozone are a result of human induced air pollution. [Fahey et al.]

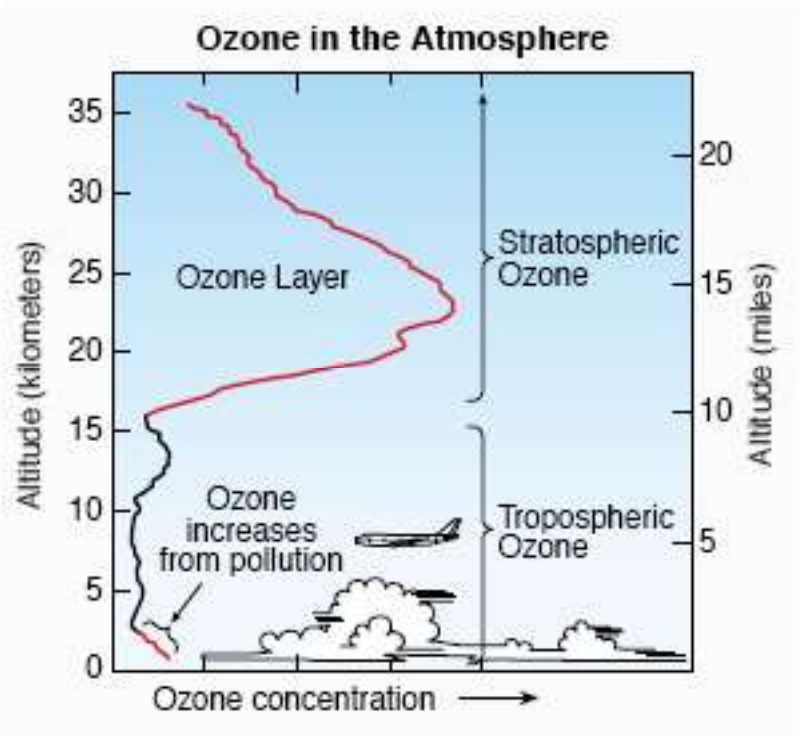

Fig.2.2 Atmospheric ozone. Ozone is present throughout the lower atmosphere. Most ozone resides in the stratospheric "ozone layer". Increases in ozone occur near the surface as a result of pollution from human activities.

2.1.1 Production and destruction

Stratospheric ozone (S-O_3) is naturally formed in chemical reactions involving ultraviolet sunlight and oxygen molecules. The production of S-O_3 is balanced by its destruction in chemical reactions, and some of the S-O_3 is transported down into the troposphere.

Tropospheric ozone (T-O_3) is produced in chemical reactions involving naturally occurring gases and gases from pollution sources. The production reactions require sunlight and primarily involve hydrocarbon and nitrogen oxide gases.
A primary pollution source for T-O_3 production is fuel combustion.
The three major processes in that are active in the T-O_3 destruction process are deposition, chemical reaction and dilution.
Deposition can be dry or moist deposition, dry deposition occurs mainly at the Earth surface when ozone comes in contact with vegetation and soil. Moist deposition occurs when ozone comes in contact with water surfaces, low-level clouds or fog.
Chemical reaction with NO is especially evident when photochemistry stops as the sun sets. O_3 and NO react on a time scale of a few minutes and the species with the lower concentration are totally consumed. This reaction increases the concentration of NO_2 since each molecule O_3 converts to one molecule of NO_2 and one of O_2. Chemical reaction can also occur involving human-produced chemicals.
Dilution occurs when cleaner air dilutes the polluted air, for example from an outburst from higher levels or a low level jet from surrounding tributary valleys [Banta et al].

Increased levels of T-O_3 are generally harmful to living systems because ozone reacts strongly to destroy or alter many other molecules. Excessive ozone exposure reduces crop yields and forest growth. In humans, ozone exposure can reduce lung capacity, cause chest pains, throat irritation, and coughing, it can also worsen pre-existing health conditions related to the heart

and lungs. In addition, increases in T-O_3 lead to a warming of Earth's surface, since the ozone absorbs infrared radiation emitted by the Earth's surface.

Photochemical smog consists mainly of tropospheric ozone. It is a result of chemical interactions of nitrogen oxides (NOx) and volatile organic compounds (VOCs), and sunlight. VOCs and NOx come from a variety of industrial and combustion processes. In typical urban areas, at least half of those pollutants come from vehicular sources.

The photochemical smog is particularly common near cities but winds can carry emissions far away from their original sources and make high ozone levels a problem also in suburban areas. [EPA]

2.1.2 The chemistry

Tropospheric ozone forms from a complex series of chemical reactions containing NOx, VOCs and sunlight. Since sunlight is required for the production, concentrations of T-O_3 are normally higher in the afternoons and during summer months.
In polluted air, ozone production occurs along the following lines:

1. Sunlight dissociates nitrogen dioxide into nitric oxide and atomic oxygen.

NO_2 + solar radiation $\rightarrow$ NO + O

2. Atomic oxygen combines with molecular oxygen in the presence of a third molecule, M to form ozone.

$O_2 + O + M \rightarrow O_3 + M$

3. The ozone is then destroyed by combining with nitric oxide.

$O_3 + NO \rightarrow NO_2 + O_2$

4. As in the first step, the nitrogen dioxide will break down into nitric oxide and atomic oxygen, in the presence of sunlight.
The atomic oxygen then combines with molecular oxygen to form ozone again, as in the second step.

Large compounds of ozone can be produced in polluted air *if* some of the nitric oxide reacts with other gases, without removing ozone in the process.

Some Volatile Organic Compounds (VOCs) are called hydrocarbons (RH) and are emitted by industry and automobiles. They can react with hydroxyl radicals, releasing atomic oxide to the hydroxyl radical.

$OH + RH \rightarrow R + H_2O$

The remaining part of the hydrocarbon molecule, which can be very complex (thereby the dot), is then able to react with molecular oxygen to form RO_2 . This molecule is very reactive and combines easily with nitric oxide to form nitrogen dioxide.

RO_2 + NO $\rightarrow$ NO_2 + Other products

This increases the ozone concentration since the VOCs prevents the nitric oxide to destroy the ozone as rapidly as it is formed. [Ahrens]

2.1.3 Time fluctuations in ozone concentration

Ozone can reside in the atmosphere a month or longer, but is often titrated with the earth's surface. This leads to fluctuations in ozone concentration on many different time-scales; seasonal, synoptic, diurnal, and sub-diurnal.
The atmospheric processes that contribute to these fluctuations are associated with the time scales. The sub-diurnal fluctuations of ozone include the effects of turbulent horizontal and vertical mixing, local titration by fresh emissions of NO, and ozone response to fast-changing emission patterns during the rush traffic hours. Also, sub-diurnal variations can be due to local meteorological wind patterns as for example sea breeze and mountain winds. The diurnal fluctuations of ozone are associated with the diurnal variation of the solar flux and the resulting differences between daytime photochemical production and nighttime removal of ozone as well as the diurnal cycle of boundary layer evolution and decay. The synoptic variations of ozone are caused by changing meteorological conditions such as the presence of a near-stagnant high-pressure system or the passage of frontal systems.
The largest overall variance in ozone concentration is due to diurnal fluctuations. [Hogrefe et al.]

The ozone concentration also varies on a yearly basis, the summer months are particularly favourable for ground-level ozone formation, since the production is dependent on the presence of sunlight, and hence, the highest hourly concentrations are observed during this time of the year [Air Resources Branch]. The winter months are known to have less amount of ground-level ozone, due to the lack of sunlight, compared to the summer months. According to the same study conducted by the Air Resources Branch, the highest hourly mean concentrations are typically observed during the spring, and particularly in April and May. This finding is partly attributed to the increased contributions of stratospheric ozone, which occur during the spring when the stratosphere is closest to the earth's surface.

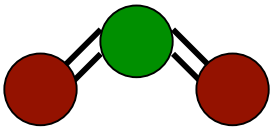

Fig 2.3: The Nitrogen dioxide molecule

2.2 Nitrogen Dixide, NO_2

Nitrogen oxides (NOx) are the generic term for a group of highly reactive gases, all of which contain nitrogen and oxygen in varying amounts. Many of the nitrogen oxides are colourless and odourless, but one common pollutant, nitrogen dioxide (NO_2) along with particles in the air can often be seen as a reddish-brown layer over many urban areas.

Common use of the term Nitrogen oxides refers to a whole family of different chemical compounds of nitrogen and oxides. In chemical reactions that produce nitrogen oxides, a mixture is often formed with the proportions depending on the specific reaction and the conditions it is performed in.

2.2.1 Production

The dry atmosphere consists of gaseous dinitrogen (N_2) to more than 70%. Life on Earth requires nitrogen (N) to survive, but the large reservoir of N_2 cannot be used directly as a nutrient by plants because they cannot absorb gaseous dinitrogen. There is only a few micro organisms that can extract dinitrogen to form reactive nitrogen (nitrogen fixation), a form of nitrogen that living species can use, and another group of micro organisms that can transform

(denitrify) it back again after it has served its purpose among the living species [Galloway]. Nitrogen fixation and denitrification were approximately equal in pre-industrial times, but in the early 20th century, manmade reactive nitrogen became necessary for meeting human needs. Processes to extract reactive nitrogen were developed accordingly and the balance was disturbed.

Human-induced increases of reactive nitrogen contribute to a wide variety of beneficial as well as detrimental changes in the health and welfare of people and ecosystems, depending on the magnitude of the reactive nitrogen [Galloway].

The artificial way of forming nitrogen oxides (NOx) is when fuel is burned at high temperatures, as in a combustion process. During combustion processes of fossil fuels, nitrogen contained in the fuel and in the combustion air is extracted to reactive nitrogen as a by-product, increasing the NOx emissions.
The amount of NOx emissions released can be reduced, depending on the pollution control technology used.

The primary manmade sources of NOx are motor vehicles, electric utilities, and other industrial, commercial, and residential sources that burn fuels.

Nitrogen oxides (NOx) and the pollutants formed from NOx can be transported over long distances, following the pattern of prevailing winds. This means that problems associated with NOx are not confined to areas where they are emitted.

The lifetime of NOx varies from hours to days, giving large spatial variations in the levels of NOx [Fuglestvedt].

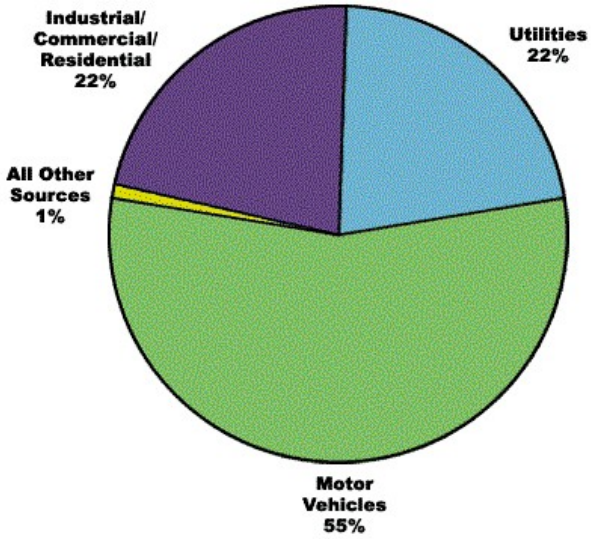

Fig 2.4: Manmade sources of NOx emissions in 2003, USA. Facts from the US Environmental Protection Agency.

2.2.2 Health and environmental impacts of Nitrogen Oxides

Nitrogen oxides cause a wide variety of health and environmental impacts because of various compounds and derivatives in the family of nitrogen oxides. Some of the impacts concerns formation of smog, acid rain, harmful particles and toxic chemicals, it can also effect the global warming, reduce visibility and deteriorate the water quality in lakes [EPA].

Smog:
Smog mainly consists of ground-level ozone and it is formed when Nitrogen oxides (NOx) and volatile organic compounds (VOCs) react in the presence of sunlight. Children, people with lung diseases such as asthma, and people who work or exercise outside are susceptible to adverse effects such as damage to lung tissue and reduction in lung function. Other impacts from ozone include damaged vegetation and reduced crop yields.
Ozone can, just as nitrogen oxides, be transported by wind currents and cause health impacts far from the original sources.

Acid rain:

When nitrogen oxides and sulphur dioxide react with other substances in the air and form acids they contribute to the formation of acid depositions, or more commonly called acid rain. The wet acid deposition refers to acidic precipitation in the form of rain, fog and snow, while the dry acid deposition refers to acidic gases and particles in the atmosphere.
Acid compounds can be carried by prevailing wind for up to hundreds of kilometres, causing damages along the way. The acid compounds causes deterioration of cars, buildings and historical monuments, and causes lakes, streams and soil to become acidic and unsuitable for many animals and a variety of plants.

Global warming:
The nitrous oxide (N_2O), a member of the NOx family is a greenhouse gas. It accumulates in the atmosphere with other greenhouse gasses and absorbs outgoing terrestrial radiation resulting in an increase in air temperature. This effect is commonly known as the greenhouse effect. The enhancement of the greenhouse effect is commonly known as global warming, and in the past century, the Earth's surface air temperature has been undergoing slight warming of between 0,3 C and 0,6 C. Many scientists believe that the main cause of this global warming is the greenhouse gas carbon dioxide (CO_2), but in recent years increasing levels of other greenhouse gasses such as nitrous oxide has shown similar effect on the surface air temperature as CO_2. The effects of an increasing air surface temperature are an ongoing debate and the research within this area is intense, but life on Earth will be affected, not only for humans but also for animals and crops [Ahrens].

Toxic chemicals:
In the air, NOx reacts readily with common organic chemicals and even ozone, to form a wide variety of toxic products, some of which may cause biological mutations. Examples of these chemicals include the nitrate radical, nitroarenes, and nitrosamines.

Visibility impairment:
Nitrate particles and nitrogen dioxide in the air can block the transmission of sunlight, reducing visibility in urban areas.
Haze is caused when sunlight encounters tiny pollution particles in the air, which reduce the clarity and colour of what we see, particularly during humid conditions.

Particles:
NOx reacts with ammonia, moisture, and other compounds to form nitric acid and related particles. These particles can be harmful to human health, with effects on breathing and the respiratory system, damage to lung tissue, and premature death. Small particles penetrate deeply into sensitive parts of the lungs and can cause or worsen respiratory disease such as emphysema and bronchitis, and aggravate existing heart disease.

Water quality:
An increased amount of nitrogen loading in water bodies, particularly coastal estuaries, disturbs the chemical balance of nutrients used by aquatic plants and animals. Additional nitrogen accelerates eutrophication, a process that leads to oxygen depletion, algal bloom, and reduces fish and shellfish populations.

This study will not look at all the nitric oxides as a whole, but will focus on one member of the NOx-family; the Nitrogen Dioxide molecule. This is mainly because this is a common pollutant to measure and there is observed data available to compare with the modelled output concentration data.

Nitrogen Dioxide (NO_2) is gas that is reddish-brown in colour and has a strong and irritating smell. In the air, nitrogen dioxide converts to form gaseous nitric acid and toxic organic nitrates. NO_2 also plays a large part in atmospheric reactions that create ground level ozone, a main part in the makeup of smog. It is also a predecessor to nitrates, which add to increased respirable particle levels in the atmosphere.

2.3 The Pacific West research area

The research area is covering a greater part of south British Columbia, Canada, and the northern part of Washington State, USA. The area is roughly defined as latitude 40N-57N and longitude 132W-110W, and its total area is approximately $9{,}4*10^6$ km^2.

Fig 2.5: Overview of Canada. The red arrow is showing the research area.

2.3.1 Lower Fraser Valley

The Lower Fraser Valley (LFV) is a triangle shaped valley surrounding the Fraser River, reaching from the Pacific Ocean and the Fraser River estuary in the Georgia Basin into the city of Hope. It is bounded by the Coastal mountain range in the north and the Cascade Mountain range in southeast.

The LFV contains some of the most productive agricultural land in Canada and is favoured by the topography, soils and mild climate. But parts of the valley host urban and industrial centres as Vancouver, Surrey and Abbotsford and the population in the area grows rapidly. More than 2 million people called the valley their home in 2005 and when the population increases, the traffic also increases, therefore air pollution concerns becomes an increasingly important issue in the area.

Fig 2.6: The Lower Fraser Valley and Vancouver.

2.4 The weather situation in the valley

The synoptic weather conditions are well known to have great impact on the distribution and concentration of pollutants, this is also the situation in the Lower Fraser Valley in British Columbia, Canada.
The Lower Fraser Valley is situated by the Pacific Northwest coast, around 41 degrees latitude. The area is most often exhibiting an impact of westerly flow, but other wind directions are present every time of the year. When in the westerly flow, the valley is highly affected by marine air that has been transported with the Westerlies over the Pacific Ocean. The air flowing over the ocean is quite clean due to wet deposition, compared to the air flowing over the American continent, which instead is constantly polluted. Therefore, the Pacific Northwest coast is particular well suited for air quality studies. If the wind is westerly, the pollution is most often originating from the area of study, and almost none particles have been advected from sources in other areas.

Weather conditions that are favourable for high values of NOx and ozone are clear skies, warm air, and reduced mixing heights. These conditions are common in the Lower Fraser Valley area during situations with weak surface pressure gradients, strong low-level inversions, warm air in low levels, and strong ridges at 500hPa that are persistent [Lord et al]. Specially favourable are situations when the strong high pressure ridge at 500hPa aligned with the Pacific Northwest coast east of 120 W, coincide with a low-level thermal trough at the surface extending northward along the Pacific coast from the southwest United States [McKendry]. A persistent situation like this can give very high concentration of ozone in the area.

Diurnal variations on smaller scales in the weather have great impact on the spatial and temporal variations of pollutants in the Lower Fraser Valley. Mesoscale phenomena are also common in this area due to contrasts in land-water temperature and topographic structure. The contrasts create thermally induced diurnal low-level circulations as sea breeze and mountain winds. These circulation systems are strongest during the summer months when the insolation is most intense and of longest duration. During summer days, the land is warmer than the water and the free atmosphere at the same level, this produces a sea breeze and an upslope wind up the terrain. At night, the land cools and you can expect a weak, if any, land breeze. Also, the mountains are now colder than the free atmosphere at the same altitude, producing a downslope (katabatic) wind replacing the upslope wind during the day [Mass].

The mountain winds acts as contributors to build up the concentration of pollutants in the Lower Fraser Valley due to the recirculation with the downslope nightly wind [Banta et al, Martilli et al]. One would believe that the polluted air in the upslope winds during the day contributes to the next day's pollution by adding the previous day's pollutants to the following with the katabatic and downvalley flows. Banta et al examined the downslope winds in an adjacent valley to the Lower Fraser Valley, and they could show that downslope winds had lower concentrations of ozone than the upslope winds. This titration of ozone is explained by dry deposition on the hillsides and/or fast chemical reactions with nitrogen oxide. The study also showed that the recirculated air layers up in the atmosphere with the polluted air on top of the cleaner air. A numerical study [Martilli et al] confirms the layering air with pollutants higher up in the atmosphere due to downslope winds. The Martilli study shows that there are three main recirculation processes, of which one of them is a day-to-day circulation where the pollutants in an upper layer of the atmosphere are fumigated to the surface layers when the convective boundary layer increases the following day.

A study of the annual and summer ozone trends between 1985 and 2000 in the Greater Vancouver/Lower Fraser Valley [Vingarzan et al] showed that the spatial mean ozone concentrations exhibited an increasing gradient from west to east with the highest concentrations to the east in the valley. During weather episodes favourable of ozone formation, the sea breeze and winds in the area acts to concentrate the pollutants to the east side of the valley, giving rise to a spatial gradient of pollutants. The westerly sea breeze contributes by "pushing" the polluted air eastwards during the day, hence reinforcing the gradient of pollutants in the valley.

3 Air quality modeling

3.1 EPA Models-3 Community Multiscale Air Quality (CMAQ) modelling system v.4.5.1

The Models-3 Community Multiscale Air Quality (CMAQ) modelling system is a third generation air quality modelling and assessment tool, which is designed to support air quality modelling applications ranging from regulatory issues to science inquiries on atmospheric science processes.
The CMAQ system uses a "one atmosphere" perspective where complex interactions between atmospheric pollutants and regional and urban scales are confronted.
The "one-atmosphere" modelling perspective is not only related with the multi-pollutant chemical interactions, but also with the dynamic description of the atmosphere. The multi-pollutant design admits CMAQ to process several pollutants, which can interact with each other and thereby enhance or decrease the emission values of a certain pollutant. The dynamical design admits CMAQ to act on different dynamic scales when processing pollutants.

CMAQ is a multi-pollutant, multiscale air quality model that contains state-of-science techniques for simulating all atmospheric and land processes that affect the transport, transformation, and deposition of atmospheric pollutants and/or their precursors on both regional and urban scales. The CMAQ model can address tropospheric ozone, acid deposition, visibility, fine particulate and other air pollutant issues that are important in air quality issues. The basic outputs include hourly concentrations for gaseous and aerosol pollutants, wet deposition, and dry deposition.

The models-3 CMAQ modelling system was first released to the public in June 1998. CMAQ version 4.5.1, which is used in this study, was released to the public in March 2006. The models-3 CMAQ modelling system consists of the Chemistry Transport Model (CTM) and additional pre-processors. The pre-processors are the initial condition processor (ICON), the boundary conditions processor (BCON) and the photolysis rates processor (JPROC). Also, the meteorology and emissions have to be processed and in this study, the meteorology pre-processing is handled by the Meteorology-Chemistry Interface Processor (MCIP), and the emission pre-processing is handled by the Sparse Matrix Operator Kernel Emissions (SMOKE) model. Fig 3.1 shows the structure of the Models-3 CMAQ modelling system with the WRF model as forecasting model.

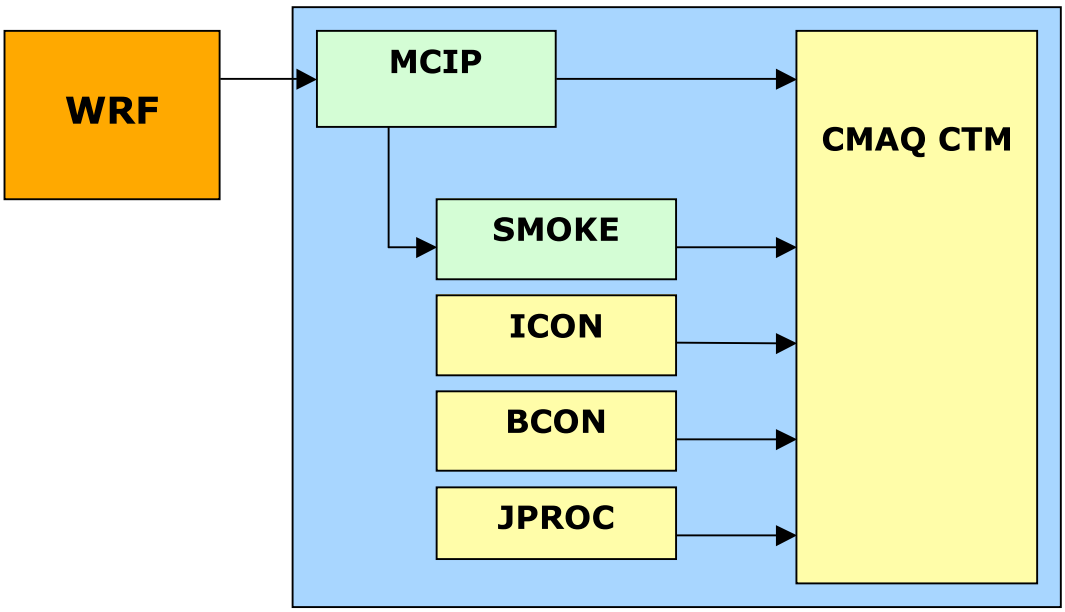

Fig 3.1: The Models-3 CMAQ modelling system in the version that is used in this air quality study.

3.1.1 The pre-processors for the CMAQ modelling system

There are, as briefly mentioned in the previous section, five pre-processors for air quality modelling with the Chemistry Transport Model (CTM) within the CMAQ modelling system. The CMAQ CTM model will be described further in section 3.2, and the five pre-processors in the following sections;
ICON, section 3.3
BCON, section 3.4
JPROC, section 3.5
MCIP, section 3.6
SMOKE, section 3.7

In this study, the MCIP pre-processor are using meteorological input from the Weather Research and Forecast model WRF, which will be described in section 4.1. The head scripts written to run CMAQ modelling system, and the grid description file can be found in appendix A.

3.2 CMAQ Chemistry transport model (CCTM)

The CCTM simulates the relevant and major atmospheric chemistry, transport and deposition processes involved throughout the modelling domains. CCTM then performs chemical

transport modelling for multiple pollutants on multiple scales.

The challenges that the CCTM model is facing are transportation of pollutants, e.g. advection and diffusion on different scales and in three dimensions, deposition of pollutants, chemical reactions, aerosols, cloud mixing, emissions injection, photolytic rate computation, plume chemistry effects, and also process analysis [US EPA CMAQ model]. Plume effects are not computed in this study, why no further explanation of this is provided.

Transport within the CCTM processor:
Advection is the transport of a quantity solely by the mass motion (velocity field) of the atmosphere [AMS glossary].
The advection scheme used in this simulation is the new global mass-consistency scheme (yamo). This scheme uses the old Piecewise Parabolic Method (PPM) advection scheme for horizontal advection and it is deriving a vertical velocity component at each grid cell that satisfies the consistency equation, using the meteorology model's density. That way the advection scheme is conserving the mass in every computational step.

Diffusion is the transport of matter solely by the random motions of molecules not moving together in coherent groups. Hence, concentration gradients are equalized by molecular and/or turbulent (eddy) motions [AMS glossary].
The minimum eddy diffusivity ($K_Z$min) has an important impact on nighttime concentration of pollutants. Meteorology models uses low values in the range 0,1-0,5 m^2/s, but running CMAQ with such low values outputs unrealistically high concentrations of primary species in areas of high emissions (for example urban areas). Using higher $K_Z$min values lead to over prediction of ozone at nighttime in rural areas. The $K_Z$min value which has been used in CMAQ in older versions than v4.5 is $1,0 m^2/s$ and it is somewhat high and therefore tends to overpredict ozone concentration as mentioned above. The newer versions of CMAQ have another $K_Z$min option, which takes into account the presence of urban areas. This option is yet only available for users running CMAQ with MM5 meteorology, why the $K_Z$min value $1,0 m^2/s$ is used in this simulation.

Deposition within the CCTM processor:
Deposition is the process where trace gases or other particles are transferred from the atmosphere to the surface of the earth [AMS glossary] Deposition is usually divided into two categories; wet deposition and dry deposition, depending on the phase of the material during the deposition process.
In wet deposition, the gas or particle is first incorporated into a droplet and then transferred to the surface via precipitation. In dry deposition, the gas or particle is transported to ground level where it is adsorbed onto the surface. Surfaces are buildings, soil, ocean, vegetation etc.
The aerosol dry deposition velocity equation has been updated to the form suggested by Venkatram and Pleim (1999):

$$v_d = \frac{v_g}{\left(1 - \exp\left(-v_g\left(R_a + R_b\right)\right)\right)}$$

Where R_b denotes the quasi-laminar boundary layer resistance, which depends on the impaction term E_{im}. The algorithm for the impaction term has also been replaced with a newer form (Giorgi, 1986).

Chemistry within the CCTM processor:
The representation of chemical interactions among atmospheric constituents is an essential element of an air quality model, since the chemical reactions in the atmosphere is fundamental in air quality modelling. The CCTM model uses the approach to model atmospheric processes

in gas-phase and in liquid-phase separately.
A chemical mechanism is a collection of reactions that transforms reactants into products, including all important intermediates. But since the chemical reactions in reality are very complicated, the chemical mechanism used by air quality modelling models are parameterised and somewhat generalized by using special conventions, which simplifies the mathematical representation of the reactions.
Mechanism species can be divided into two categories; organic and inorganic species. There are very few important inorganic species and they are almost always represented explicitly in all chemical mechanisms. The important inorganic species are, among others, ozone, nitric oxide, nitrogen dioxide, and sulphur dioxide. The different chemical mechanisms available for use in for example air quality studies mainly differ in the representation of the reactions for organic species.

Gas-phase, aqueous, and aerosol chemistry within CCTM:
The chemical mechanism used in this study is the cb4_ae3_aq mechanism, which is based on the Carbon Bond Mechanism IV (CB4 mechanism). The CB4 mechanism includes 36 species and 93 reactions, including 11 photolytic reactions. The CB4 uses nine primary organic species (species omitted directly to the atmosphere). The mechanism was developed for simulating photochemistry on urban and regional scale in the late 80's [Gery et al.], and tend to overpredict ozone concentrations by a small percentage. The mechanism has undergone several changes since its publication in 1989 and all of these changes have been incorporated into CMAQ.
As the name of the chemical mechanism, cb4_ae3_aq implies, the CB4 mechanism has been modified to incorporate both aqueous chemistry and aerosol formation processes.
The Euler Backward Iterative (EBI) solver is used for this study in chemical computations for CMAQ. The EBI solver has been found to be the most computationally efficient solver in the CMAQ model [US EPA highlights June 2004].

Aerosols within the CCTM model:
Aerosols are finely divided liquid or solid particles uniformly dispersed in a gas-phase medium, such as air [AMS glossary].
Incorporating aerosols in air quality modelling is quite hard since not only particle size is important, but you also need to choose total number of particles, mass and size of particles. Also, the emittance of aerosols into the atmosphere can be made in a number of ways, both natural (blowing winds, volcano activity, creation of particles by chemical reactions in the atmosphere) and artificial (human activities as combustion and agriculture).
The aerosol component used in CMAQ is derived from the Regional Particulate Model (RPM) which divide particles into two groups, fine and coarse particles, which generally have separate sources and chemical reactions. The fine particles have a diameter less than 2,5 m and the coarse particles have a diameter between 2,5 and 10 m.
In version 4.5 of CCTM, a new aerosol module (Aero4) is incorporated which includes considerations of sea salt aerosols. However, in this study, the older module, Aero3 is used which differs from the Aero4 module only by the inclusion of sea salt aerosols.

Clouds within the CCTM model:
Clouds are important in air quality modelling since they hold both physical and chemical processes affecting the pollutants. The pollutant concentration in the atmosphere is affected by clouds in terms of convective mixing (vertical transport), scavenging (clouds and precipitation), aqueous chemistry (dissociation into ions and/or reaction with other compounds), and removal of pollutants by wet deposition, and concerns both gas-phase

species and aerosols.
The cloud model in CMAQ incorporates parameterisations of different types of clouds in the different scales, both precipitating and non-precipitating clouds, an aqueous chemistry model for sulphur, and a simple mechanism for scavenging. The cloud model can be divided into two main components; a sub-grid cloud model, and a resolved cloud model. The sub-grid cloud model handles convective clouds smaller than the horizontal grid resolution, both precipitating and non-precipitating convective clouds. The resolved cloud model handles clouds bigger than the horizontal resolution of the model and which has been resolved by the meteorological model.
The sub-grid cloud scheme is used in CMAQ only if the horizontal grid resolution is larger than 12 km. Both the sub-grid model and the resolved model takes into account the scavenging, wet deposition, convective mixing and the aqueous chemistry within the clouds. The sub-grid cloud scheme was derived from the RADM model v2.6 and simulates in a representative cloud within a grid cell. The pollutant vertical mixing algorithm has been modified based on the ACM model for the last version of CMAQ, allowing in-cloud transport from a source layer to all other layers within the cloud [Appel et al.].
The resolved cloud scheme is based upon the output from the meteorological model since the resolved clouds covers the entire grid cell. The meteorological model computes mixing, convection, and precipitation. Using the total of condensed cloud water and rainwater reported by the meteorological model, the CMAQ model then simulates the processes within the cloud; scavenging, wet deposition, and aqueous chemistry.

Within the CCTM, there is a subroutine that has two basic functions; including interpolation of the clear-sky photolysis rate table (created by JPROC, section 3.5) and application of a cloud correction factor to the clear-sky values

Process analysis within CCTM:
Process analysis is a diagnostic tool that can be used by the modelling analyst to quantify contributions of individual science processes to model predicted concentrations. Such information is useful for understanding the model's behaviour, for example; understanding a model's predictions and determining why predictions change when the model configuration or when model inputs are changed.

For further information about the CMAQ model, please see the CMAQ Science documentation at the CMAS Model documentation site;
http://www.cmascenter.org/help/documentation.cfm

3.3 Initial condition processor (ICON)

The ICON processor provides concentration fields for all individual chemical species within each grid cell in the modelling domain for the beginning of a simulation, as required by the CMAQ CTM model. The individual model species include gas-phase mechanism species, aerosols, non-reactive species and tracer species, and the output concentration files are all 3-dimensional gridded files.

Since initial conditions are required only for the start of a model simulation, the ICON processor will generate initial conditions for only the first time step in a simulation. The ICON processor generates initial concentrations using a predefined vertical profile during the first day in a simulation, and using CMAQ simulation results during the following days. The predefined vertical concentration profiles give species concentrations as a function of height and are spatially and temporally independent. The profile represents relatively clean air

conditions in the eastern USA and is formulated from available measurements and modelling studies.
The initial concentrations can also be generated by the ICON processor by using existing 3 dimensional gridded concentration files from CMAQ simulations. These files are both temporally and spatially resolved and used when nesting the model into a finer grid. If not nesting is necessary, the CMAQ concentration file from the previous run can be used directly as input initial concentrations file to the current CMAQ run.

3.4 Boundary condition processor (BCON)

The BCON processor generates boundary conditions for individual model species for the grids surrounding the modelling domain. The individual model species include gas-phase mechanism species, aerosols, non-reactive species and tracer species.
Concentration fields of all model species at the boundaries of the modelling domain throughout the simulation are required as boundary conditions to the CCTM.

Since boundary conditions are required throughout a simulation, one set of boundary conditions will be generated at each time step for the modelling period as 3 dimensional boundary files. Just as for the ICON processor, the BCON processor can generate boundary concentrations for the cells immediately surrounding the modelling domain by using a predefined vertical concentrations profile. The predefined vertical profiles give species concentrations as a function of height and are minimally spatially dependent and temporally independent. The profile represents relatively clean air conditions in the eastern USA and is formulated from available measurements and modelling studies.
The boundary concentrations can also be generated by using existing 3-dimensional gridded concentration files from CMAQ simulations. These files are both temporally and spatially resolved and used when nesting the model into a finer grid is necessary.

3.5 Photolysis rates processor (JPROC)

Many chemical reactions in the atmosphere are initiated by the photo dissociation of numerous trace gases. These photo dissociative reactions are responsible for most of the smog build-up detrimental to humans, animals, plant life and materials. In order to accurately model and predict the effects of air pollution, good photo dissociation reaction rate (photolysis rate) estimates must be made. Photo dissociation is the conversion of solar radiation into chemical energy to activate and dissociate chemical species. Examples of species that photo dissociate include many important trace constituents of the troposphere such as NO_2 (nitrogen dioxide), O_3 (ozone), HCHO (formaldehyde), CH_3CHO (acetaldehyde), HONO (nitrous acid), the NO_3 (nitrate) radical, and H_2O_2 (hydrogen peroxide).
The simulation accuracy of the entire chemical system is highly dependent upon the accuracy of photolysis rates, which are the primary sources of radicals in the troposphere.
JPROC produces a clear-sky photolysis rate look-up table. The look-up table consists of photolysis rates at 7 altitudes, 6 latitudes, and hour angles. The look-up table is recalculated for each simulation day and is dependent upon the chemical mechanism.

The photolysis rate changes with time of day, longitude, latitude, altitude, and season, and is governed by the astronomical and geometrical relationships between the sun and the earth. It is also greatly affected by the earth's surface albedo as well as by various atmospheric scatterers and absorbers.

3.6 Preparation of meteorological input for CMAQ with the Meteorology-Chemistry Interface Processor (MCIP), v3.x

The Meteorology-Chemistry Interface Processor (MCIP) is a meteorological data pre-processor, which is used to convert meteorological data and generate gridded two- and three-dimensional meteorological data files as output.
Since most meteorological models are not built for air quality modelling purpose, MCIP deals with issues related to data format translation, conversion of units of parameters, diagnostic estimations of parameters not provided, extraction of data for appropriate window domains, and reconstruction of meteorological data on different grid and layer structures.
Hence, MCIP links meteorological models as the WRF model with the Chemical Transport Model (CTM) of the Models-3 Community Multiscale Air Quality (CMAQ) modelling system, to provide a complete set of meteorological data needed for air quality simulations [Byun et al].

The inputs for MCIP consist of operational inputs and meteorological model output files. MCIP writes the bulk of its two- and three-dimensional meteorological and geophysical output data in a transportable binary format (netCDF) using the Models-3 input/output applications program interface (I/O API) library. [Byun et al]

When the input meteorological data form the WRF model are recast with the proposed set of governing equations using MCIP, chemical transport models can follow the dynamic and thermodynamic descriptions of the meteorological data closely.[KÄLLA??? troligtvis science documentation for CMAQ]

The MCIP version used in this study is a version of the MCIP v 3.0, which is further developed specially for the WRF model and is currently not official to use (May, 2006), thereby the denotation 3.x.

3.7 Preparation of emission input for CMAQ with the Sparse Matrix Operator Kernel Emissions (SMOKE) model, v2.2

Advanced numerical air quality models (AQMs) have been developed to understand the interactions among meteorology, emissions (both manmade and biogenic), and pollutant chemistry and dynamics. Emission data from emission models and inventories for the modelling domain are one of the most important inputs for these air quality models, and the Sparse Matrix Operator Kernel Emissions model (SMOKE) is one among several emission processors that can provide these data to the AQMs.

The Sparse Matrix Operator Kernel Emissions (SMOKE) Modelling System was created by the former MCNC Environmental Modelling Center to allow emissions data processing methods to integrate high-performance-computing sparse matrix algorithms. MCNC EMC was later reorganized to Barons Advanced Meteorological Systems EMC, and they are now handling the development of the SMOKE Modelling System.

The first version of SMOKE was released to the public in February 1998 and the version used in this study, version 2.2, was released in September 2005. This version is also the first SMOKE version developed to handle meteorological input from the WRF model.

The SMOKE system provides a mechanism for preparing specialized inputs for air quality modelling research, and it makes air quality forecasting possible.
SMOKE can process criteria gaseous pollutants such as carbon monoxide (CO), nitrogen

oxides (NO_x), volatile organic compounds (VOC), ammonia (NH_3), sulphur dioxide (SO_2); particulate matter (PM) pollutants such as PM 2.5 microns or less ($PM_{2.5}$) and PM less than 10 microns (PM_{10}); as well as a large array of toxic pollutants, such as mercury, cadmium, benzene, and formaldehyde.

SMOKE is not an air quality model itself, but is primarily an emission processing system. This means that its main purpose is to provide an efficient tool for converting the resolution of the emission inventory data into the formatted emission input files required by an air quality model.

The AQ models typically require emissions data on an hourly basis, for each model grid cell (and perhaps model layer), and for each model species. Emission inventories are typically available with an annual-total emissions value for each emissions source, or perhaps with an average-day emissions value. To achieve the input requirements of the AQ model, emissions processing must at least transform inventory data by temporally allocating annual emissions to hour-by-hour emissions based on activity data, by spatially allocating aggregated emissions to a predefined model grid, by chemical speciation, and by layer assignment.

Currently, SMOKE supports area-, mobile-, and point-source emissions processing and also includes biogenic emissions modelling.
The input data for SMOKE in this study, which depends on the research area, is meteorology data from the WRF model prepared by the meteorology pre-processor MCIP, emissions of CO, NH_3, NOx, PM_{10}, $PM_{2.5}$, SO_2, and VOC based on EPA's 2001 National Emission Inventory and provided by the Canadian RWDI (Rowan Williams Davies & Irwin inc.), biogenic land use files prepared using the Multimedia Integrated Modelling Systems (MIMS) Spatial Allocator, and surrogate files describing the detailed emissions, also provided by RWDI.

3.7.1 The SMOKE processing

SMOKE uses sparse matrix operations when modelling emissions. Figure 3.2 shows an example of how the matrix approach organizes the emissions processing steps for anthropogenic emissions, with the final merging step to create the model-ready emissions. This example does not include all processing steps, which is different for the different source categories in SMOKE, but it does include the major processing steps.
More specific, the inventory emissions are arranged as a vector of emissions, with associated vectors that include characteristics about the sources. SMOKE also creates matrices that will apply the gridding, speciation, and temporal factors to the vector of emissions. In many cases, these matrices are independent from one another, and can therefore be generated in parallel. The processing approach ends with the merge step, which combines the inventory emissions vector (now an hourly inventory file) with the control, speciation, and gridding matrices to create model-ready emissions. This study consistently excluded the control program and files.

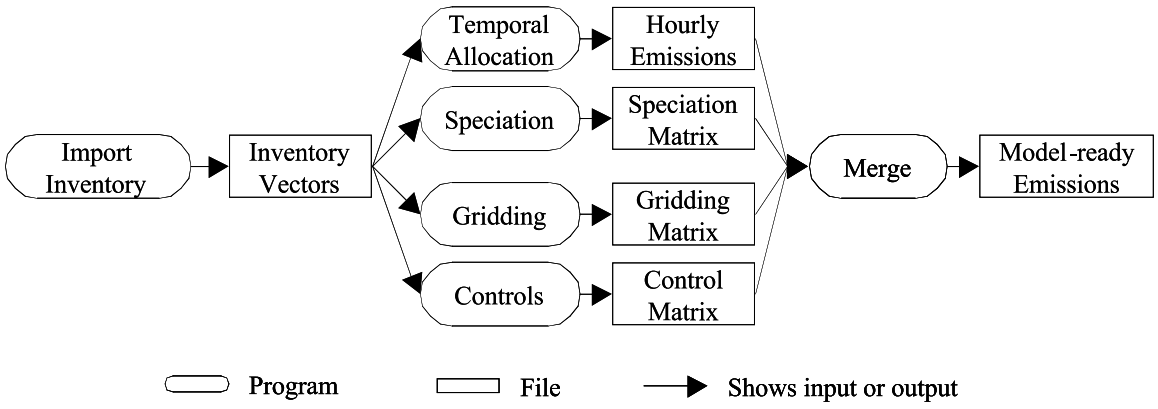

Fig 3.2: Flow diagram of major SMOKE-processing steps needed by all source categories.

The emission sources SMOKE is processing are all anthropogenic and are merged into four groups; area sources, point sources, biogenic sources, and mobile sources. The area sources are stationary non-point sources and include for example dry cleaners and gas stations, the point sources are specific point of pollution, for example factory smokestacks and industries. The biogenic sources are biological sources like plants and animals, which emit pollutants. These sources include animal management operations, oak and pine tree forests. The mobile and non-road sources include mobile air polluters like airplanes, cars, motorcycles and boats. In this study, the mobile inventory also consists of non-road sources, which should be treated as area sources, and therefore the combined non- road and mobile sources are processed as extra area sources.

Special settings for the SMOKE runs for this study is

1. For area sources:
   No special settings
2. For Point sources:
   No Plume in Grid computation
   Not running elevpoint
3. For mobile sources:
   No Mobile6 processing, which are a special processor for the toxics in the atmosphere.
   Mobile sources processed as area sources since this study uses an inventory of mobile (on-road) sources combined with non-road (area) sources.
4. For biogenic sources:
   Running a meteorology scanning processor for settings of season and daylight.

4 The meteorology input

4.1 The Weather Research and Forecast Model (WRF) v2.1.2

The Weather Research and Forecasting (WRF) Model is a next-generation mesoscale numerical weather prediction system designed to provide a common framework for both operational numerical weather prediction and atmospheric research. It was developed to eventually supersede the established but aging existing models such as the Mesoscale Model MM5 at the National Center for Atmospheric Research (NCAR), the (ETA) model at (NCEP), and the (RUC) system of (FSL).
The WRF model is suitable for a broad spectrum of applications across scales ranging from meters to thousands of kilometres, but is specially targeted for the 1-10km grid scale and intended mostly for operational weather forecasting, regional climate prediction, air quality

simulation, and idealized dynamical studies.

The first version, WRF 1.0 was released in the end of November 2000, and the latest version, WRF 2.1.2 was released in January 2006. The version that is running in research purpose by the Weather Forecast Research team of the Geophysical Disaster Computational Fluid Dynamics Centre at University of British Columbia and is used in this study, WRF 2.1.2 was updated on January 30, 2006.

4.1.1 The WRF system

The WRF system consists of the *WRF model* itself, *pre-processors* for producing initial and lateral boundary conditions for idealized, real-data, and one-way nested forecasts, *postprocessors* for analysis and visualization, and a three-dimensional variational data assimilation *(3DVAR) program*. The WRF system is illustrated in Figure 4.1.

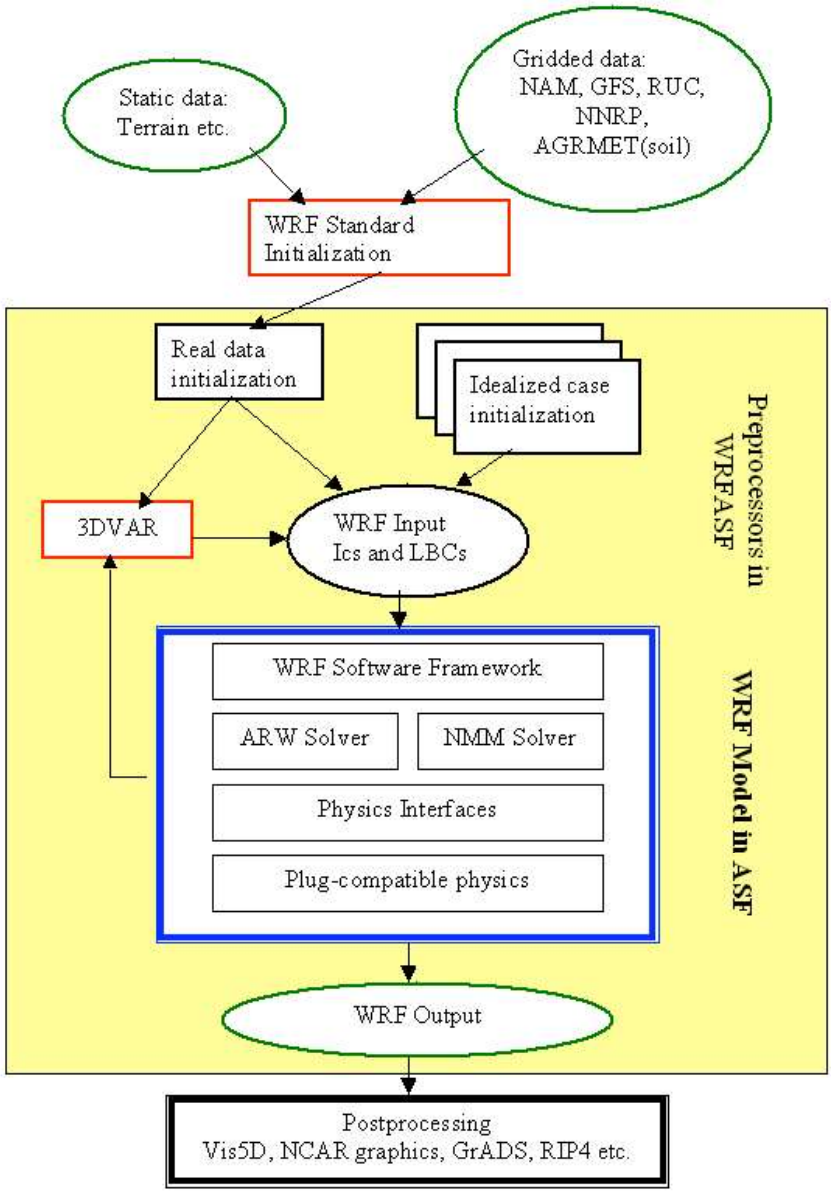

Fig 4.1: Schematic of the WRF system.

With the exception of the standard initialisation (SI) program, each of the pre-processors and 3DVAR are parallel programs implemented using the WRF Advanced Software Framework

(WRF ASF). The WRF ASF is further described in chapter 4.1.2

The function of the Standard Initialisation is to take real-data analyses on another grid, define the WRF horizontal grid, and vertical levels in mass coordinates, generate map, elevation and land use information for WRF, and horizontally and vertically interpolate fields to the WRF grid. The WRF model can be run with either idealized initialisation or real-data initialisation.

The WRF Model (large box in the figure 4.1) contains two dynamical cores; The NCAR-developed Advanced Research WRF (*ARW*), and the NOAA/NCEP's operational implementation of WRF, the Non-hydrostatic Mesoscale Model (*NMM*).

The WRF-NMM core is based on a fully compressible hydrostatic NWP model using mass based vertical coordinate, which has been extended to include the non-hydrostatic motions. The non-hydrostatic dynamics has been introduced through an add-on module, which can be turned on and off [Janjic 2003].
The NMM core uses a terrain-following hybrid (sigma-pressure) vertical coordinate. NMM conserves mass, kinetic energy, enstrophy (mean square vorticity) and momentum, as well as a number of additional first and second order quantities using 2^{nd} order finite differencing.

The WRF-ARW core is based on a Eulerian solver for the fully compressible non-hydrostatic equations.
Further details on this core can be found in section 4.1.4.

The dynamical core that is used for the research of this thesis and also in operational use by the Weather Forecast Research team at the Geophysical Disaster Computational Fluid Dynamics Centre at University of British Columbia, is the Advanced Research WRF (ARW).

4.1.2 Three-level hierarchy software design

The WRF model is organized functionally as a three-level hierarchy superimposed over the model subroutine call tree.
The three levels are the driver layer, the model layer and the mediation layer. The idea of three-level structure is so that users of the WRF model easily can implement their schemes with little need to understand other parts of WRF code.

The driver layer is responsible for top-level control of initialization, time-stepping, I/O, instantiating domains, maintaining the nesting hierarchy between domain type instances, and setting up and managing domain decomposition, processor topologies, and other aspects of parallelism. The driver deals only with domains and does not see the data fields they contain. The driver layer, or WRF Software Framework, is common for both dynamical solvers, ARW and NMM.

The model layer comprises the subroutines that perform actual model computations, for example advection, diffusion, and physical parameterizations.

The mediation layer is the bridge between the model and driver layers and it connects the dynamics with the physics. It contains information pertaining to both the model layer and the driver layer.
The different dynamical solvers, ARW and NMM, call the physics drivers, which are the interfaces between the solver and individual physics schemes [Michelakes et al. 1998, Skamarock et al. 2005].

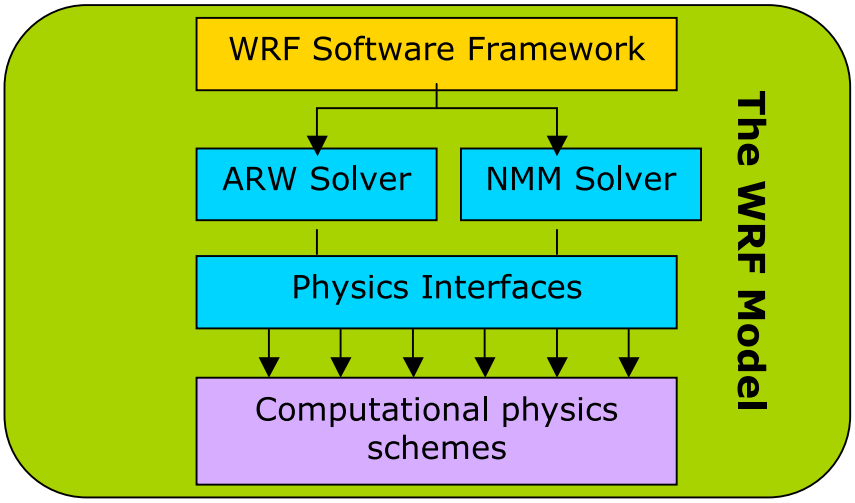

Fig 4.2: Three-level hierarchy;
Top, yellow=Driver layer; Middle, blue=Mediation layer; Bottom, violet=Model layer.

4.1.3 The Physics within the WRF model

Physics components that have been included in WRF is; microphysics, cumulus parameterisation, long wave radiation, short wave radiation, planetary boundary layer, surface layer, land-surface parameterisation, turbulence and subgrid eddyscale diffusion. For all these components, there are several different solver schemes to choose from. For the WRF model to be compatible with the model constellation examined in this thesis, some of the schemes are predominant to use. For a detailed description of both the physical schemes in use, and the dynamics options, see appendix C.

4.1.4 The Advanced Research WRF (ARW) solver

The equation set in ARW is Euler non-hydrostatic with a run-time hydrostatic option available, the equation set is also fully compressible and conservative for scalar variables. The equations are cast in flux form, using a mass (terrain-following hydrostatic-pressure) vertical coordinate, and the top of the model is a constant pressure surface. The horizontal grid used is Arakawa C-grid staggering. The ARW solver uses a time-split high-order Runge-Kutta method to integrate a conservative formulation of the compressible non-hydrostatic equations. The model also supports one-way, two-way, and moving nest options. For spatial discretization, the WRF ARW solver uses high-order advection options in both horizontal and vertical. Full Coriolis term is included [Skamarock et al].

4.1.4.1 Governing equations in the ARW-WRF model parameterisation

The ARW dynamics solver integrates the compressible, non-hydrostatic Euler equations, which are cast in flux form using variables that have conservation properties. The equations are formulated using a terrain-following (mass) vertical coordinate η [Skamarock et al. 2005].

The terrain-following hydrostatic-pressure vertical coordinate is denoted by η and defined as

$$\eta = (p_h - p_{ht})/\mu \qquad (4.1)$$

where

$$\mu = p_{hs} - p_{ht} \qquad (4.2)$$

p_h is the hydrostatic component of the pressure, and p_{hs} and p_{ht} refer to values along the surface and top boundaries, respectively.

η varies from a value of 1 at the surface to 0 at the upper boundary of the model domain. A visual description of the vertical coordinate can be found to the right, in fig 4.3.

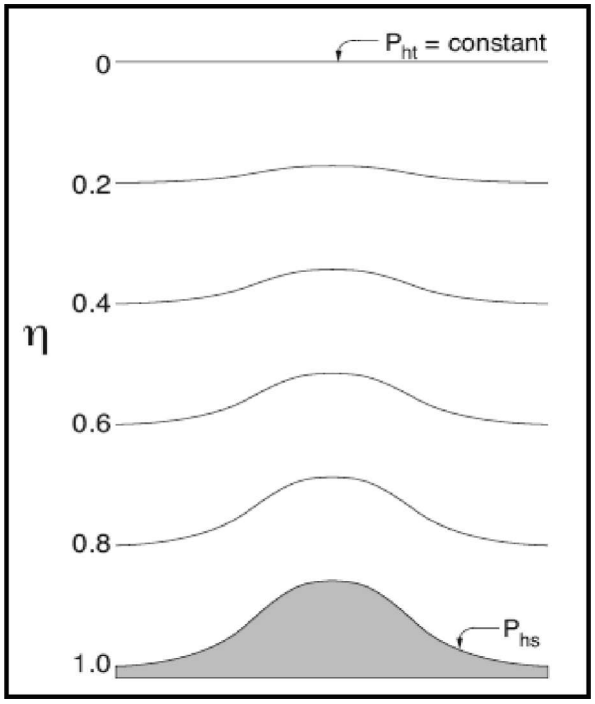

Figure 4.3: ARW vertical coordinate η.

4.1.4.2 Flux-form Euler equations

Using the variables defined above, the flux-form Euler equations can be written as

$$F_U = \partial_t U + \left(\nabla \bullet \overline{V} u\right) - \partial_x\left(p\phi_\eta\right) + \partial_x\left(p\phi_x\right) \qquad (4.3)$$

$$F_V = \partial_t V + \left(\nabla \bullet \overline{V} v\right) - \partial_y\left(p\phi_\eta\right) + \partial_y\left(p\phi_y\right) \qquad (4.4)$$

$$F_W = \partial_t W + \left(\nabla \bullet \overline{V} w\right) - g\left(\partial_\eta p - \mu\right) \qquad (4.5)$$

$$F_\theta = \partial_t \theta + \left(\nabla \bullet \overline{V}\theta\right) \qquad (4.6)$$

$$0 = \partial_t \mu + \left(\nabla \bullet \overline{V}\right) \qquad (4.7)$$

$$0 = \partial_t \phi + \mu^{-1}\left[\left(\overline{V} \bullet \nabla\phi\right) - gW\right] \qquad (4.8)$$

along with the diagnostic relation for the inverse density

$$\partial_\eta \phi = -\alpha\mu \qquad (4.9)$$

and the equation of state

$$p = p_0\left(R_d\theta / p_0\alpha\right)^\gamma \qquad (4.10)$$

$\gamma = c_p / c_v = 1.4$ is the ratio of the heat capacities for dry air, R_d is the gas constant for dry air, and p_0 is a reference pressure (typically 105 Pascals). The left-hand-side terms $F_U, F_V, F_W,$ and F_θ represents forcing terms arising from model physics, turbulent mixing, spherical projections, and the earth's rotation.

In ARW, the governing equations also include the effects of moisture in the atmosphere, and projections to the sphere. Currently, the ARW solver supports three projections to the sphere; the Lambert Conformal, polar stereographic, and Mercator projections. The Lambert Conformal projection is used in this study.

The momentum variables are redefined due to a map-scaling factor, and the governing equations, including map factors and rotational terms can be written as

Momentum conservation equations:

$$F_U = \partial_t U + m\left[\partial_x (Uu) + \partial_y (Vu)\right] + \partial_\eta (\Omega u) + \mu_d \alpha \partial_x p + (\alpha/\alpha_d)\partial_\eta p \partial_x \phi \quad (4.11)$$

$$F_V = \partial_t V + m\left[\partial_x (Uv) + \partial_y (Vv)\right] + \partial_\eta (\Omega v) + \mu_d \alpha \partial_y p + (\alpha/\alpha_d)\partial_\eta p \partial_y \phi \quad (4.12)$$

$$F_W = \partial_t W + m\left[\partial_x (Uw) + \partial_y (Vw)\right] + \partial_\eta (\Omega w) - m^{-1} g\left[(\alpha/\alpha_d)\partial_\eta p - \mu_d\right] \quad (4.13)$$

Conservation equation for potential temperature:

$$F_\theta = \partial_t \theta + m^2\left[\partial_x (U\theta) + \partial_y (V\theta)\right] + m\partial_\eta (\Omega\theta) \quad (4.14)$$

Mass conservation equation:

$$0 = \partial_t \mu_d + m^2\left[U_x + V_y\right] + m\partial_\eta (\Omega) \quad (4.15)$$

Geopotential equation:

$$0 = \partial_t \phi + \mu_d^{-1}\left[m^2\left(U\phi_x + V\phi_y\right) + m\Omega\phi_\eta - gW\right] \quad (4.16)$$

Conservation equation for scalars:

$$F_{Q_m} = \partial_t Q_m + m^2\left[\partial_x (Uq_m) + \partial_y (Vq_m)\right] + m\partial_\eta (\Omega q_m) \quad (4.17)$$

with the redefined momentum variables as

$U = \mu_d u/m \quad V = \mu_d v/m \quad W = \mu_d w/m \quad \Omega = \mu_d \dot{\eta}/m$

where $m = \dfrac{(\Delta x, \Delta y)}{distance\_on\_earth}$ (4.18)

The left-hand-side terms of the momentum equations (4.11)-(4.13) contain the Coriolis and curvature terms along with mixing terms and physical forcing.

To reduce the truncation errors in the horizontal pressure gradient calculations in the discrete solver, the governing equations are rewritten using perturbation variables, using $p = \bar{p}(z) = p'$, $\phi = \bar{\phi}(z) = \phi'$, $\alpha = \bar{\alpha}(z) = \alpha'$, and $\mu_d = \bar{\mu}_d(x,y) = \mu_d'$

The equations (4.11)-(4.17), rewritten in perturbation variables together with the diagnostic relation for the full pressure (vapour plus dry air);

$$p = p_0\left(R_d \theta_m / p_0 \alpha_d\right)^\gamma \quad (4.19)$$

represents the equations solved in the ARW.

5 Statistics

The forecast skill of the WRF/CMAQ air quality modeling system have been evaluated using the statistical parameters; the Pearson product-moment coefficient of linear correlation, the unpaired peak prediction accuracy, the root mean square error, and the gross error. All statistical measures are here presented in the context of evaluation of forecasts and the formulas used have been reproduced from earlier research [Delle Monache et al.] and literature [Wilks].

The notations used in this chapter are the following;

$C_o(t)$= The observed 1-hour averaged concentration at hour t.
$C_p(t)$= The predicted 1-hour averaged concentration at hour t.
$C_o(d)_{max}$= The observed maximum concentration during day d.
$C_p(d)_{max}$= The predicted maximum concentration during day d.
$\overline{C_o(t)}$= The average of the 1-hour averaged observed concentrations during the period.
$\overline{C_p(t)}$= The average of the 1-hour averaged predicted concentrations during the period.
N_{hour} = The number of 1-hour average concentrations over the period.
N_{day} = The number of days over the period.

5.1 The Pearson product-moment coefficient of linear correlation

This coefficient is also known as the "linear correlation coefficient" and it is a measure of how well a linear equation describes the relation between two variables X and Y measured on the same object. A single-value measure of association is obtained by the ratio of the covariance of the two variables to the product of the two standard deviations.

Definition.

$$Correlation(station) = \frac{\sum_{t=1}^{N_{hour}} \left\{ \left[C_o(t, station) - \overline{C_o(station)} \right] \left[C_p(t, station) - \overline{C_p(station)} \right] \right\}}{\sqrt{\sum_{t=1}^{N_{hour}} \left[C_o(t, station) - \overline{C_o(station)} \right]^2 \sum_{t=1}^{N_{hour}} \left[C_p(t, station) - \overline{C_p(station)} \right]^2}}$$

Since the denominator is always positive, it acts as a scaling constant. Thus, the Pearson correlation coefficient is a non-dimensionalized covariance.

The Pearson correlation coefficient is bounded by -1 and 1, i.e. $-1 \le r_{xy} \le 1$

If $r_{xy} = -1$ or $r_{xy} = +1$, then there is a perfectly linear association between the variables x and y. If $r = 0$, then the two variables x and y is not associated or correlated at all.

5.2 The unpaired peak prediction accuracy (UPPA)

The unpaired peak prediction accuracy (UPPA) measures the ability of predicting the maximum value of the variable x in a certain spot during a time period (for example one day). This test handles both the magnitude of the peak and the timing.

Definition. $$UPPA(station) = \frac{1}{N_d} \sum_{d=1}^{N_{day}} \frac{\left| C_p(d, station)_{\max} - C_o(d, station)_{\max} \right|}{C_o(d, station)_{\max}}$$

The unit is an error percent.

5.3 The root mean square error (RMSE)

The root mean square error (RMSE) gives a measure of the error magnitude when trying to predict the value of a variable x.

Definition. $$RMSE(station) = \sqrt{\frac{1}{N_{hour}} \sum_{t=1}^{N_{hour}} \left[C_p(t, station) - C_o(t, station) \right]^2}$$

The unit is the same as the forecast variable.

5.4 The gross error

The gross error gives a good hint about the forecast performance at higher concentration values. Since these higher values are important regarding health-issues, it is of great interest to evaluate the forecast at those concentrations.

Definition. $$gross\,\Diamond error(station) = \frac{1}{N_{hour}} \sum_{t=1}^{N_{hour}} \frac{\left| C_p(t, station) - C_o(t, station) \right|}{C_o(t, station)}$$

The gross error gives information about the error magnitude, just as the root mean square error, but as a portion of the concentration, and hence the unit is in percent.

6 Data

This study examines the ozone and nitrogen dioxide concentration in the Lower Fraser Valley during four days in the spring 2006. The time period of interest is 00 UTC 15/5 – 23.59 UTC 18/5 (local time 5pm 14/5 – 2.59 pm 18/5).

6.1 The observed data

The control data of the hourly concentrations of ozone and nitrogen dioxide data was provided by the Emergency Weather Net Canada and came from five weather stations situated in the Lower Fraser Valley; Vancouver airport, Langley central, Central Abbotsford, Chilliwack airport, and Hope Airport. Temperature data for the period has also been collected from this database. The data is stored and visualized by the Geophysical Disaster Computational Fluid Dynamics Centre at the University of British Columbia. The data is real-time weather information and the mainly purpose of the Emergency Weather Net Canada is to provide planners, emergency managers and disaster relief efforts with local weather information.

Fig 6.1 The five stations where real data is collected from the Emergency Weather Net. From left to right: Vancouver Airport – Langley central – Central Abbotsford – Chilliwack Airport – Hope Airport.

The Langley weather station breaks down at 05.00 UTC 15/5 and returns zero values during the rest of the period, therefore, the Langley central station is excluded from the database. Further, in the concentration data where the instruments return zero values, obviously due to

missing recordings, proper values are interpolated from the values the hours before and after the missing values.
The weather stations are situated from west to east in the following order: Vancouver airport – Langley central – Central Abbotsford – Chilliwack airport – Hope airport.
The concentration data used in this study can be found in appendix B.
Also, some meteorological observations data was used to investigate the modelled ozone concentrations more properly. The solar radiation data was provided by the Greater Vancouver Regional District (GVRD), and the wind and cloud data was gathered from the Environmental Canada website "Weatheroffice".

6.2 The WRF/CMAQ air quality output

The modelled data of the ozone, O_3 and nitrogen dioxide, NO_2 concentrations is computed with the Models-3 CMAQ modelling system together with emissions data from the RWDI (Rowan Williams Davies & Irwin inc.), and meteorology data from the Weather Research and Forecasting model, WRF.
The WRF model needed to be run in a different projection than the WRF model in operational use at UBC, why a special run was prepared for this thesis. The WRF model was started on the 1st of May, and it was therefore given a very short spin-up time before distributing data to the WRF/CMAQ model. The WRF/CMAQ model was set up to run for 14 days in May, 2006 and data was collected for 15/5, 16/5, 17/5 and 18/5, giving the model a spin-up time of 10 days.

This WRF/CMAQ air quality output is a 3-dimensional gridded datafile and for comparing this data with the real data from the emergency weather net data, data from the four places (Langley is not evaluated due to missing recordings in real data) in the Lower Fraser Valley is extracted from the model output using MATLAB. The four stations; Vancouver airport, Central Abbotsford, Chilliwack airport and Hope is recovered using their coordinates and the modelled concentration of ozone and nitrogen dioxide are extracted for the stations in the lowest model layer. Example surface plot can be viewed in appendix D.

6.3 The synoptic situation during the episode of study; analyses and satellite images

The analysis of the synoptic weather situation covers two days before and the four days during the study. This approach is for getting to know how the weather situation has developed not only during the study, but also until the period of study.
The analysis data contains;

- The ETA analysis of the 850hPa temperature (C), relative humidity (%), and wind (m/s). For example, see appendix E:1 [COLA (web)].
- The ETA analysis of the geopotential heights, and the vorticity. For example, see appendix E:2 [COLA (web)].
- The ETA analysis of the 200hPa streamlines and isotachs (m/s). For example, see appendix E:3 [COLA (web)].
- The Environment Canada analysis of the 500hPa. For example, see appendix E:4 [Environment Canada (web)].
- Satellite images for IR data, visible data and water vapour data. For example, see appendix E:5 [WW2010 (web)].
- Surface analysis from NOAA National Weather Service (2 days) and Environment Canada (4 days) For example, see appendix E:6 [NOAA (web), Environment Canada (web)].

7 Results and Analysis

7.1 Synoptic conditions

The weather situation two days before the episode of study:
At the surface, a high-pressure ridge of warm air is developing over the western parts of North America. The ridge is moving into the southwestern parts of Canada and is gaining strength during the period, resulting in higher temperatures. A low-pressure system is weakening while heading east, moving from the west coast of BC towards the interior of Canada. The winds over British Columbia are weak, and disoriented.
In the upper-level atmosphere, the BC is situated between a ridge and a coming trough, and the upper-level flow is therefore south-south westerly and quite strong over the research area. There are positive vorticity to the north and negative vorticity to the south of the research area, but the negative vorticity is spreading during the period, giving the area a negative, high pressure enhancing touch.

The weather situation during the episode of study:
At the surface, the high-pressure ridge with weak winds is spreading north, covering greater parts of western Canada. A low-pressure system with stronger winds is developing in the eastern Pacific Ocean, outside the coast of BC. During the four-day period, this low-pressure system is moving closer to BC, bringing more humid air towards the research area. In the end of the episode, the high-pressure ridge is withdrawing and the temperature is decreasing.
In the upper-level atmosphere, the ridge over western North America is slowly moving eastwards as the trough over the northeast Pacific Ocean is closing in. The trough is weakening a bit during the episode while the ridge is maintaining its strength although withdrawing towards the US. The upper-level flow is turning from south south westerly to southwesterly. The vorticity is negative throughout the period but the positive vorticity is moving in as the trough is closing up.

The satellite images for the period are confirming the high-pressure situation implicated by the analysis. During the whole period, several low-pressure systems are twisting over the Pacific Ocean. Dry air is travelling towards the Vancouver area, origination from 20 N and the area experiences almost no clouds, part from a few middle high clouds at the beginning of the period. At the end of the episode of study, more humid air is forcing in from the approaching low pressure systems over the Pacific Ocean together with a cloud cover connected to the lows.

7.2 Mesoscale conditions

The temperature in the Lower Fraser Valley during the four-day episode showed a pattern with both diurnal and spatial variation, Fig 7.1. Hope, which is situated in the inner parts of the valley, had the highest daily maximum temperatures with the first day as the warmest (32,8 C) and the following days with slightly decreasing temperatures. Night temperatures were between 11,7 C and 15,1 .

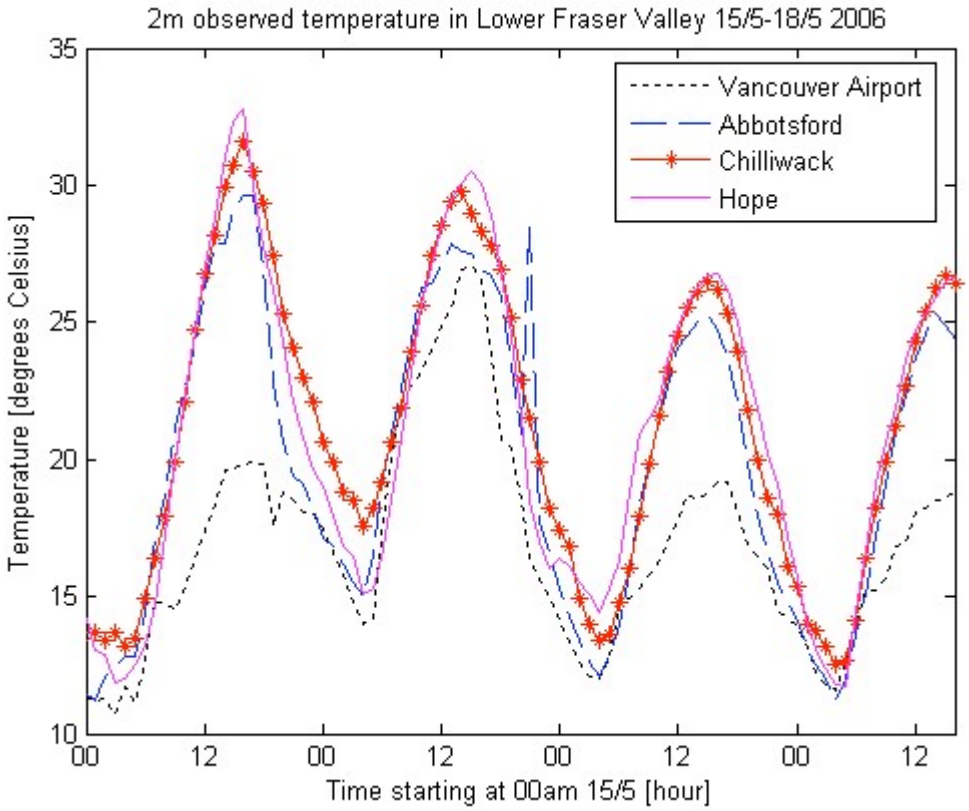

Fig 7.1: Observed 2-meter temperature in lower Fraser Valley 15/5-18/5. Dotted line is Vancouver Airport, broken line Central Abbotsford, line with stars Chilliwack Airport, and plain line is Hope Airport. Temperature is measured in degrees Celsius and time starts at 00 PDT (Pacific daylight Time) 15/5.

Vancouver Airport, situated close to the sea and hence in the outer parts of the valley had the lowest daily maximum temperatures, 6-12 C lower than the other stations every day, except for the second day when the temperature was just slightly lower than the other stations. Nightly minimum temperatures were among the lowest nightly temperatures for the stations, spanning between 10,7 C and 14 C.
Abbotsford and Chilliwack are all spatially situated in between Vancouver Airport and Hope. The highest daily temperatures in the Valley was as mentioned in Hope and the maximum temperatures were then falling towards the Pacific coast as can be seen in Fig 7.1, following the pattern of the Hope station with decreasing temperatures throughout the four day episode. Maximum and minimum temperature data can be found in appendix F.

The existence of a possible sea breeze during daytime or a land breeze during night time can be found in Fig. 7.14, chapter 7.9.4. The top graph shows the observed wind direction and the bottom graph shows the observed wind speed at Vancouver airport during the period 15/5-18/5 2006. Observed data from the Vancouver airport station is visualized with a plain line in both graphs.
The westerly winds during daytime and easterly winds during night time day two, three and four are part of a sea- and land breeze circulation. Wind speeds are also largest during daytime with very weak winds at night. Additional observed data for the other three stations is not available.

7.3 Observed data from the Emergency Weather Net

The temporal distribution of nitrogen dioxide is following a diurnal pattern, Fig 7.2. Peak concentrations are found in the evening and night at all stations, and lowest concentrations are

found in the morning and during lunchtime. For two of the stations situated in the inner parts of the valley, Chilliwack airport and Hope airport, the temporal variations are very small in the beginning of the episode, with low peak concentrations during the second night, 15-16/5.

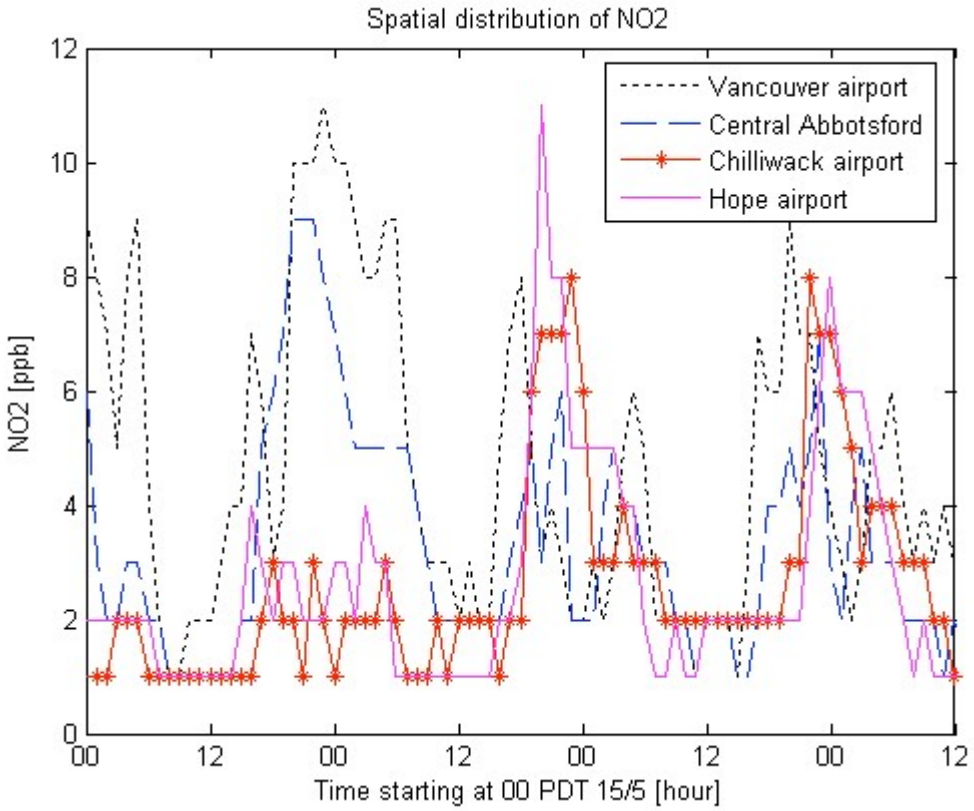

Fig 7.2: Spatial distribution of nitrogen dioxide in Lower Fraser Valley. Nitrogen dioxide concentration is measured in parts per million (ppm) and the graph shows 4 consecutive days in May, 2006(15/5-18/5). Dotted line is Vancouver Airport, broken line Central Abbotsford, line with stars Chilliwack Airport, and plain line is Hope Airport. Time on graph is measured in PDT (Pacific Daylight Time).

The spatial distribution of nitrogen dioxide in Fig 7.2 is found to be quite complex and no particular spatial pattern can be found among the stations in the valley. During the first two nights of the episode, 14-15/5 and 15-16/5, the stations closer to the sea shows the highest peak concentrations. During the third night, 16-17/5, the highest peak concentrations are found in the inner parts of the valley and by the coast. During the fourth night, 17-18/5, the peak concentrations are almost equal in the valley.
After two nights of high nitrogen dioxide concentrations, 9-11 ppb, the Vancouver airport station and the Central Abbotsford station exhibits a dip around 00 PDT during the nights 16-17/ and 17-18/5 instead of a peak. Also, the two stations further inside the valley, Chilliwack airport and Hope airport, exhibits low nitrogen dioxide concentrations during the first two nights and higher concentrations during the last two nights.

To sum up, the Vancouver Airport station close to the sea exhibits high peak concentrations during the whole episode, although dips are present in the last two day's peaks. Hope airport and Chilliwack airport exhibits low peak concentrations in the beginning of the episode, and higher peak concentrations at the end of the episode. Central Abbotsford exhibits high peak concentrations in the beginning of the episode but they are dropping throughout the episode, Abbotsford also experiences similar dips in the peaks as Vancouver airport, during the last two days. Overall, the peak concentrations are dropping for all stations during the last night, 17-18/5.

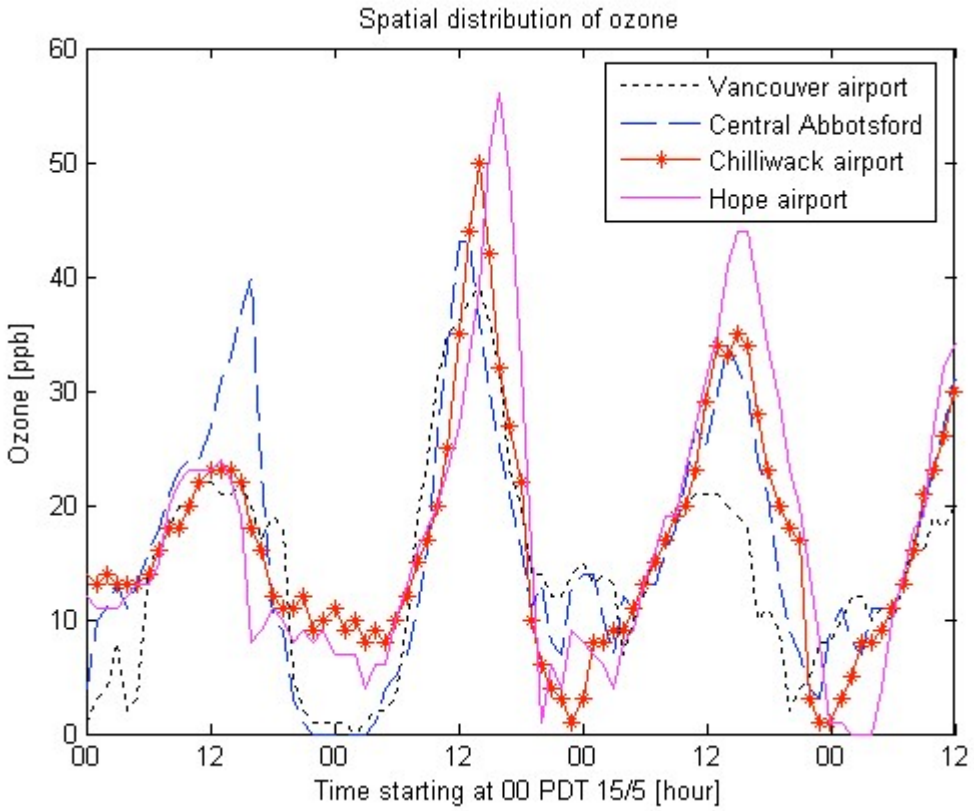

Fig 7.3: Spatial distribution of Ozone in Lower Fraser Valley. Ozone concentration is measured in 10^{-3}ppm and the graph shows four consecutive days in May, 2006 (15/5-18/5). Dotted line is Vancouver Airport, broken line Central Abbotsford, line with stars Chilliwack Airport, and plain line is Hope Airport. Time on graph is measured in PDT (Pacific Daylight Time).

The spatial distribution of ozone in Lower Fraser Valley varies during the four day episode in May, Fig 7.3. The inner parts of the valley had higher peak concentrations than the outer parts, closer to the sea. Hope, which is the station farthest inside the valley mostly had the highest peak ozone concentrations, followed by Chilliwack, Abbotsford and Vancouver Airport. The stations are all situated in the valley in this order, counting from Hope furthest inside the valley to Vancouver Airport by the coastline.
Observed data therefore shows a trend in the spatial distribution of ozone concentration in Lower Fraser Valley, where the highest concentrations during daytime are found furthest inside the valley and the lowest concentrations during daytime is found close to the coast. The circumstances are the opposite during night time, when Vancouver Airport shows slightly higher ozone concentrations than the stations situated farther inside the valley.

The ozone concentration in the lower atmosphere does not only show variations in the spatial distribution, but also variations in the temporal distribution, Fig 7.3. The temporal variation at the stations in the valley during the four day episode in May, 2006 is found to be as large as 55 ppb in one station (Hope at 17.00-21.00 16/5). The ozone concentrations are at their peak in the afternoon and drops to around zero during night time. The first day of the episode, all stations except Central Abbotsford shows low peak concentrations and the highest peak concentrations are measured in the afternoon 16/5 for all four stations, and decreasing the following days. The stations situated farthest inside the valley, Hope airport and Chilliwack airport are both exhibiting decreasing concentrations night time during the episode, while the other two stations, Vancouver airport and Central Abbotsford are exhibiting the opposite relation, with increasing concentrations night time.

7.4 Modelled nitrogen dioxide versus observed data

The nitrogen dioxide distribution in Lower Fraser Valley is shown in Fig 7.4. Observed data from the Emergency Weather Net (plain line) is compared with modelled data (line with stars) at four stations in the valley.

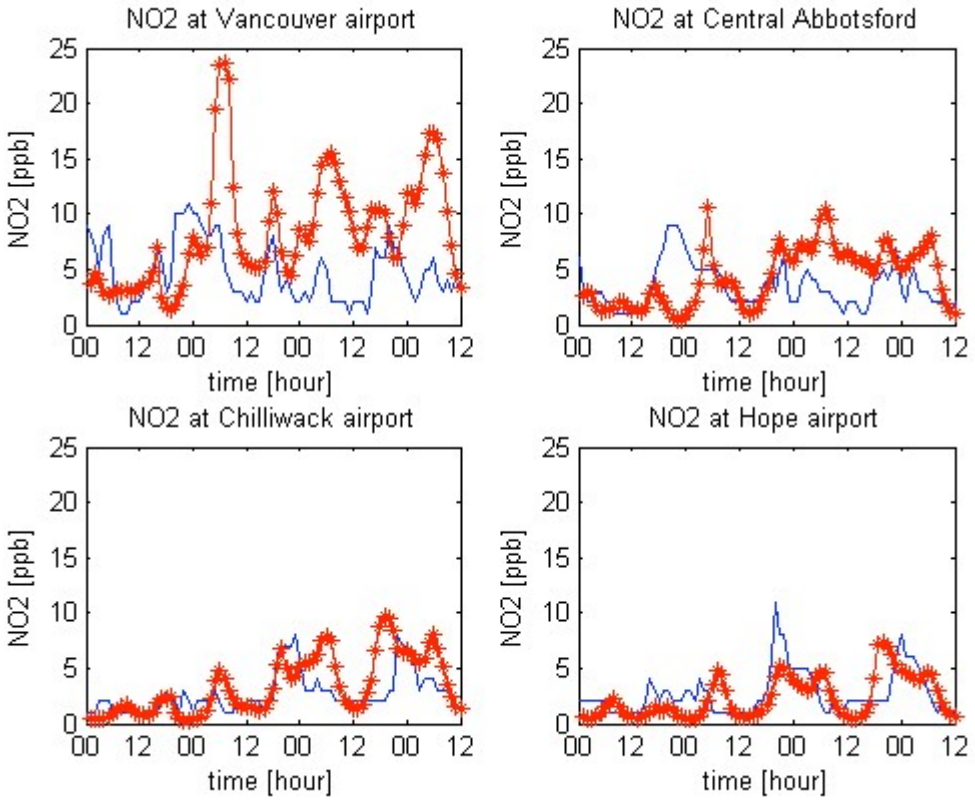

Fig 7.4: Distribution of nitrogen dioxide in Lower Fraser Valley. Line with stars marks the modelled nitrogen dioxide concentration, and the plain line marks the observed nitrogen dioxide concentration. Top left shows the nitrogen dioxide concentration at Vancouver Airport, top right Central Abbotsford, bottom left Chilliwack Airport and bottom right Hope Airport. Concentrations are measured in 10^{-3}ppm, and timeline starts at 00 PDT 15/5.

The WRF/CMAQ model has captured the magnitude of the real data well, except at Vancouver Airport, where the model overestimates the nitrogen dioxide concentration. The modelled nitrogen dioxide does not fit the real data curves very well at any of the four stations in this study. A vague diurnal pattern in the modelled data can be resolved from the bottom two figures, but the top figures shows no pronounced diurnal pattern.

7.5 Modelled ozone versus observed data

Modelled ozone concentration (line with stars) was compared to observed data from the Emergency Weather Net (plain line) at the four stations in the valley, Fig 7.5.
The modelled ozone concentration at the four stations where much higher than the observed data. The difference was between 0,020 ppm and 0.030 ppm during the whole period.

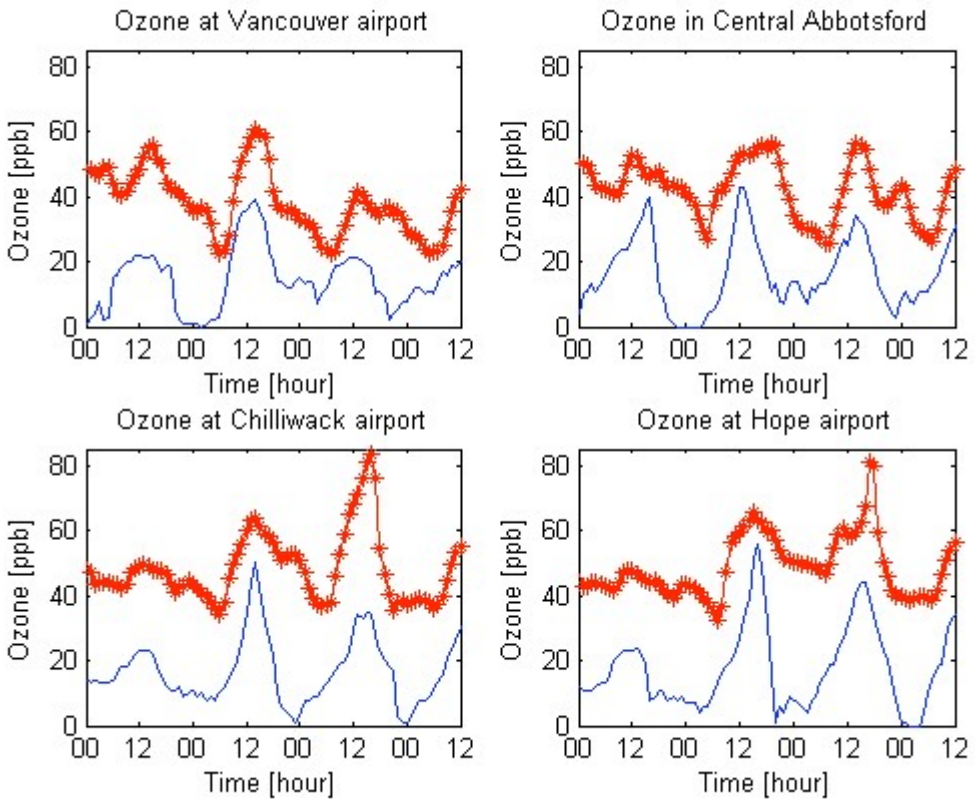

Fig 7.5: Distribution of ozone in Lower Fraser Valley. Line with stars marks the modelled ozone concentration, and the plain line marks the observed ozone concentration. Top left shows the ozone concentration at Vancouver Airport, top right Central Abbotsford, bottom left Chilliwack Airport and bottom right Hope Airport. Concentrations are measured in 10^{-3}ppm, and time starts at 00 PDT 15/5.

A diurnal variation can be found not only in the observed data, but also in modelled ozone concentration. Observed data gives the peak maximum concentrations on the second day at all stations, but modelled maximum concentrations peaks only on the second day at Vancouver Airport and slightly in Abbotsford. In Chilliwack and Hope, the modelled maximum ozone concentrations peak on the third day. Maximum concentrations occur on the same time for both the modelled ozone and the observed data, but modelled minimum concentrations is a few hours slow compared to the observed data.
The model shows a decreasing trend at Vancouver Airport during the four-day period, while at the other stations there is no increasing or decreasing trend (Abbotsford) or a slightly increasing trend in ozone concentrations.

7.6 Statistics

Linear correlation

Fig 7.6 shows the linear correlation of both ozone and nitrogen dioxide for the modelled dataset and the observed dataset.
Nitrogen dioxide correlation, line with stars in Figure 7.6, is overall very poor throughout the period. At Vancouver airport, the correlation is poor all period except during the first six hours 15/5. The nitrogen dioxide correlation is acceptable first day in Abbotsford, otherwise very poor. In Chilliwack and Hope, the nitrogen dioxide correlation is very poor during the first two days, but acceptable during the last two days.

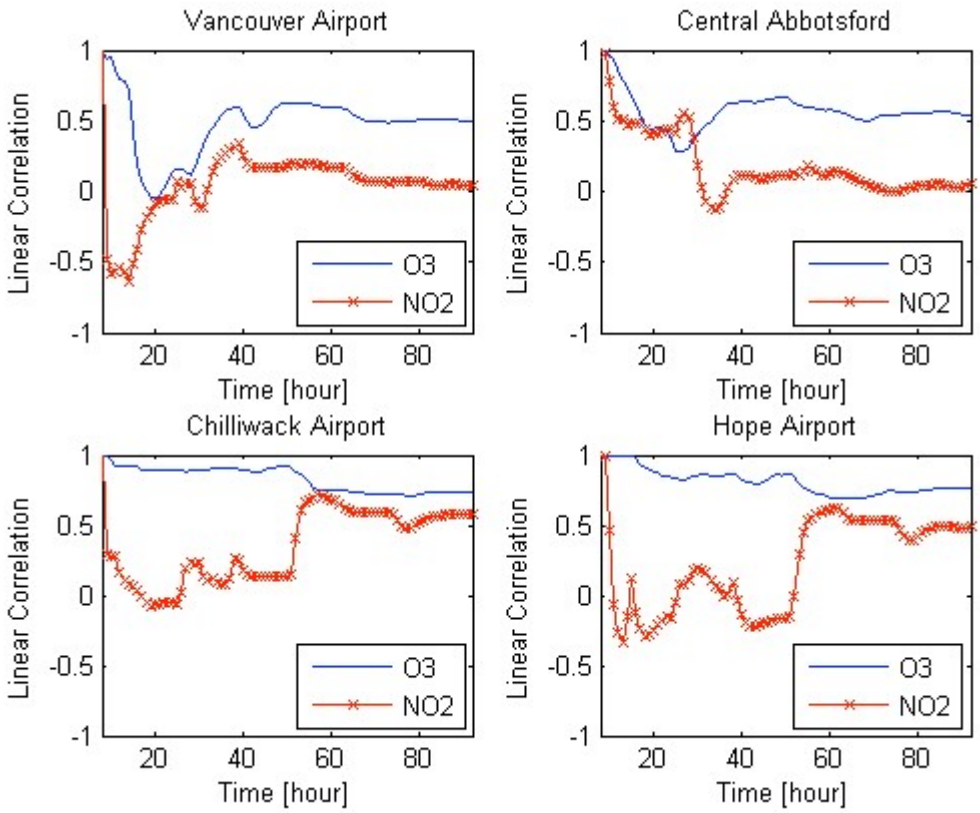

Fig 7.6: Linear Correlation for ozone and nitrogen dioxide at four stations in Lower Fraser Valley. Blue line marks ozone correlation, and the red line marks nitrogen dioxide correlation. Linear correlation is between –1 and 1, with –1 and 1 meaning perfect correlation and 0 meaning no correlation. Time starts at 00 PDT 15/5.

The plain line in Fig 7.6 represents the ozone correlation. The best correlation is found at the two stations furthest inside the valley, Chilliwack and Hope. At Vancouver airport, the correlation is very poor during the first day, but is improved to an acceptable level during the rest of the study. The ozone correlation in Abbotsford is acceptable during the whole period, and in Chilliwack and Hope, the correlation is good throughout the period.

Root mean square error

The root mean square error for the modelled and real datasets is investigated for both ozone and nitrogen dioxide. Fig 7.7 shows the error distribution and its development in time for the two pollutants.

The root mean square error (RMSE) is a measurement of the magnitude of the error of a predicted variable. This error is very high for ozone, around 25 to 30 ppb throughout the study for all stations, top graph in Fig 7.7.

The RMSE for nitrogen dioxide is overall much better for all stations. Best agreement with observed data had Chilliwack and Hope with a maximum RMSE of 2 ppb. The station closer to the coast, Vancouver airport and Abbotsford, had higher errors, but still acceptable.

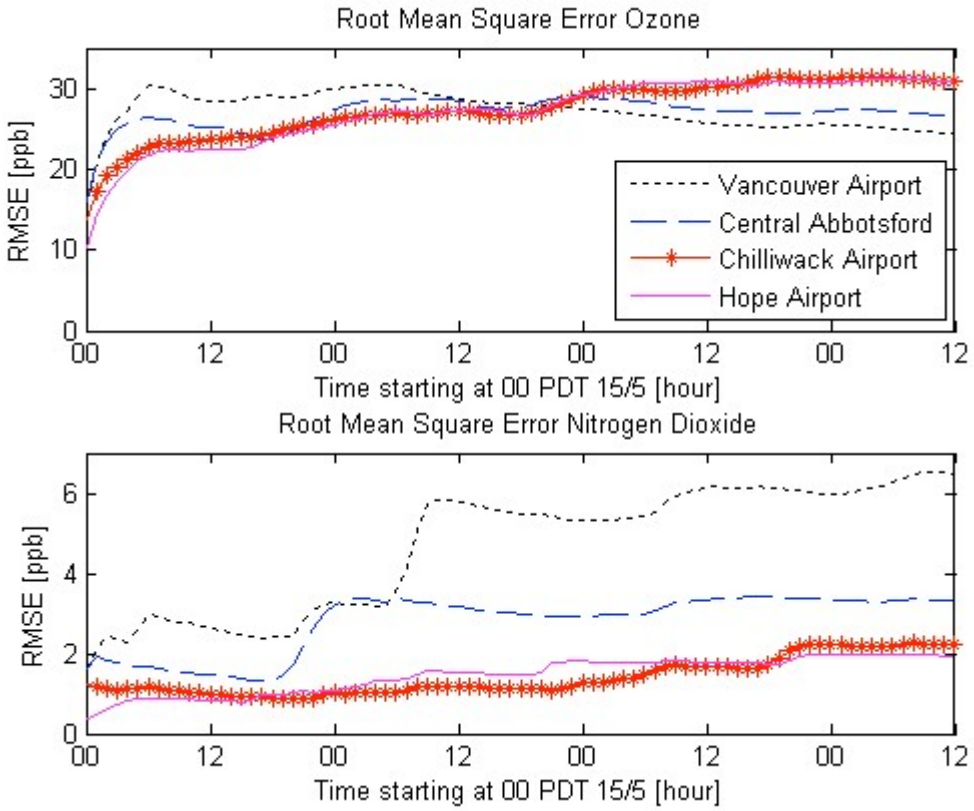

Fig 7.7: Root mean square error (RMSE) for ozone and nitrogen dioxide at four stations in Lower Fraser Valley. Top graph shows RMSE for ozone and bottom graph shows RMSE for nitrogen dioxide. The legend in top graph is suitable for bottom graph as well. RMSE is a magnitude of the error of prediction, measured in 10^{-3}ppm Time starts at 00 PDT 15/5.

Gross error

Fig 7.8 shows the development of the gross error for both ozone and nitrogen dioxide of the modelled and observed datasets.

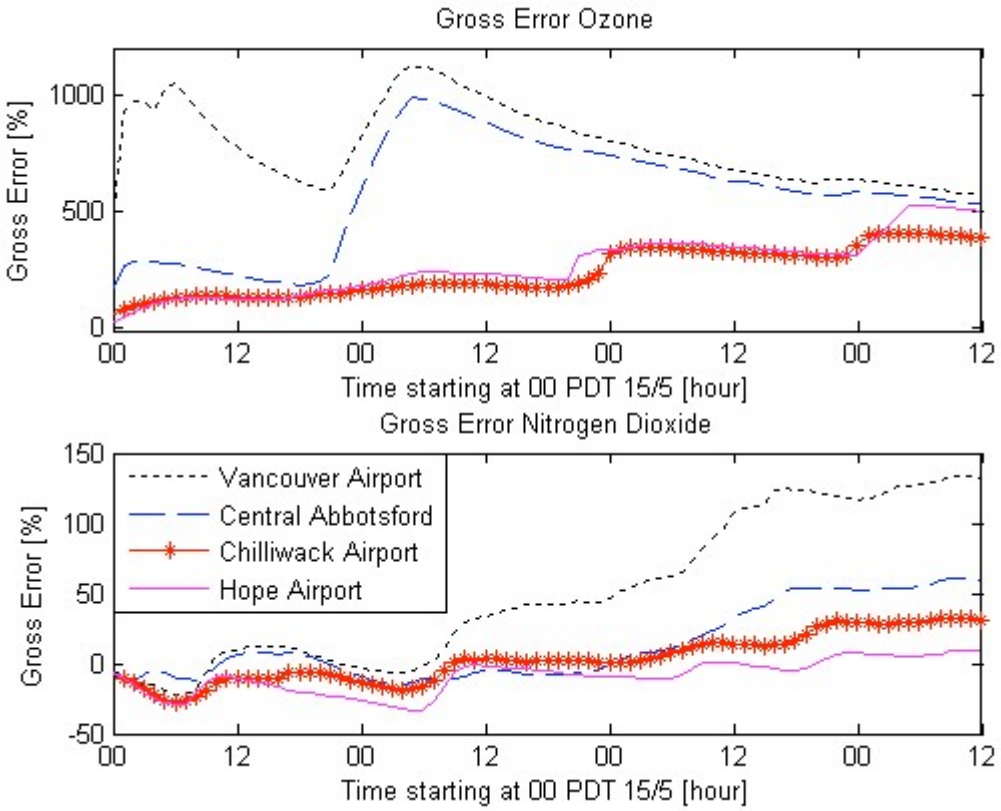

Fig 7.8: Gross error for ozone and nitrogen dioxide at four stations in Lower Fraser Valley. Top graph shows gross error for ozone and bottom graph shows gross error for nitrogen dioxide. The legend in bottom graph is suitable for top graph as well. Gross error is the magnitude of the error of prediction, measured in percent, %. Time starts at 00 PDT 15/5.

The gross error is a measure of the error magnitude in percent. Acceptable values for the gross error of a forecasting dataset are between ± 30% and ± 35%. The gross error for the modelled ozone compared to observed data is far from good. The "best" error is again found in Chilliwack and Hope, but these errors are still much higher than the acceptable values.

The gross error for nitrogen dioxide (bottom graph, Fig 7.8) shows better results than for ozone. For the two stations furthest inside the valley, the errors are acceptable nearly throughout the whole period. The error in Abbotsford is acceptable during the first two days, but the error grows and is not acceptable during the last two days. Vancouver airport shows very poor results during the last three days, but the error is acceptable during the first day, 15/5.

Unpaired peak prediction

The unpaired peak prediction accuracy (UPPA) measures the model´s ability to predicting the maximum value of the variable in a certain spot during a time period. Table 7.1 shows the results of the UPPA at each station during every day of the period and also as a mean of the four-day period.

Table 7.1: Unpaired peak prediction accuracy (UPPA) for ozone and nitrogendioxide. Modelled concentrations are compared to real concentrations collected from the Emergency Weather Net. UPPA is computed once a day for both species, and a mean value for the four-day period.

Unpaired Peak Prediction Accuracy

Ozone	Vancouver Airport	Central Abbotsford	Chilliwack Airport	Hope Airport
15/5	153,10%	31,39%	117,36%	99,39%
16/5	56,22%	30,57%	27,07%	16,84%
17/5	98,57%	65,29%	138,20%	84,47%
18/5	104,46%	62,20%	65,94%	51,65%
Mean	103,09%	47,36%	87,12%	63,09%

Nitrogen dioxide	Vancouver Airport	Central Abbotsford	Chilliwack Airport	Hope Airport
15/5	-29,83%	-61,62%	-49,68%	-45,09%
16/5	115,58%	31,74%	-3,43%	-52,86%
17/5	72,12%	109,14%	21,82%	48,15%
18/5	188,57%	14,12%	14,86%	-33,60%
Mean	86,61%	23,34%	-4,11%	-20,85%

Acceptable values of the unpaired peak prediction accuracy of a forecasting dataset are between ± 15% and ± 20%. As can be seen in the table, none of the stations except the Hope station day two, delivers acceptable values for ozone. The second day is the best predicted peak for every station, with an error between 16,84% and 56,22%. As for the nitrogen dioxide concentrations, Chilliwack is the station that best predicts the peaks having three out of four days with acceptable values. Central Abbotsford also has one day, the last day, with acceptable values. No day is particularly well predicted for all stations.

To sum up, the modelled concentrations agrees poorly with the observed dataset. Modelled ozone concentrations are quite well correlated with observed data, but both the root mean square error and the gross error are not acceptable. Also, the unpaired peak prediction accuracy did not present acceptable values.
The modelled nitrogen dioxide concentrations failed in correlation with observed data, only for two of the stations, the correlation was acceptable the last two days. During the whole study the root mean square error and the gross error were acceptable for the same two stations, Chilliwack and Hope. The RMSE and gross error was ok at Vancouver airport during the first day, but not the rest of the period. Abbotsford had acceptable values for the same errors during the first two days. Chilliwack had the best unpaired peak prediction accuracy among the stations with two, almost three peaks having acceptable values. Central Abbotsford had acceptable UPPA's during day four.

Visually, the modelled ozone concentration is much higher than observed values, and the errors would naturally be big here, Fig 7.5. Modelled nitrogen dioxide concentrations on the other hand are ok in magnitude but not well modelled compared to observed data, Fig 7.4. To evaluate if the model just overestimates ozone by a factor X, the modelled ozone is now manipulated by removing a certain amount of the ozone concentrations. The same statistics tests as above are then computed on the new manipulated dataset to find out if the error results improve.

7.7 Manipulated modelled ozone

The modelled ozone was manipulated to better fit the observed data at the four different stations in Lower Fraser Valley, Fig 7.9. The modelled ozone was diminished with 24 ppb at all stations.

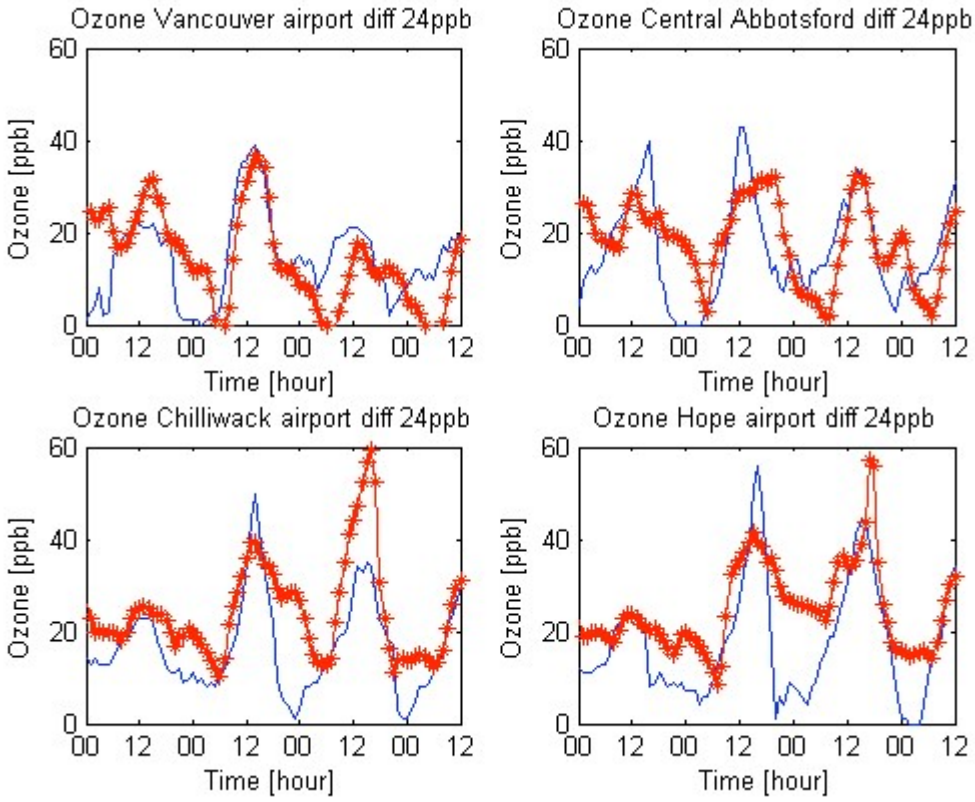

Fig 7.9: Manipulated distribution of ozone versus observed data. Line with stars marks the manipulated modelled ozone concentration, and the plain line marks the real ozone concentration. Top left shows the ozone concentration at Vancouver Airport, top right Central Abbotsford, bottom left Chilliwack Airport and bottom right Hope Airport. Concentrations are measured in 10^3ppm, and timeline starts at 00 PDT 15/5.

The manipulated ozone concentration fits the observed ozone concentration much better when 24 ppb is removed from all data. The concentration at Vancouver airport is well forecasted, especially from day two and forward. The manipulated concentrations in Central Abbotsford are a bit low during the first two days, but the last two days, the forecast captures the peak concentrations very well. Both the model data and the observed data give us the second day as the day with the highest ozone concentrations at Vancouver airport and Central Abbotsford. The forecasts for Chilliwack and Hope predict the third day to have the highest ozone concentrations, although in the reality, the second day has the highest concentrations. The manipulated concentrations simulate the second day to have lower concentrations than in reality.

To sum up, the diurnal variation and the timing in peaks is predicted well by the WRF/CMAQ model, and the overall magnitude fits the observed curve reasonable well, only the nightly dips in concentration agrees poorly in time. For the two stations furthest inside the valley, Chilliwack and Hope the nightly dips agrees very poorly also in magnitude.

7.8 Statistics manipulated ozone

The same four statistics tests used above in this study to evaluate the modelled concentrations of nitrogen dioxide and ozone, where also used to evaluate the manipulated ozone concentrations. Fig 7.10 shows the results from linear correlation, root mean square error and gross error when comparing the manipulated dataset to the observed dataset.

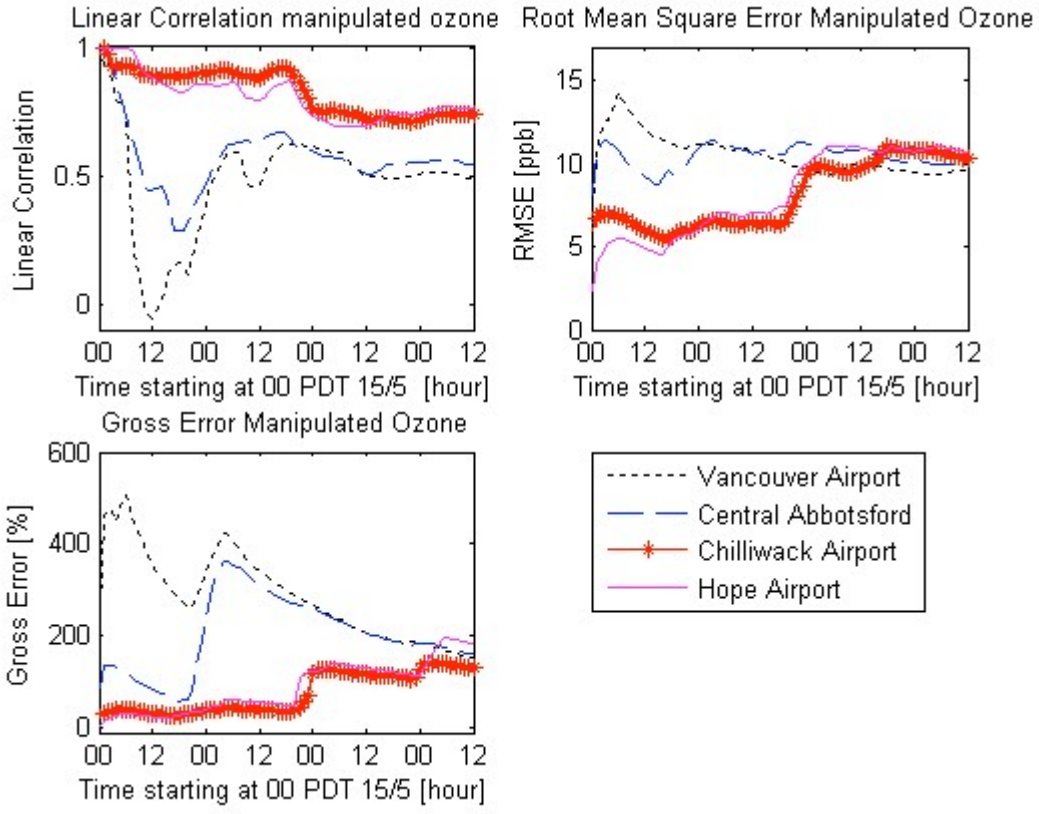

Fig 7.10: Statistics for the manipulated ozone concentrations. Top left graph shows the linear correlation, top right graph shows the root mean square error and bottom left graph shows the gross error for the manipulated and observed datasets. Dotted line is Vancouver Airport, broken line Central Abbotsford, line with stars Chilliwack Airport, and plain line is Hope Airport. Time on graph is measured in PDT (Pacific Daylight Time).

The *linear correlation* result for the manipulated dataset, top left graph in Fig 7.10, is the same as the result for the true modelled ozone concentration, see Fig 7.6. This since the manipulation made to the modelled dataset was just to subtract the modelled concentrations with a factor. The manipulation doesn't change the linear correlation of the dataset. Again, the correlation at Vancouver airport is very poor during the first day, but is improved to an acceptable level during the rest of the study. The correlation in Abbotsford is acceptable during the whole period, and in Chilliwack and Hope, the correlation is good throughout the period.

The *root mean square error* (RMSE), top right graph in Fig 7.10, is diminished by 60% to 80% for all four stations, due to the manipulation. The error is now between 5 –12 ppb throughout the period, with the lowest values during the first two days in Chilliwack and Hope. The RMSE is pending around 10 ppb throughout the period at Vancouver airport and Abbotsford, and also during the last two days in Chilliwack and Hope.

The *gross error*, bottom left graph in fig 7.10, is also strongly improved for the manipulated dataset compared to the true modelled dataset. Acceptable values for the gross error of a forecasting dataset are between ± 30% and ± 35%. The Chilliwack and Hope stations are experiences such low error values during the first two days of study. During the second day's evening, both stations record a rapid degeneration of the error, and during the rest of the

period the error is growing towards 130% and 170% respectively. The gross error at Vancouver airport and Central Abbotsford is not close to acceptable although it is has improved. The gross error has improved by 50% to 80% for all four stations due to the manipulation.

The *unpaired peak prediction accuracy* is the fourth statistics test, measuring the accuracy of the predicted peaks in the dataset. This test was also expected to improve, since it not only measures the timing of the peaks, but also the agreement of the magnitude of concentration at the peaks. Table 7.2 shows the results from the test when manipulated modelled ozone concentrations were compared to observed ozone concentrations.

Table 7.2: Unpaired peak prediction accuracy (UPPA) for manipulated ozone. Adjusted modelled concentrations are compared to observed concentrations collected from the Emergency Weather Net. UPPA is computed once a day, and a mean value for the four-day period is also calculated.

Unpaired Peak Prediction Accuracy

Manipulated Ozone	Vancouver Airport	Central Abbotsford	Chilliwack Airport	Hope Airport
15/5	44,01%	-28,61%	13,01%	-0,61%
16/5	-5,32%	-25,24%	-20,93%	-26,01%
17/5	-15,71%	5,30%	69,63%	29,93%
18/5	-9,83%	-15,22%	-2,73%	-9,89%
Total	3,29%	-18,59%	14,74%	-1,65%

As mentioned in chapter 7.6, acceptable values of the unpaired peak prediction accuracy (UPPA) of a forecasting dataset are between ± 15% and ± 20%. As can be seen in Table 7.2, these requirements are met as mean values for all four stations. Also, the majority of the daily tests are passing these requirements. At Vancouver airport and Chilliwack airport, three out of four days have acceptable values. And in Central Abbotsford and Hope airport, two out of four days shows acceptable values.

To sum up, the linear correlation of the manipulated and observed datasets did not improve, but the correlation already had acceptable values throughout the period (except for Vancouver airport during the first day). Both the root mean square error (RMSE) and gross error was improved by a large percent, due to very large errors in magnitude for the true modelled dataset. These large errors were diminished by the subtraction of 24 ppb ozone from the true modelled dataset. The RMSE is improved to between 5 and 12 ppb at all stations with the lowest values in Chilliwack and Hope during the first two days. The gross error has improved, but only two stations, Chilliwack and Hope shows acceptable values during the first two days of the study. The unpaired peak prediction accuracy met the requirements of an acceptable forecasting dataset in 62,5% of the peaks, and 87,5% of the peaks were in the range of ± 30% accuracy.

7.9 Overestimated ozone

The modelled ozone concentrations and the observed ozone concentrations differed with between 20 and 30 ppb, the modelled concentrations where larger than the observed data. To find out why the WRF/CMAQ model overestimated the ozone, several parameters from the WRF model, affecting the ozone was investigated. These parameters are the temperature (which has been compared to observed data from the four stations in the area of investigation), the solar radiation, the height of the mixing layer, and the winds.

7.9.1 Temperature

The hourly temperature at the four stations; Vancouver Airport, Abbotsford, Chilliwack and Hope, was compared to the 2 meter hourly temperature from the WRF model. The comparison is shown in Fig 7.11 below.

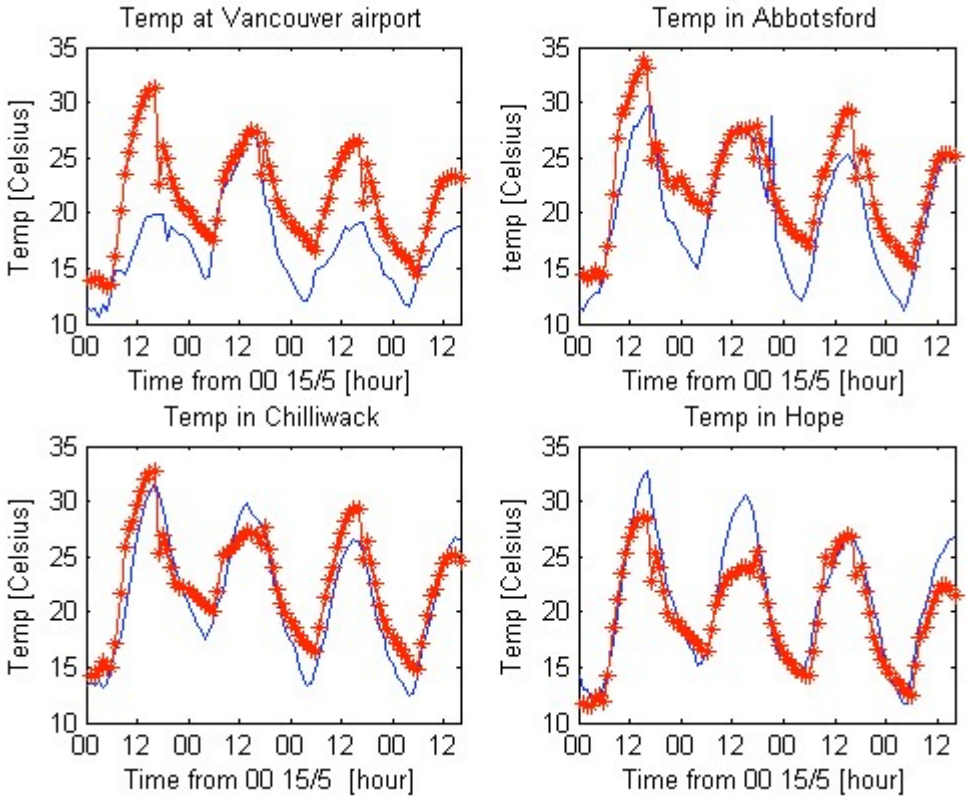

Fig 7.11: Observed temperature versus modelled temperature in Lower Fraser Valley. Top left shows the temperature at Vancouver Airport, top right Central Abbotsford, bottom left Chilliwack Airport and bottom right Hope Airport. Line with stars marks the modelled temperature from WRF, and plain line marks the observed temperature. Temperature is measured in degrees Celsius, and timeline starts at 00 PDT15/5.

The model overestimates the temperature at the stations closest to the coast, Vancouver Airport and Central Abbotsford, on three out of four days. Both maximum and minimum temperatures are overestimated. The maximum temperature is well predicted at both stations on the second day, 16/5. The model best captures the real temperature in Chilliwack, even though the minimum temperatures are modelled too high. The model underestimates the maximum temperatures, but captures the minimum temperatures well in Hope.
The four-day trend of falling daily maximum and minimum temperatures is captured well at all four stations, as well as the diurnal variation. The maximum temperatures are reproduces well in time by the model, but the model's minimum temperatures are captured later than the observed data.

7.9.2 Solar radiation

Solar radiation data from the WRF model and radiation data from the Greater Vancouver Regional District database is illustrated in Fig 7.12. The observed solar radiation shows a diurnal rhythm with peak values of approximately 800-820 W/m^2. The modelled solar radiation data also shows a diurnal rhythm, but peak values are approximately 900 W/m^2. Peaks are occurring around lunchtime local time for both datasets. The dip in modelled radiation data around 16.00 local time is due to inconsistency in data when the meteorology data files are changing days (~00 UTC).

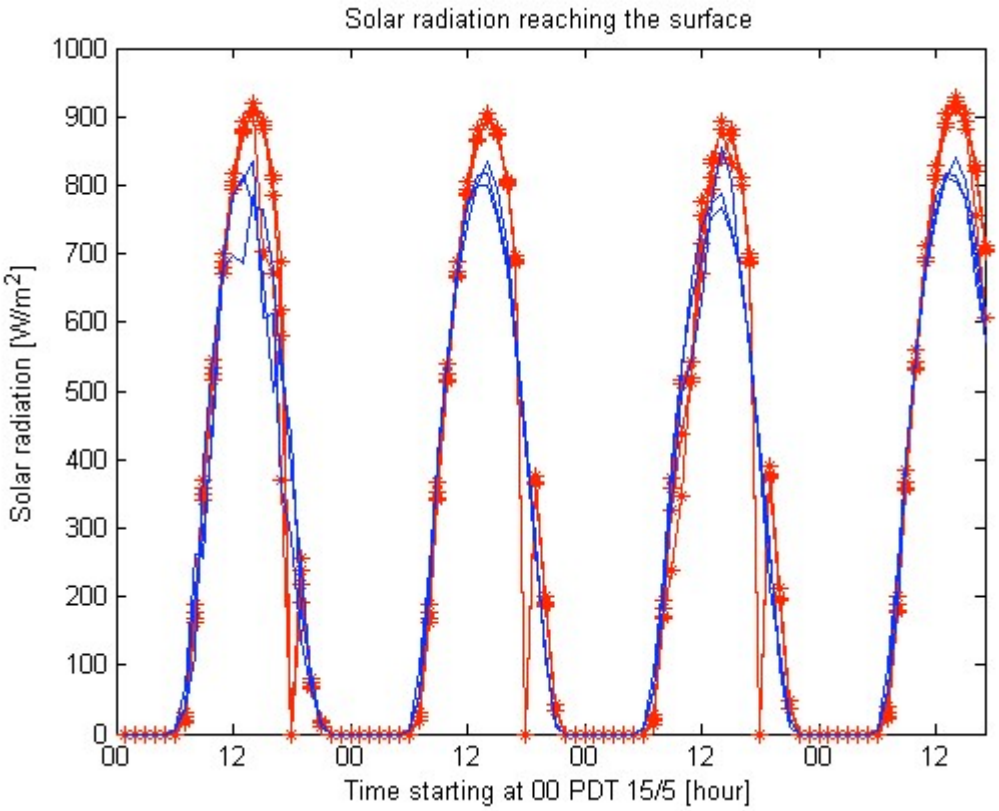

Fig 7.12: Solar radiation reaching the surface during four consecutive days, 15/5-18/5. The graph shows the solar radiation measured in Watts per square meter for four stations within the Lower Fraser Valley. Plain blue line marks the observed radiation data and red line with stars marks the modelled radiation data. Time starting at 00 PDT 15/5.

7.9.3 Cloud coverage

The cloud cover at Vancouver airport during the period is shown in Fig 7.13. Top graph describes the observed cloud cover from the Weatheroffice, Environment Canada, and bottom graph describes the modelled cloud cover from the WRF model.
The WRF model clearly underestimates the cloud cover at Vancouver airport, as easily can be seen from Fig 7.13. While observed data very seldom reports “clear skies”, the model reports “clear skies” often, especially during day two, three, and day four. The modelled cloud cover never reports “cloudy”, and it reports “mostly cloudy” only three times during the whole period. Observations more frequently report “mostly cloudy” or “cloudy”, Fig 7.13 top graph.

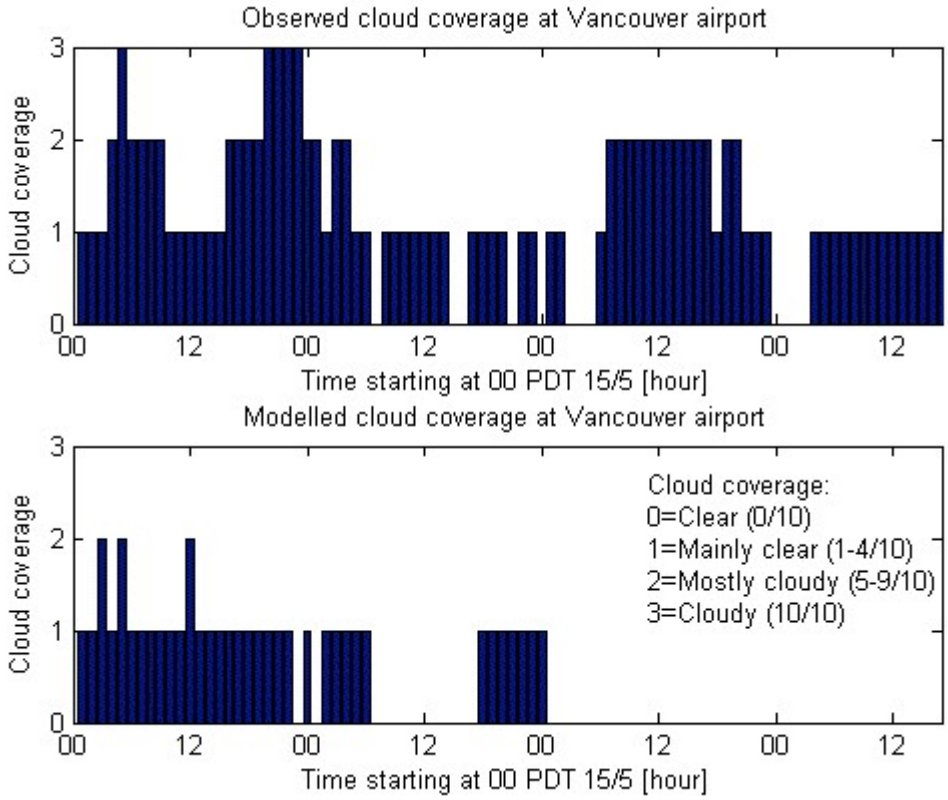

Fig 7.13: Observed and modelled cloud coverage at Vancouver airport 15/5-18/5. Top graph shows the observed cloud coverage and bottom graph shows the modelled cloud coverage. On the Y-axis: 0 means clear skies and 0/10 cloud cover, 1 means mainly clear skies and 1-4/10 cloud cover, 2 means mostly cloudy and 5-9/10, and 3 means cloudy and 10/10 cloud cover.

7.9.4 Winds

Fig 7.14 shows the observed wind direction and wind speed compared to the wind direction and wind speed modelled by WRF at Vancouver airport.

The observed winds were weak, varying between 0 and 7 m/s, with a pronounced diurnal rhythm during the four-day period in May. This diurnal variation showed weak nightly winds, and stronger daily winds. The modelled winds at Vancouver airport were weaker than the observed but the diurnal variation was clearly pronounced also in this data.

The model predicts easterly winds during the first day, unlike the observed westerly data. The modelled wind is then turning westerly during the second day and continues westerly throughout the period, except during nighttime. The nightly winds are quite varying and very weak. The observed winds are also mainly westerly during the last three days with weak easterly nightly winds.

The modelled data shows tendencies to simulate a sea- and land breeze during the second, third and fourth day, judging by the wind directions, top graph. The modelled wind direction captures the westerly sea breeze quite well, but is a couple of hours slow to capture the beginning of the nightly land breeze.

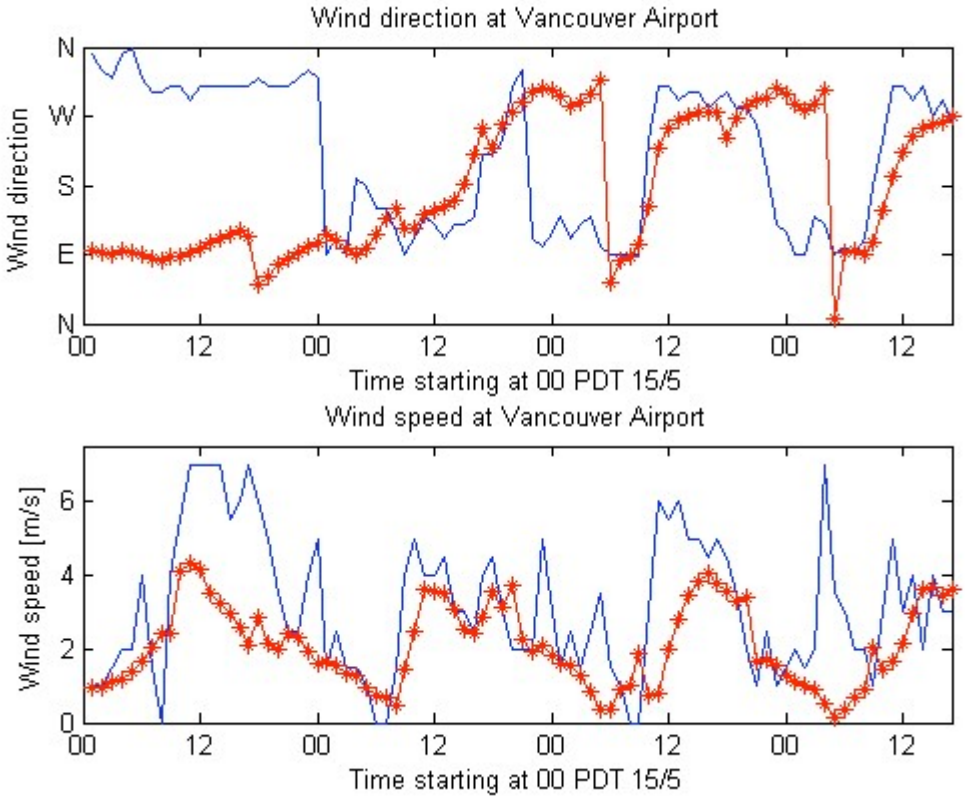

Fig 7.14: Wind direction and wind speed at Vancouver airport. Line with stars marks the modelled winds and plain line marks observed winds. Top graph shows wind direction and bottom graph shows wind speed.

The diurnal variation in wind speed, bottom graph, is captured well by the WRF model, but the peak wind speeds are too low. The wind speed is underestimated by as much as 2-3 m/s during day one and three, but only by approximately 1m/s during day two and four.

7.9.5 Modelled planetary boundary layer and mixing height

The mixing layer is a convective boundary layer that is characterised by its turbulence. This turbulence originates from mechanical and/or buoyant turbulence, depending on the situation. Strong winds and wind shear generate mechanical turbulence and heating at the earth's surface causes the buoyantly generated mixed layers. In the situation with fair weather during this study, the mixing layer is mainly generated by buoyant turbulence.

The planetary boundary layer, PBL, is a layer in the atmosphere reaching from the earth's surface to a statically stable layer or temperature inversion in the troposphere. The PBL is variable in both time and depth, and depending on time and atmospheric conditions, it changes characteristics, se Fig 7.15. During fair weather days over land, the PBL has a marked diurnal cycle, and during daytime a mixed layer of vigorous

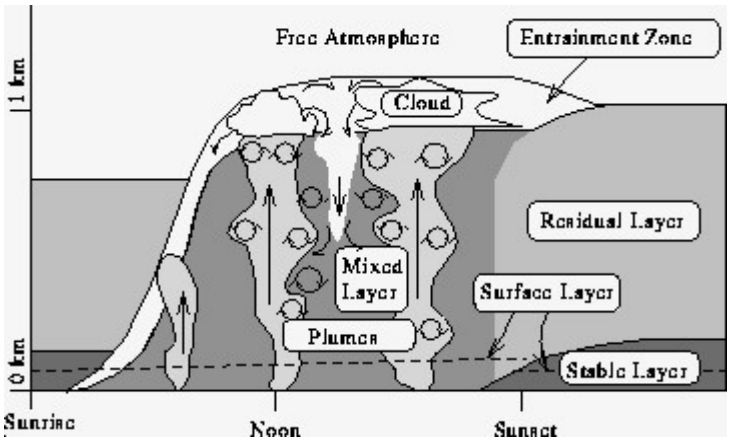

Fig 7.15 Illustration of the diurnal variations for the Planetary Boundary Layer. Mixing layer starting to build up at sunrise and passing on to residual layer at sunset.

turbulence grows in depth. The mixing layer reaches its maximum depth in the afternoon and is extended over the whole depth of the planetary boundary layer.
The extent of the mixing layer is important since an inversion layer caps it. This inversion layer also captures the pollutants and hence, a lower mixing layer enhances the concentration of the pollutants. The modelled planetary boundary layer height during a period as in this study would consist of mainly mixing layer during daytime, and Fig 7.16 shows the extent of this.

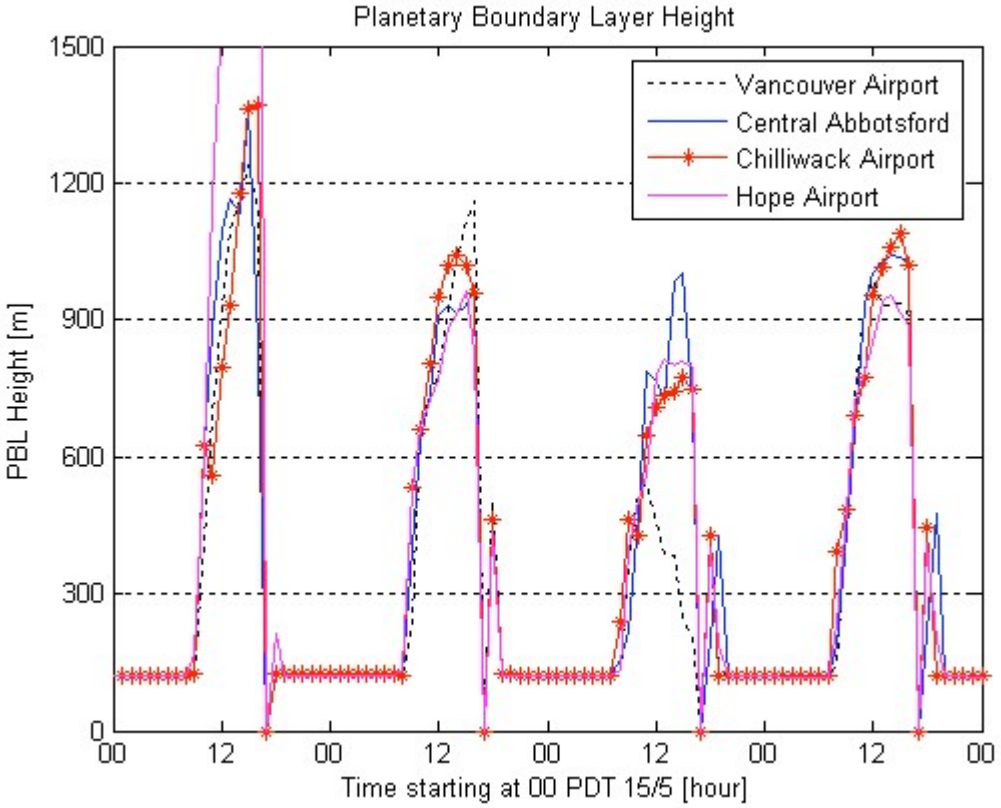

Fig 7.16: The modelled height of the planetary boundary layer during four consecutive days, 15/5-18/5. The graph shows the height measured in metres for four stations within the Lower Fraser Valley. Time starting at 00 PDT 15/5.

The modelled planetary boundary layer during daytime varies in height between 800 and 1300m throughout the period. The maximum values occur on the first day, 15/5, where Hope records a value of 2500m (out of range in Fig 7.16) This value seems unreasonable high since all the others in the valley are in the range 1200-1300m. Lowest values occur on the third day, 17/5, for all stations except Abbotsford with values between 750 and 800m, only Vancouver Airport has as low as 550m, but this seems unlikely to be true, judging by the sudden drop in the morning. Abbotsford shows almost equally height on both day two and three, around 1000m. Hence, the mixing height is quite low during the latest three days of the period it is growing in depth on the fifth day (not viewable).

8 Discussion, conclusions and summary

The quality of the air we breathe is of great interest for everyone. Pollutants as ozone and nitrogen dioxide can for example cause severe health issues, destroy crops, and enhance global warming. To protect ourselves from serious damage, we need to be able to forecast the concentrations of these harmful pollutants. Many different air quality models are in use all over the world, providing citizens with forecasts and warnings of unhealthy air quality. This study focuses on the topic to use the Weather research and Forecasting model as a driver of

the Community Multiscale Air Quality model, and to produce forecasts for British Columbia. The models are run during May 2006 and the forecasts for the period 15/5-18/5 are evaluated. The focus is to evaluate the forecasted concentrations of ozone and nitrogen dioxide in the Lower Fraser Valley by comparing them to observed data from the Emergency Weather Net. The Lower Fraser Valley is a region in British Columbia where approximately 2 million people live and it also host many industries and a widespread agricultural production.
The synoptic and mesoscale conditions, which are very important for both the magnitude and the spatial distribution in the valley, are also investigated.

Synoptic conditions

As mentioned in chapter 2.4, conditions favourable for high values of nitrogen oxides and ozone in the Lower Fraser Valley are small surface pressure gradients, strong low-level inversions, warm air in low levels, and strong ridges at 500 hPa that are persistent. The synoptic situation during the four-day episode in May, 2006 was characterized by weak winds and high temperatures in a high-pressure ridge at the surface, few clouds and dry air. At 500 hPa, a high-pressure ridge is slowly moving eastwards while maintaining its strength. The ridge was covering Lower Fraser Valley during seven days before continuing eastward, hence being semi-persistent.
Also, the especially favourable synoptic conditions described by McKendry with a strong ridge aligned with the Pacific Northwest coast, east of 120 and a low-level thermal through extending northward from the south western parts of United States seems to be mostly fulfilled.
Taking these conditions into consideration, the synoptic situation seems favourable for high values of pollutants as ozone in the Lower Fraser Valley area during the four-day episode.

Mesoscale conditions

The diurnal temperature variations in the valley were large during the four-day episode in May. The days were sunny, calm and warm producing high maximum temperatures, while quite low minimum temperatures were measured during night, se chapter 7.2.
Spatially, there were also differences where the western part of the valley, closest to the ocean, had lower temperatures than the eastern parts further inside the valley. Since the solar insolation was pronounced due to few clouds in the sky, and the ocean water outside the Fraser Valley in May is much colder than the land surface temperature during daytime, a sea breeze would easily be produced nearby the ocean. A sea breeze could explain the colder daytime temperatures closer to the water, and it would also affect the spatial distribution of pollutants in the valley, resulting in lower concentrations near the coast and higher concentrations further inside the valley. A land breeze would affect the spatial distribution of pollutants in the opposite way, with the lowest concentrations inside the valley and highest concentrations near the coast. A potential sea breeze would also have the effect of reducing mixing heights, which enhances the concentration of pollutants of the affected inland areas.
As can be seen in the observed wind data in Fig 7.14, there were sea- and land breezes present, at least in the western part of the valley during day two, three, and four (16/5-18/5).

Diurnal variations in the observed data

As described in chapter 2.1.2 the nitrogen dioxide molecule reacts with sunlight and dissociates, creating nitrogen oxide and atomic oxygen. This behaviour can be seen in the observed data in Fig 7.2 where the lowest concentrations of nitrogen dioxide are found in the morning and during lunchtime, when the sun is most active. The concentration of nitrogen dioxide is continuously low until the evening when the concentration increases rapidly. At the same time, the ozone concentrations are low during the morning but are increasing as the

insolation starts in the morning. The peak concentrations occur in the afternoon, around 16.00 PDT, see Fig 7.3. The increasing ozone concentrations during the day are due to the formation of ozone from molecular oxygen and atomic oxygen, with the latter created in the dissociation process of nitrogen dioxide to nitrogen oxide. The ozone concentration then drops rapidly during the evening while the concentration of nitrogen dioxide increases. This relation is most certainly due to the destruction of ozone which forms nitrogen dioxide, as described in chapter 2.1.2. This relation between ozone and nitrogen dioxide is also confirmed in other studies where a positive dependence of the ozone production due to incoming sun radiation, and a negative dependence of ozone production on nitrogen dioxide production due to a photolysis process (dissociation of ozone results in increasing levels of nitrogen dioxide) has been found [Minoura].

The high ozone concentrations measured at the stations (at the most 56 ppb at Hope airport 16/5) confirms the hypothesis that the synoptic conditions were favourable for high ozone concentrations. Also, the spatial distribution of ozone described in chapter 7.3, where the daily ozone concentrations were increasing further into the valley and the nightly ozone concentrations were decreasing further into the valley confirms the hypothesis of the effects of a diurnal sea and land breeze.

Observed data versus modelled data

Nitrogen dioxide and ozone are the two pollutants evaluated in this study. By comparing the forecasted concentrations of these two pollutants with corresponding observed data at four different places in the Lower Fraser Valley, the accuracy of the WRF/CMAQ model are investigated.

As can be seen in chapter 7.3, Figure 7.4, the modelled nitrogen dioxide concentrations agreed quite poorly with the observed concentrations in the valley. The expected diurnal variations that were found in the observed concentrations at all four stations could only be found in the forecasted concentrations for two stations during the last two days of study. The linear correlation for all stations were unacceptable, only for the two stations furthest inside the valley, the correlation was acceptable during the last two days. Both these stations, Chilliwack and Hope, also showed acceptable values for the root mean square error and gross error throughout the period. The root mean square error and gross error was acceptable at Vancouver airport during only the first day and Abbotsford station had ok error values during the first two days. The unpaired peak prediction accuracy was, due to lack of diurnal rhythm in the data, unacceptable for all stations but the Chilliwack station, which showed good accuracy during the last three days. To sum up, the nitrogen forecast for the two stations furthest inside the valley, Chilliwack and Hope, was acceptable during the last two days of study, but only the Chilliwack station managed to forecast the peaks of concentration in a proper way. The nitrogen dioxide forecast for Vancouver airport and Abbotsford was beneath contempt.

Modelled ozone concentrations showed a good diurnal rhythm but the forecasted concentrations were very high, Figure 7.5. Unfortunately, the forecasted concentrations were much higher than the observed ozone concentrations, and this overestimation of ozone led to very high root mean square errors and gross errors. The overestimation also resulted in bad unpaired peak prediction accuracy for all stations since this measurement takes into account not only the timing of the peak, but also the magnitude of the peak. The linear correlation for the forecasted ozone concentrations compared to the observed ozone concentrations was good

except during the first day for the two stations closest to the coast, Vancouver airport and Abbotsford.

Since the correlation between the forecasted and observed ozone datasets was good during the period, and the forecasted ozone concentrations showed a similar diurnal rhythm as the observed ozone concentrations, the modelled ozone dataset was manipulated by subtraction with an amount of concentration to see if the errors would improve.
The new, manipulated forecast agreed much better with the observed ozone concentrations as can be seen in Fig 7.9. The linear correlation stayed the same as expected, and both the root mean square error and gross error was improved by a large percent. These originally large errors were diminished with 50-80% by the subtraction of 24 ppb ozone from the "true" forecasted dataset. The unpaired peak prediction accuracy was also largely improved due to the decrease in magnitude of the concentration, 62,5% of the peaks were in the range ± 20% accuracy, and 87,5% were in the range ± 30%.
The unpaired peak prediction accuracy is a very useful tool in determining whether the dataset is good in air quality respect. This, since the peaks are the most interesting parts from a health point of view. Citizens want to know if the peak concentration will exceed healthy values and if precautions have to be made. Unpaired peak prediction accuracy within ± 20% is said to be acceptable for a forecast, and therefore the manipulated forecast is quite good in air quality respect.

Overestimation of ozone by WRF/CMAQ
Why is the WRF/CMAQ model forecasting too high concentrations of ozone? The reasons for this overprediction are further evaluated below.
The WRF/CMAQ model overestimates the ozone concentration by an amount of between 20 and 30 ppb during the studied four-day period, as can be seen in Fig 7.5. The reason for this overestimation is not simple to determine; is it the chemistry model (CMAQ CTM) computing bad values, or are there other reasons for these heightened concentrations? First of all, it is important to determine which factors can contribute to this enhanced ozone concentration.

1. If the solar insolation is not as great in reality as the meteorological model forecasts it to be, the models would predict higher ozone concentrations than the reality. This because the sunlight is a necessary ingredient in the formation of ozone (chapter 2.1.2). More incoming radiation would help to produce more ozone.
2. The temperature is important on ozone formation. The ozone concentration tends to increase with increasing temperatures [Joe et al.].
3. Clear or almost clear skies are favourable for higher ozone concentrations since this means that very few clouds that are preventing the insolation.
4. Stagnant high-pressure situations favour higher ozone concentrations, hence wind speed should be weak. A sea breeze circulation is acceptable, see item number 5.
5. The mixing height is also important since lower mixing heights can lead to increased pollutant concentrations due to capping inversions. A well-developed sea breeze will have the effect of reducing mixing heights on affected inland areas, also a high-pressure ridge in the area leads to subsidence and lower mixing heights. [Snyder]
6. The chemical mechanism within CMAQ CTM; CB4, enhances the predicted ozone concentrations by some percentage, se chapter 3.2.
7. The eddy diffusivity coefficient within CMAQ CTM, $K_H$min, is not adapted to urban environments since this is not possible when input meteorology is WRF, see chapter 3.2. The coefficient therefore helps to overestimate the ozone concentration in urban areas, which is the case in the Lower Fraser Valley.

8. High modelled concentrations of NO_2. Sunlight dissociates nitrogen dioxide into nitric oxide and atomic oxygen, the atomic oxygen can then react with molecular oxygen and form ozone, see chapter 2.1.2.

Meteorology data from the WRF model was compared to observed meteorology data during the four-day period in May. Item 1 to 4 in the list above; solar radiation, temperature, cloud cover and winds was investigated more carefully. Modelled mixing height was also considered.

Solar radiation: When comparing to the observed radiation data provided by the GVRD, it is clear that the modelled solar radiation is overestimated by the WRF model by almost 100 W/m^2. Since the ozone concentration in the troposphere is highly dependent on the amount of sunlight reaching the surface of the Earth, see chapter 2.1.2, this overestimation of radiation most certainly enhances the modelled concentration of ozone.
Temperature: The trend is that the WRF model overestimates the temperature at the stations closest to the coast, Vancouver airport and Abbotsford, captures the observed temperature best in Chilliwack, and underestimates the temperature furthest inside the valley, in Hope. This overestimation of temperature nearby the coast may be related to higher ozone concentrations in this area, but the underestimation of temperature inside the valley may also lead to lower forecasted concentrations in this region.
Clear skies: The model predicts less cloud cover than observations report during the whole period. Clear skies or mainly clear skies is forecasted by the model 97% of the period, while such cloud cover is present 65% of the period. Less cloud cover heightens the ozone concentrations since clouds prevent insolation. Hence, the modelled reduced cloud cover presumably enhances the modelled ozone concentration.
Weak wind speed: The WRF model underestimates the wind speed during the whole period by 1-3m/s. Thus, the model expects the maximum wind speed during day one to be around 4m/s instead of the observed 7m/s. Since the pollutants are spread by the wind, see chapter 2.1.3 and 2.2.1, the modelled weaker wind speeds most certainly enhances the modelled ozone concentration in the valley.
Mixing height: The mixing layer reaches its maximum depth in the afternoon and is then extended over the whole depth of the planetary boundary layer. The extent of the mixing layer is determined by a capping inversion layer, which also captures the pollutants in the mixing layer Hence, a lower mixing layer enhances the concentration of the pollutants. The modelled maximum planetary boundary height, or the modelled mixing height, is quite low during the last three days of the episode. The lowest modelled mixing layer depth occurs on the third day for Chilliwack and Hope, and it is therefore a good guess that the model forecasts the highest ozone concentrations on this day for the two stations. Abbotsford shows equally modelled mixing heights on day two and three and thus, the modelled ozone concentrations would be almost equally on these two days. It is not possible to determine the lowest modelled mixing height for the Vancouver Airport station. When comparing to the modelled ozone concentrations, it is obvious that the mixing height is important for the concentration of pollutants. Both Chilliwack and Hope is forecasted to have their maximum ozone concentrations on day three, and Abbotsford forecasts almost equally high maximum concentrations day two and three.
Unfortunately, no soundings from the Lower Fraser Valley could be collected and hence, there is no observed mixing height data to compare and to verify the forecasts with. The mixing height would most likely be low in reality too, due to the subsidence in the area and the developing land- and sea breeze as can be seen in observed wind data.

CMAQ CTM settings: The CB4 chemical mechanism and the eddy diffisivity coefficient in use in CMAQ CTM has, as mentioned above and in chapter 3.2, a tendency to overpredict the ozone.
Modelled concentrations of nitrogen dioxide: The WRF/CMAQ captures the magnitude of the NO_2 concentrations reasonable well, se chapter 7.4. The only station showing distinctly larger modelled concentrations of nitrogen dioxide than observed values, is Vancouver airport. This would lead to enhanced ozone concentrations in the area closest to the station, but the nitrogen dioxide concentrations should not be a factor contributing to the high modelled ozone concentrations in other parts of the region.

Summary:
The main goal for this thesis was to create a third ensemble member to add to the two air quality models in use at UBC, Vancouver. This goal was reached, but the new air quality model, WRF/CMAQ was not put in operational mode since the current operational WRF model is run in a different projection than was possible for this thesis.
The synoptic and mesoscale situation was favourable for high ozone concentrations in the area, and the observed data showed that this was the case.
The WRF/CMAQ model was evaluated by comparing modelled ozone and nitrogen dioxide concentrations with observed ozone and nitrogen dioxide concentrations. The result was not very satisfying since the WRF/CMAQ model not successfully forecasted proper concentrations of the pollutants nitrogen dioxide and ozone. The nitrogen dioxide forecasts had almost the right magnitude as the observed data, but the diurnal variations were not captured at the testsites. The ozone forecasts overpredicted the concentrations largely, but the diurnal variations were good at the testsites.
The reasons for this overprediction of ozone was investigated and it came to light that the WRF model overestimated the solar radiation, underestimated the cloud cover, and also underestimated the winds at all testsites. The WRF model also overestimates the nitrogen dioxide concentrations and temperature nearby the coast, but underestimates the temperature in Hope. All these factors, except the underestimated temperature in Hope, enhances the ozone concentration. The modelled mixing height was low during the period and could also have contributed to the heightened ozone concentrations. Also, the CMAQ CTM model uses a chemical mechanism and an eddy diffusivity coefficient, which both tends to enhance modelled ozone concentrations. The amount of overestimation of the ozone concentration due to the CCTM model would not be more than to a small percentage though.
Since the WRF/CMAQ model overestimated the ozone concentration by approximately 24 ppb and the diurnal variations were good, I would say that the main error for the forecasted would be in the WRF model forecasting the input meteorology, even though it is not clear how much the misprediction of meteorology would enhance the ozone concentration. The WRF model is known to be a good forecasting model but as mentioned in chapter 6.2, the WRF model was given only a short spin-up time before its output was used as input to the WRF/CMAQ model. This fact could have reduced the WRF model's ability to correct predict the meteorology.

9 Future work
Example of future work related to this thesis would be to use different options in the models in use; WRF, MCIP, SMOKE, and CMAQ, or to give the different models a proper spin-up time before collecting data. It would also be interesting to compare the performance of a WRF/CMAQ constellation to the WRF-Chem model. The WRF-Chem model is an option in running WRF to produce chemical output without using an air quality model as CMAQ.

A topic that was originally ment to be investigated in this thesis was to examine how the performance of the WRF/CMAQ model stands towards the other two ensemble members at UBC; MM5/CMAQ and MC2/CMAQ.

10 Acknowledgements

I would like to thank my supervisor at University of British Columbia professor Roland Stull for providing me the opportunity to conduct this work at the University of British Columbia in Vancouver. I also would like to thank Henryk Modzelewski, George II Hicks, Bruce Thompson, Thomas Nipen, Luca Delle Monache, Judi Krzyzanowski and all other in my research group; the Weather Forecast Research Team (WFRT) in the Geophysical Disaster Computational Fluid Dynamics Centre at the University of British Columbia for all help and encouragement during my five months in Vancouver. I also want to thank my Swedish supervisor Hans Bergström for believing in me and supporting me with ideas and cheering when coming home from Canada.
A special thanks to Michael, my family and friends at home who have supported me on a long distance.
I would also like to thank Limei Ran and Alison Eyth at University of North Carolina for all the help with the MIMS program, Tanya Otte for providing me a special version of MCIP, also a big thanks to the CMAS personel, specially Zac Adelman for the unvaluable help with the CMAQ CCTM model and the SMOKE model. Thanks to the Greater Vancouver Regional District (GVRD) who has helped me with radiation data and Michael Rensing at BC ministry of environment for the good ideas and motivation.

Finally, some words of wisdom that I've learnt while working on this thesis:
* You can get help in the least expected ways, don't hesitate to ask.
* There is at least one bug in every program.

11 References

Articles:

Ahrens, C. Donald 2000. Meteorology Today: An introduction to weather, climate, and the environment 6th ed. Brooks/Cole pp.38-39 ISBN 0-534-37201-5

Ahrens, C. Donald 2000. Meteorology Today: An introduction to weather, climate, and the environment 6th ed. Brooks/Cole pp.447-448 ISBN 0-534-37201-5

Air Resources Branch; Ministry of Environment, Lands and Parks, June 1998: Air quality report for British Columbia: Ground-level ozone concentrations (1986-1997). Victoria, BC. http://www.env.gov.bc.ca/air/vehicle/index.html

Appel W.K, Gilliland A, Eder B: An operational evaluation of the 2005 release of models-3 CMAQ version 4.5. National oceanic and atmospheric administration – Air resources laboratory.
http://www.cmascenter.org/help/model_docs/cmaq/4.5/Model_Performance_Evaluation.pdf

Banta R, Shepson P, Bottenheim J, Anlauf K, Wiebe H.A, Gallant A, Biesenthal T, Olivier L, Whu C, McKendry I, Steyn D, 1997: Nocturnal cleansing flows in a tributary valley. Atmospheric Environment volume 31, Issue 14, pp 2147-2162.

Byun D, Pleim J, Tai Tang R, Bourgeois A, 1999.: Meteorology-Chemistry Interface Processor (MCIP) for Models-3 Community Multiscale Air Quality (CMAQ) Modelling

System. Chapter 12 in Science Algorithms of the EPA Models-3 Community Multiscale Air Quality (CMAQ) modelling system.
EPA/600/R-99/030

Delle Monache L, Deng X, Zhou Y, Stull R, 2006. Ozone ensemble forecasts: 1 A new ensemble design.
Journal of geophysical research. Volume 111, D05307.

EPA, United States Environmental Protection Agency
"NOx – How Nitrogen oxides affect the way we live and breathe"
EPA-456/F-98-005
September 1998

Fahey, D.W. et al. Twenty questions and answers about the ozone layer. Scientific Assessment of Ozone Depletion 2002. World Meteorological Organization, Global Ozone Research and Monitoring Project – Report No.47.

Fuglestvedt Jan S., Berntsen Terje K., Isaksen Ivar S. A., Mao Huiting, Liang Xin-Zhong and Wang Wei-Chyung, 1998
Climatic forcing of nitrogen oxides through changes in tropospheric ozone and methane; global 3D model studies
Atmospheric Environment volume 33 Issue 6, pp 843-1013

Galloway JN, Cowling EB, Seitzinger SP, Socolow RH (2002). Reactive Nitrogen: Too Much of a Good Thing? AMBIO: A Journal of the Human Environment: Vol. 31, No. 2 pp. 60–63. Also: http://www.bioone.org/

Gery M.W., Whitten G. Z., Killus J. P., Dodge M. C. (1989). A photochemical kinetics mechanism for urban and regional scale computering modeling. Journal of geophysical research: Vol 94, No D10, pp12925-12956. Also:
http://www.agu.org/pubs/crossref/1989/89JD00793.shtml

Hogrefe C., Rao S.T., Kasibhatla P., Hao W., Sistla G., Mathur R., McHenry J. 2001. Evaluating the performance of regional-scale photochemical modelling systems: Part II – Ozone predictions. Atmospheric Environment 35 pp. 4175-4188

Janjic Z, 2003: A nonhydrostatic model based on a new approach. Springer-Verlag. Meteorology and Atmospheric Physics 82, pp.271–285

Joe H, Steyn D, Susko E, 1996. Analysis of trends in tropospheric ozone in the Lower Fraser Valley, British Columbia. Atmospheric Environment Vol 30, No 20, pp 3413-3421.

Lord E, Cannon A, 2003: Forecasting ground-level ozone in the Lower Fraser Valley. From the 2003 Georgia Basin/Puget Sound Research Conference.
www.psat.wa.gov/Publications/03_proceedings/PAPERS/ORAL/5b_lord.pdf

Martilli A, Steyn D, 2004: Pollutant recirculation in the Lower Fraser Valley (British Columbia, Canada) – Numerical study with MC2. From the 13th conference on the applications of air pollution meteorology with the air and waste management association. August 2004. Session 4.

http://ams.confex.com/ams/AFAPURBBIO/techprogram/program_221.htm

Mass C, 1982: The topographically forced diurnal circulations of western Washington State and their influence on precipitation. Monthly weather review 110, pp 170-183.

McKendry I, 1984: Synoptic circulation and summertime ground-level ozone concentrations at Vancouver, British Columbia. Journal of applied meteorology, volume 33, pp 627-641.

Michalakes J, Dudhia J, Gill D, Klemp J, Shamarock W, 1998: Design of a Next-generation Regional Weather research and Forecast Model: Towards Teracomputing, World Scientific, River Edge, New Jersey, 1998, pp. 117-124.

Michalakes J, Dudhia J, Gill D, Henderson T, Klemp J, Skamarock W, Wang W: The Weather Research and Forecast Model: Software architecture and performance.
Mesoscale and Microscale Meteorology Division, National Center for Atmospheric Research, Boulder, Colorado 80307 U.S.A.
http://www.wrf-model.org/wrfadmin/docs/ecmwf_2004.pdf

Minoura, H, 1999: Some characteristics of surface ozone concentration observed in an urban atmosphere. Atmospheric research 51, pp 153-169

Vingarzan R, Taylor B, 2003: Trend analysis of ground-level ozone in the Greater Vancouver/Fraser Valley area of British Columbia. Atmospheric environment 37, pp 2159-2171.

Wilks D. Statistical Methods in the Atmospheric Sciences; An introduction. Volume 59 in International Geophysics Series. Academic Press, San Diego. 1995. ISBN 0-12-751965-3

Science Algorithms of the EPA Models-3 Community Multiscale Air Quality (CMAQ) Modelling System, United States Environmental Protection Agency, March 1999 EPA/600/R-99/030

Skamarock W, Klemp J, Dudhia J, Gill D, Barker D, Wang W, Powers J, 2005: A description of the Advanced Research WRF Version 2. NCAR Tech Notes-468+STR
NCAR TECHNICAL NOTE June 2005
http://www.mmm.ucar.edu/wrf/users/docs/arw_v2.pdf

SMOKE v2.2 User's Manual
Publishing date: 2005/11/07
Carolina Environmental Program (CEP)- The University of North Carolina at Chapel Hill
Center for Environmental Modelling for Policy Development (CEMPD) a part of CEP

Snyder, B, 2002. Meteorological summary of the Pacific Air Quality 2001 field study. Environment Canada, Atmospheric science section.
http://www.pyr.ec.gc.ca/georgiabasin/reports/pacific_2001_summary/MetReport_final_GBEI_e.pdf

US Environmental Protection Agency, Office of Mobile Sources. Automobiles and ozone. Fact sheet OMS-4 1993.
EPA 400-F-92-006

2003 Annual Progress Report on The Canada-Wide Acid Rain Strategy for Post-2000
Federal/Provincial/Territorial
Ministers of Energy and Environment
ISSN 1488-948X
PN 1351 © Canadian Council of Ministers of the Environment 2006

Webpages:

AMS Glossary. American Meteorological Society Glossary.
http://amsglossary.allenpress.com/glossary

Canadian Council of Ministers of the Environment (CCME)
http://www.ccme.ca

COLA Weather and climate data
http://wxmaps.org/pix/analyses.html

Environmental Canada
www.ec.gc.ca
http://www.weatheroffice.ec.gc.ca/analysis/index_e.html

NOAA National Weather Service
http://www.hpc.ncep.noaa.gov/html/sfc_archive.shtml

SMOKE User's manual
http://cf.unc.edu/cep/empd/products/smoke/version2.2/

The WRF-NMM users webpage
http://www.dtcenter.org/wrf-nmm/users

The WRF users webpage
http://www.mmm.ucar.edu/wrf/users

The Weather Research & Forecasting Model webpage
http://www.wrf-model.org

US EPA CMAQ model
http://www.epa.gov/asmdnerl/CMAQ/cmaq_model.html

US EPA Highlights June 2004.
http://www.epa.gov/asmdnerl/Library/Highlights/2004/june.html

WW2010: The Weather World 2010 project. The University of Illinois
http://ww2010.atmos.uiuc.edu/(Gh)/wx/satellite.rxml

Figures:

2.1: The ozone molecule. Own creation.
2.2: Atmospheric ozone. Source Fahey et al. See literature reference .
2.3: The nitrogen dioxide molecule. Own creation.

Table references:

Appendix A: Codes from the WRF/CMAQ modeling system.

The grid description file used for the runs with the WRF/CMAQ air quality modelling system:

```
‘ ‘
‘LAMCON_49N121W’
2                    30.000              60.000              -121.000            -121.000            49.000
‘ ‘
‘PWEST_12’
‘LAMCON_49N121W’   -474000.000   -522000.000   12000.000   12000.000   70   89   1
‘ ‘
```

The headscript used to run the different models in the WRF/CMAQ air quality modelling system:

Wrfcmaq_full_rsc.run

```
#!/bin/tcsh
cd /users/cmaq_wrf/bin/new/log
# --- General settings
set day =    060518
set GIORNO =     18
set JULIAN =    138  # May 18, 2006 [DDD]
set JDATE =     139  # JULIAN + 1
set PREVDAY =   137  # JULIAN - 1
set GIORNO_INC = 19 # GIORNO + 1
set YESTER    =  17
set MESE =       05
set ANNO =       06
set YEAR  =      06
set MESE_INC =   05
set ANNO_INC =   06

set tmpl = /users/cmaq_wrf/bin/new/serial_12_full.rsc.csh
set cmd = /usr/local/pbs/bin/qsub
set serial = `$cmd –v
YYMMDD=$day,GIORNO=$GIORNO,MESE=$MESE,ANNO=$ANNO,GIORNO_INC=$GIORNO_INC,MESE_INC=$MESE_INC,AN
NO_INC=$ANNO_INC,JULIAN=$JULIAN,YESTER=$YESTER $tmpl | cut -d'.' -f1`
exit
```

Serial_12_full.rsc.csh

```
#!/bin/csh
#PBS -N WRFCMAQ12ser
#PBS -l nodes=1:ppn=1,walltime=07:20:00

# --- ********** General Inputs
echo 'SJ: source General Inputs - START'
setenv DAG               $GIORNO
setenv DAY               ${ANNO}${MESE}${DAG}
setenv YESTERDAY   $ANNO$MESE$YESTER
setenv G_STDATE      20${ANNO}${JULIAN}         # Julian start date
setenv ESDATE          20${ANNO}${MESE}${DAG}    # Start date of emis time-based files
setenv MSDATE          20${ANNO}${MESE}${DAG}    # Start date of met  time-based files
setenv G_STTIME       000000                  # Start time (HHMMSS)
setenv G_RUNLEN      250000                  # Run length (HHMMSS)
setenv NDAYS           2             # Duration in days of emis timebased files
set    YEAR     =   20${ANNO}
setenv G_TSTEP         010000                  # Time step  (HHMMSS)
set MDAYS =  2              # Duration in days of met timebased files
#  --- MCIP start/end + time string
set MCIP_START =    20${ANNO}-${MESE}-${DAG}_00:00:00.0000       #[UTC]
set MCIP_END   =    20${ANNO}-${MESE}-${GIORNO_INC}_00:00:00.0000 #[UTC]
echo 'SJ: source General Inputs – END'

# --- Clean-up log dir
cd /users/cmaq_wrf/bin/new/log
rm WRF*

 ## MCIP already run! Output in /temp/cmaq_wrf/out_mcip..
echo ' --- **** MCIPlarge (Run for WRFCMAQ) ****---'
# NOTE: before running qsub.mcip_12km need to clear output dir
```

```
cd /temp/cmaq_wrf/out_mcip/PWEST_12/4.5.1/OutDir
rm GRID*
rm MET*
cd /users/cmaq_wrf
tcsh
cd cmaq
source set_env_orig
cd /users/cmaq_wrf/cmaq/m3home/working/mcip3.1
echo 'SJ: source qsub.mcip large domain testrun - START'
source qsub.mcip.12km.large
echo 'SJ: source qsub.mcip large domain testrun - END'

# --- MCIP OUTPUT size check
cd /temp/cmaq_wrf/out_mcip/PWEST_12/4.5.1/OutDir
set size = `ls -l METCRO3D_${DAY} | awk '{print($5)}'`
echo METCRO3D_${DAY}
echo $size
if ($size <= 325373500) then  # 89x70x34
   echo 'SJ: MCIP OUTPUT size check FAILED!'
endif
echo 'SJ: MCIP OUTPUT (METCRO3D_*.12km) size check SUCCESSFULL'
#-------------------------------------------------------------------------------
setenv SMOKEDAY $DAG
# --- ********** SMOKE 12 km ************
source /users/cmaq_wrf/bin/orig_path
# NOTE: before running SMOKE need to clear output dir
cd /users/cmaq_wrf/smoke_v2.2/data/ge_dat
rm bioseason.*pwest.ncf
cd /users/cmaq_wrf/smoke_v2.2/data/inventory/base2001.new
rm a*e
rm p*
cd area_dat
rm C*
rm N*
rm P*
rm S*
rm V*
cd ../pnts_dat
rm C*
rm N*
rm P*
rm S*
rm V*
cd /users/cmaq_wrf/smoke_v2.2/data/reports/base2001.new/static
rm a*
rm p*
rm r*
cd ../scenario
rm a*
rm p*
rm r*
cd /users/cmaq_wrf/smoke_v2.2/data/reports/base2001.newmb/scenario
rm a*
rm r*
cd /users/cmaq_wrf/smoke_v2.2/data/run_base2001.new/output/cmaq.cb4p25
rm agts*_12.*
rm bgts*_12.*
rm pgts*_12.*
cd ../merge
rm egts*_12.*
cd ../../scenario
rm atmp.*
rm atsup.*
rm play.*
rm pt*.*
cd ../static
rm ag*.*_12.*
rm as*
rm pg*.*_12.*
rm ps*
rm repiven*
cd logs
rm *.log
cd /users/cmaq_wrf/smoke_v2.2/data/run_base2001.newmb/output/cmaq.cb4p25
rm agts_l*
#cd /temp/cmaq_wrf/cmaq.wrf/m3home/data/smokev2.2/$DAY
```

```
#rm egts*
cd /users/cmaq_wrf/smoke_v2.2/data/run_base2001.newmb/scenario
rm at*
cd /users/cmaq_wrf/smoke_v2.2/data/run_base2001.newmb/static/logs
rm smkinven*
rm smkmerge*
rm smkreport*
rm temporal*
rm rawbio*
rm metscan*
rm grdmat*
rm spcmat*
###########  SMOKE  ###########
cd /users/cmaq_wrf
tcsh
source .cshrc
cd $SMKROOT/assigns
echo 'smkroot is'
echo $SMKROOT
echo 'SJ: source ASSIGNS.pwest.12km.txt - START'
echo $G_STDATE $G_STTIME $G_TSTEP $G_RUNLEN $ESDATE $MSDATE $NDAYS $MDAYS
source ASSIGNS.pwest.12km.txt $G_STDATE $G_STTIME $G_TSTEP $G_RUNLEN $ESDATE \
                    $MSDATE   $NDAYS    $MDAYS   $YEAR     $DAY
cd $SCRIPTS/run
#  --- Area emissions
echo 'SJ: Area emissions -START'
rm run.ar
ln -s smk_ar_pwest12.2k1base.csh run.ar
source /users/cmaq_wrf/bin/orig_path
source qsub.ar

# --- Point emissions
echo 'SJ: Point emissions -START'
rm run.pt
ln -s smk_pt_pwest12.2k1base.csh run.pt
source /users/cmaq_wrf/bin/orig_path
source qsub.pt

# --- Biogenic emissions
echo 'SJ: Biogenic emissions -START'
rm run.bg
ln -s smk_bg_pwest12.2k1base.csh run.bg
source /users/cmaq_wrf/bin/orig_path
source qsub.bg

# --- Merge area, biogenic and point emissions with mrgrid into a gridded outputecho 'SJ: Merge area, biogenic and point emissions -START'
rm run.mrgabp
ln -s smk_mrgabp_pwest12.2k1base.csh run.mrgabp
source /users/cmaq_wrf/bin/orig_path
source qsub.mrgabp

### A,B,P output into run_base2001.new,  M output into run_base2001.newmb
### Need to merge this output in the end!

## ---  Mobile and nonroad treated like area sources since having pregridded inventories as input. Not running Mobile6.
cd $SMKROOT/assigns
echo 'SJ: source ASSIGNS.pwest.12km.mb.txt - START'
source ASSIGNS.pwest.12km.mb.txt $G_STDATE $G_STTIME $G_TSTEP $G_RUNLEN $ESDATE\
                    $MSDATE   $NDAYS    $MDAYS   $YEAR     $DAY
cd $SCRIPTS/run
# ---  Mobile and nonroad emissions
echo 'SJ: Mobile and nonroad emissions -START'
rm run.armb
ln -s smk_armb_pwest12.2k1base.csh run.armb
source /users/cmaq_wrf/bin/orig_path
source qsub.armb

# --- Merge all emissions to create CMAQ input files
# Merging A,B,P outputfile EGTS3D_L with M outputfile AMGTS_L
echo 'SJ: Merge all emissions -START'
rm run.mrgrid
ln -s smk_mrgrid_pwest12.2k1base.csh run.mrgrid
source /users/cmaq_wrf/bin/orig_path
source qsub.mrgrid

unsetenv DAG
```

```
setenv DAG $SMOKEDAY
cd /temp/cmaq_wrf/cmaq.wrf/m3home/data/smokev2.2
mkdir $DAY
mv egts_l.20${ANNO}${MESE}*.PWEST_12.base2001.new.ncf
/temp/cmaq_wrf/cmaq.wrf/m3home/data/smokev2.2/$DAY/egts_l.20${ANNO}${MESE}${DAG}.2.PWEST_12.base2001.new.ncf
mv egts3d_l.20${ANNO}${MESE}*.PWEST_12.base2001.new.ncf
/temp/cmaq_wrf/cmaq.wrf/m3home/data/smokev2.2/$DAY/egts3d_l.20${ANNO}${MESE}${DAG}.2.PWEST_12.base2001.new.ncf

# --- SMOKE OUTPUT size check
cd /temp/cmaq_wrf/cmaq.wrf/m3home/data/smokev2.2/$DAY
set smoke_files = (`ls -x egts_l* `)
foreach file ($smoke_files)
  set size = `ls -l $file | awk '{print($5)}'`
  echo $file
  echo $size
    if ($size <= 213500000) then
## 70x89x17x24x21 (CxRxLxTxV)
     echo 'SJ: SMOKE OUTPUT size check FAILED!'
     exit
  endif
end
echo 'SJ: SMOKE OUTPUT size check SUCCESSFULL'
#-------------------------------------------------------------------------------
#********** CMAQ/Serial 12 km ---
cd /users/cmaq_wrf
cd CMAQ
source set_env_test

echo ' ---*** BCON Boundary condition preprocessor ***---'
# NOTE: before running qsub.bcon_12km, need to clear output dir
cd /temp/cmaq_wrf/cmaq.wrf/m3home/data/bcon
mv BCON_cb4_PWEST_12_profile ./old
cd $WORK/bcon
echo 'SJ: source qsub.bcon_12km - START'
source qsub.bcon_12km $G_STTIME $G_RUNLEN $DAY
echo 'SJ: source qsub.bcon_12km - END'

## BCON OUTPUT size check
cd /temp/cmaq_wrf/cmaq.wrf/m3home/data/bcon
set size = `ls -l BCON_cb4_PWEST_12_profile | awk '{print($5)}'`
 if ($size <= 953000) then
  # 89x70x17
  echo 'SJ: BCON OUTPUT size check FAILED!'
endif
echo 'SJ: BCON OUTPUT size check SUCCESSFULL'
#exit

echo '---*** ICON Initial condition preprocessor ***---'
# --- Check if the previous day finished succesfully...if yes, setting for a "warm start", otherwise, setting for a "cold start"
cd /temp/cmaq_wrf/cmaq.wrf/m3home/data/cctm/$YESTERDAY
set size = `ls -l CCTM_pwest_12CONC.e1* | awk '{print($5)}'`
if ($size <= 1109814000) then  # 80x60x17
  setenv IC profile  # use default profile file
  echo 'SJ: COLD START'
else
  setenv IC m3conc   # use CMAQ CTM concentration files (nested runs)
  echo 'SJ: WARM START'
endif
# NOTE: before running qsub.icon_12km, need to clear output dir
cd /temp/cmaq_wrf/cmaq.wrf/m3home/data/icon
#mv ICON_cb4_PWEST_12_profile ./old      #if second day
mv ICON_cb4_PWEST_12* ./old              #following days
cd $WORK/icon
echo 'IC, G_STDATE, G_STTIME, DAY'
echo $IC $G_STDATE $G_STTIME $DAY
echo 'WRF: source qsub.icon_12km - START'
source qsub.icon_12km $IC $G_STDATE $G_STTIME $DAY
echo 'WRF: source qsub.icon_12km - END'

# --- ICON OUTPUT size check
cd /temp/cmaq_wrf/cmaq.wrf/m3home/data/icon
set size = `ls -l ICON_cb4_PWEST_12_* | awk '{print($5)}'`
echo ICON_cb4_PWEST_12_*
echo $size
if ($size <= 18228000) then
  echo 'SJ: ICON OUTPUT size check FAILED!'
```

```
endif
echo 'SJ: ICON OUTPUT size check SUCCESSFULL'

## JCON processor already run and output stored in /temp/cmaq_wrf/cmaq.wrf/m3home/data/jproc.
# ---*** JCON Photolysis preprocessor
#cd $WORK/jproc
#echo 'SJ: source qsub.jproc - START'
#source qsub.jproc
#echo 'SJ: source qsub.jproc - END'
#------------------------------------------------------------------------
echo '**************----- CCTM -----***************'
echo 'dag, mese, anno, julian'
echo ${DAG} ${MESE} ${ANNO} ${JULIAN}
setenv EXTN ${ANNO}${MESE}${DAG}
setenv STTIME 010000 #HHMMSS
setenv NSTEPS 250000
setenv ST 600  # STTIME/10000*60 [min. from 00 UTC]
setenv NS 26  # NSTEP/10000 + 1 [number of output hours]
cd /users/cmaq_wrf/CMAQ
source set_env_test
#------------------------------------------------------------------------
# --- NOTE: before running run.master.pwest12 need to clear output dirs, and also check if the previous day finished succesfully... if yes,
setting for a "warm start" otherwise, setting for a "cold start"
#Remove old logfiles
cd $WORK/cctm
rm e1a.log
rm e1b.log
#Remove old outputfiles
cd $M3DATA/cctm/
rm CCTM_pwest_12*
#------------------------------------------------------------------------
# Checking for warm or cold start! Is there any output from yesterday's run?
cd $M3DATA/cctm/$YESTERDAY
set size2 = `ls -l CCTM_pwest_12CONC.* | awk '{print($5)}'`
if ($size2 >= 50000000) then
  echo 'WARM START'
  set NEW_START=false
else
  echo 'COLD START'
  set NEW_START=true
endif
cd $WORK/cctm/BLD
ln -s BLD_pwest12 BLD
#------------------------------------------------------------------------
# check whether this is a cold start (first day of modeling) or for subsequent runs (second day .....)
  if ( ${NEW_START} == true ) then
    setenv NEW_START  false
    setenv GC_ICpath  /temp/cmaq_wrf/cmaq.wrf/m3home/data/icon
    setenv GC_ICfile  ICON_cb4_PWEST_12_profile
  else
    echo $YESTERDAY
    setenv GC_ICpath  /temp/cmaq_wrf/cmaq.wrf/m3home/data/cctm/$YESTERDAY
    setenv GC_ICfile  $GC_ICpath/CCTM_pwest_12CONC.*
  endif
#------------------------------------------------------------------------
#Run daily script!
      echo 'run daily script'
      echo ${G_STDATE}
   #$WORK/cctm/run.cctm_pwest_12 $G_STDATE $EXTN #First day's run
   $WORK/cctm/run.cctm_pwest_12_2 $G_STDATE $EXTN # Following days
#------------------------------------------------------------------------
# Store the output files
cd $M3DATA/cctm
mkdir $DAY
mv CCTM_pwest_12ACONC.e1b ./$DAY/CCTM_pwest_12ACONC.e1b
mv CCTM_pwest_12AEROVIS.e1b ./$DAY/CCTM_pwest_12AEROVIS.e1b
mv CCTM_pwest_12CONC.e1b ./$DAY/CCTM_pwest_12CONC.e1b
mv CCTM_pwest_12DRYDEP.e1b ./$DAY/CCTM_pwest_12DRYDEP.e1b
mv CCTM_pwest_12WETDEP1.e1b ./$DAY/CCTM_pwest_12WETDEP1.e1b
cd $WORK/cctm
mv e1b.log $M3DATA/cctm/$DAY/elb.log
echo 'SJ - KLAR'
exit 0
```

Appendix B: Data from Emergency Weather Net

Ozone concentrations by order: Langley central, Hope airport, Vancouver airport, Central Abbotsford, and Chilliwack airport. Time meassured in GMT, Greenwitch Mean Time.

2006-05-15	00:00	23	28	22	29	35
2006-05-15	01:00	23	21	19	19	35
2006-05-15	02:00	20	3	16	17	23
2006-05-15	03:00	16	3	17	15	17
2006-05-15	04:00	7	10	15	9	17
2006-05-15	05:00	0	15	5	2	7
2006-05-15	06:00	0	15	1	2	2
2006-05-15	07:00	0	14	1	3	7
2006-05-15	08:00	0	12	1	4	14
2006-05-15	09:00	0	11	3	10	13
2006-05-15	10:00	0	11	4	11	14
2006-05-15	11:00	0	11	8	13	13
2006-05-15	12:00	0	12	2	11	13
2006-05-15	13:00	0	13	3	13	13
2006-05-15	14:00	0	13	15	16	14
2006-05-15	15:00	0	15	16	18	16
2006-05-15	16:00	0	20	18	21	18
2006-05-15	17:00	0	22	20	23	18
2006-05-15	18:00	0	23	20	24	20
2006-05-15	19:00	0	23	22	24	22
2006-05-15	20:00	0	23	22	27	23
2006-05-15	21:00	0	24	21	31	23
2006-05-15	22:00	0	22	21	33	23
2006-05-15	23:00	0	19	22	37	22
2006-05-16	00:00	0	8	20	40	18
2006-05-16	01:00	0	9	17	23	16
2006-05-16	02:00	0	11	19	10	12
2006-05-16	03:00	0	10	18	9	11
2006-05-16	04:00	0	8	5	3	11
2006-05-16	05:00	0	9	2	1	12
2006-05-16	06:00	0	8	1	0	9
2006-05-16	07:00	0	9	1	0	10
2006-05-16	08:00	0	7	1	0	11
2006-05-16	09:00	0	7	1	0	9
2006-05-16	10:00	0	7	0	0	10
2006-05-16	11:00	0	4	1	0	8
2006-05-16	12:00	0	6	2	1	9
2006-05-16	13:00	0	6	2	4	8
2006-05-16	14:00	0	10	3	5	10
2006-05-16	15:00	0	13	10	7	12
2006-05-16	16:00	0	16	19	11	15
2006-05-16	17:00	0	18	24	16	17
2006-05-16	18:00	0	20	31	26	20
2006-05-16	19:00	0	23	35	34	25
2006-05-16	20:00	0	27	36	43	35
2006-05-16	21:00	0	33	38	43	44
2006-05-16	22:00	0	39	39	36	50
2006-05-16	23:00	0	51	36	30	42
2006-05-17	00:00	0	56	32	25	32
2006-05-17	01:00	0	49	23	21	27
2006-05-17	02:00	0	32	20	16	22
2006-05-17	03:00	0	16	14	11	10
2006-05-17	04:00	0	1	14	13	6
2006-05-17	05:00	0	6	12	8	4

2006-05-17	06:00	0	4	12	7	3
2006-05-17	07:00	0	9	14	13	1
2006-05-17	08:00	0	8	15	14	3
2006-05-17	09:00	0	7	13	14	8
2006-05-17	10:00	0	6	14	10	8
2006-05-17	11:00	0	4	13	7	9
2006-05-17	12:00	0	8	7	12	9
2006-05-17	13:00	0	9	10	11	11
2006-05-17	14:00	0	13	12	13	13
2006-05-17	15:00	0	16	16	13	15
2006-05-17	16:00	0	19	19	16	17
2006-05-17	17:00	0	19	19	19	19
2006-05-17	18:00	0	23	20	22	20
2006-05-17	19:00	0	27	21	27	23
2006-05-17	20:00	0	31	21	25	29
2006-05-17	21:00	0	35	21	30	34
2006-05-17	22:00	0	41	20	34	33
2006-05-17	23:00	0	44	19	32	35
2006-05-18	00:00	0	44	18	30	34
2006-05-18	01:00	0	39	10	24	28
2006-05-18	02:00	0	34	11	21	23
2006-05-18	03:00	0	29	9	13	20
2006-05-18	04:00	0	23	2	9	18
2006-05-18	05:00	0	20	4	7	17
2006-05-18	06:00	0	14	5	4	3
2006-05-18	07:00	0	8	8	3	1
2006-05-18	08:00	0	1	8	9	1
2006-05-18	09:00	0	1	10	11	3
2006-05-18	10:00	0	0	12	8	5
2006-05-18	11:00	0	0	12	7	8
2006-05-18	12:00	0	0	10	11	8
2006-05-18	13:00	0	4	11	11	9
2006-05-18	14:00	0	10	10	11	11
2006-05-18	15:00	0	14	14	14	14
2006-05-18	16:00	0	18	17	16	16
2006-05-18	17:00	0	19	16	20	21
2006-05-18	18:00	0	27	19	23	23
2006-05-18	19:00	0	32	18	27	26
2006-05-18	20:00	0	34	20	31	30
2006-05-18	21:00	0	35	21	31	32
2006-05-18	22:00	0	37	19	30	35
2006-05-18	23:00	0	39	19	28	31

Nitrogen dioxide concentrations by order: Langley central, Hope airport, Vancouver airport, Central Abbotsford, and Chilliwack airport.

2006-05-15	00:00	3	1	2	1	1
2006-05-15	01:00	2	2	3	3	1
2006-05-15	02:00	3	7	4	4	3
2006-05-15	03:00	4	6	3	4	3
2006-05-15	04:00	6	4	4	7	2
2006-05-15	05:00	0	2	9	10	5
2006-05-15	06:00	0	1	10	9	6
2006-05-15	07:00	0	2	10	7	5
2006-05-15	08:00	0	2	9	6	1
2006-05-15	09:00	0	2	8	3	1
2006-05-15	10:00	0	2	7	2	1
2006-05-15	11:00	0	2	5	2	2
2006-05-15	12:00	0	2	8	3	2
2006-05-15	13:00	0	2	9	3	2

2006-05-15	14:00	0	2	4	2	1
2006-05-15	15:00	0	1	2	2	1
2006-05-15	16:00	0	1	1	1	1
2006-05-15	17:00	0	1	1	1	1
2006-05-15	18:00	0	1	2	1	1
2006-05-15	19:00	0	1	2	1	1
2006-05-15	20:00	0	1	2	1	1
2006-05-15	21:00	0	1	3	1	1
2006-05-15	22:00	0	1	4	1	1
2006-05-15	23:00	0	2	4	2	1
2006-05-16	00:00	0	4	7	2	1
2006-05-16	01:00	0	3	6	5	2
2006-05-16	02:00	0	2	3	6	3
2006-05-16	03:00	0	3	4	7	2
2006-05-16	04:00	0	3	10	9	2
2006-05-16	05:00	0	2	10	9	1
2006-05-16	06:00	0	2	10	9	3
2006-05-16	07:00	0	2	11	8	2
2006-05-16	08:00	0	3	10	7	1
2006-05-16	09:00	0	3	10	6	2
2006-05-16	10:00	0	2	9	5	2
2006-05-16	11:00	0	4	8	5	2
2006-05-16	12:00	0	3	8	5	2
2006-05-16	13:00	0	3	9	5	3
2006-05-16	14:00	0	1	9	5	2
2006-05-16	15:00	0	1	5	5	1
2006-05-16	16:00	0	1	4	4	1
2006-05-16	17:00	0	1	3	3	1
2006-05-16	18:00	0	1	3	2	2
2006-05-16	19:00	0	1	3	2	1
2006-05-16	20:00	0	1	2	2	2
2006-05-16	21:00	0	1	3	2	2
2006-05-16	22:00	0	1	2	2	2
2006-05-16	23:00	0	1	2	2	2
2006-05-17	00:00	0	2	5	2	1
2006-05-17	01:00	0	2	7	3	2
2006-05-17	02:00	0	3	8	4	2
2006-05-17	03:00	0	6	5	5	6
2006-05-17	04:00	0	11	3	3	7
2006-05-17	05:00	0	8	4	5	7
2006-05-17	06:00	0	8	3	6	7
2006-05-17	07:00	0	5	2	2	8
2006-05-17	08:00	0	5	2	2	6
2006-05-17	09:00	0	5	3	2	3
2006-05-17	10:00	0	5	2	3	3
2006-05-17	11:00	0	5	3	5	3
2006-05-17	12:00	0	4	5	4	4
2006-05-17	13:00	0	4	6	4	3
2006-05-17	14:00	0	2	5	3	3
2006-05-17	15:00	0	1	2	3	3
2006-05-17	16:00	0	1	2	3	2
2006-05-17	17:00	0	2	2	2	2
2006-05-17	18:00	0	1	2	2	2
2006-05-17	19:00	0	1	1	1	2
2006-05-17	20:00	0	2	2	2	2
2006-05-17	21:00	0	2	2	2	2
2006-05-17	22:00	0	2	2	2	2
2006-05-17	23:00	0	2	1	1	2
2006-05-18	00:00	0	2	3	1	2
2006-05-18	01:00	0	2	7	2	2

2006-05-18	02:00	0	2	6	4	2
2006-05-18	03:00	0	2	6	4	2
2006-05-18	04:00	0	2	9	5	3
2006-05-18	05:00	0	2	7	4	3
2006-05-18	06:00	0	4	7	5	8
2006-05-18	07:00	0	6	5	7	7
2006-05-18	08:00	0	8	4	3	7
2006-05-18	09:00	0	6	3	2	6
2006-05-18	10:00	0	6	2	4	5
2006-05-18	11:00	0	6	3	5	3
2006-05-18	12:00	0	5	5	3	4
2006-05-18	13:00	0	4	5	3	4
2006-05-18	14:00	0	3	6	3	4
2006-05-18	15:00	0	2	4	2	3
2006-05-18	16:00	0	1	3	2	3
2006-05-18	17:00	0	2	4	2	3
2006-05-18	18:00	0	1	3	2	2
2006-05-18	19:00	0	1	4	1	2
2006-05-18	20:00	0	1	3	2	1
2006-05-18	21:00	0	1	3	1	2
2006-05-18	22:00	0	2	4	2	2
2006-05-18	23:00	0	1	3	1	2

Appendix C: The physics and dynamics within the Weather and Research Forecast model v 2.1.2 in use

Physics	
Long wave radiation	RRTM scheme. A spectral-band scheme using the correlated-k method. It uses pre-set tables to accurately represent longwave processes due to water vapor,ozone, carbondioxide, and trace-gases, as well as accounting for optical depth.
Short wave radiation	MM5 Dudhia shortwave scheme. The scheme has a simple downward integration of solar flux, accounting for clear-air scattering, water vapor absorption, and cloud albedo and absorption.
Microphysics (atmospheric heat and moisture tendencies, microphysical rates, and surface rainfall)	Purdue Lin et al scheme. includes six classes of hydrometeors; water vapor, cloud water, rain, cloud ice, snow, and graupel. It is a relatively sophisticated microphysics scheme and is well suitable for use in research studies. The scheme ios taken from the Purdue cloud model.
Convective parameterization (atmospheric heat and moisture/cloud tendencies, surface rainfall)	Kain-Fritsch scheme. The Kain-Fritsch scheme is really a modification of the original scheme, due to testing with the ETA model. The scheme utilizes a simple cloud model with moist updrafts and downdrafts, including the effects of entrainment, detrainment, andrelatively simple microphysics.
Surface parametrization	MM5 similarity theory. Based on Monin-Obukov with Carslon-Boland viscous sub-layer and similarity functions from look-up tables.
Land-surface parametrization	5-layer thermal diffusion: Soil temperature scheme only using 5 layers.
Planetary boundary layer (boundary layer fluxes and vertical diffusion)	Yonsei University (YSU) PBL scheme. The YSU scheme is the next generation of the Medium range forecast model (MRF) PBL scheme, also using counter-gradient terms to represent fluxes due to non-local gradients. The scheme also uses an explicit treatment of the entrainment layer at the PBL top, where the entrainment is made proportional to the surface buoyancy flux.
Dynamics	
Dynamical core	Advanced Research WRF core. Eulerian mass
Turbulence and mixing	Evaluates 2nd order diffusion term on coordinate surfaces
Eddy diffusion coefficient	Horisontal Smagorinsky first order closure
Upper level damping	Without damping
Horisontal and vertical diffusion constants	Both 0 m^2/s

Appendix D: The WRF/CMAQ air quality output

D1: Ozone concentration over British Columbia 18/5 12.00 & 18/5 15.00

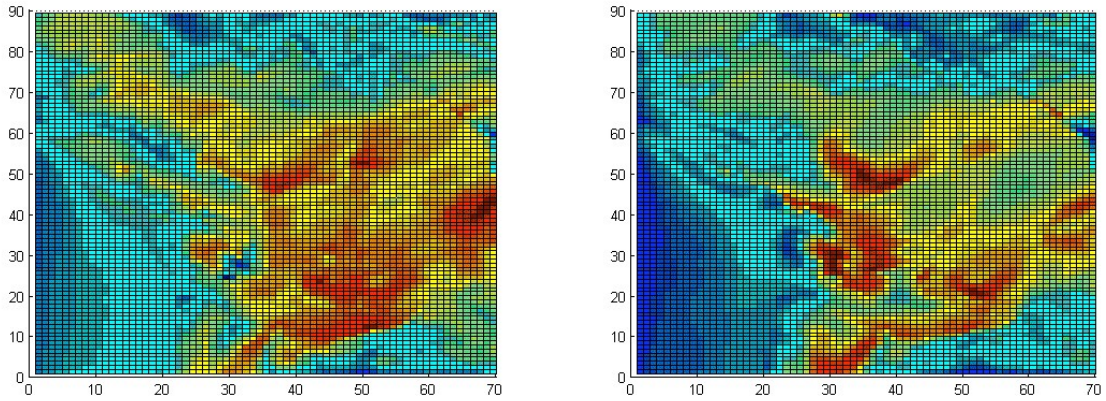

D2: Nitrogen dioxide concentration over British Columbia 17/5 21.00 & 18/5 00.00

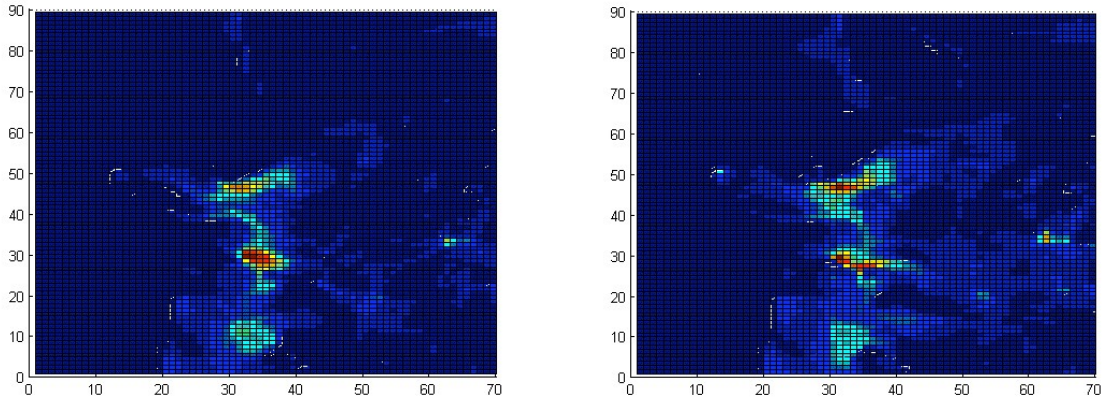

Appendix E: The Synoptic situation

E:1 ETA analysis 850mb Temperature ,Relative Humidity, Wind

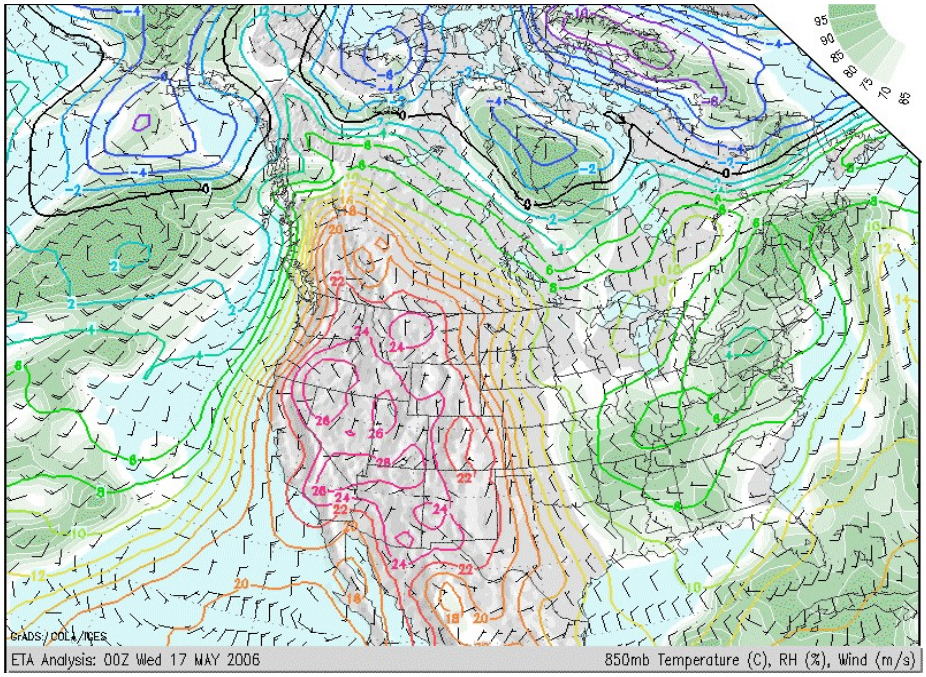

E:2 ETA analysis 500mb Geopotential heights, Vorticity

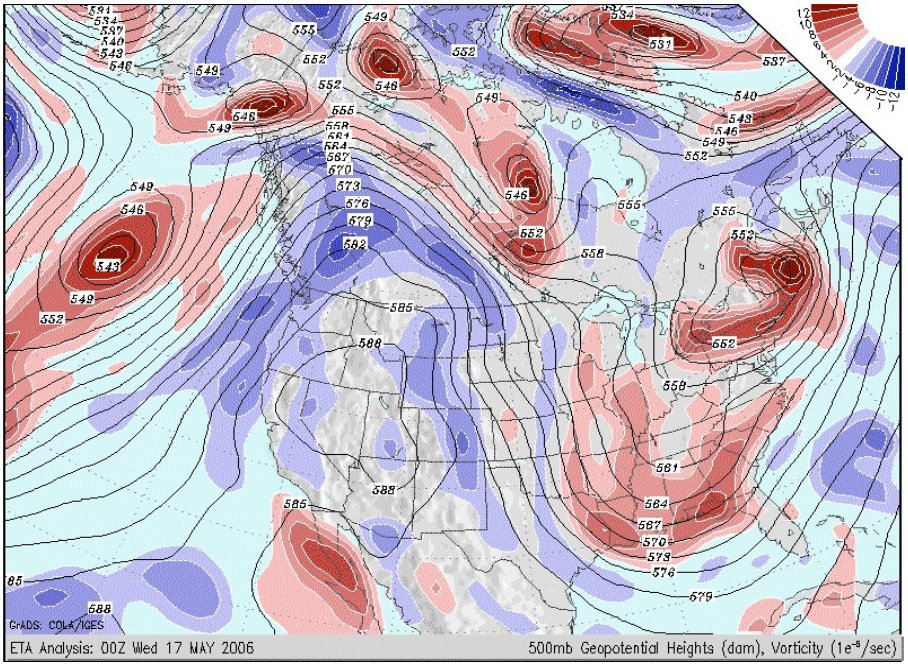

E:3 ETA analysis 200mb Streamlines, Isotachs

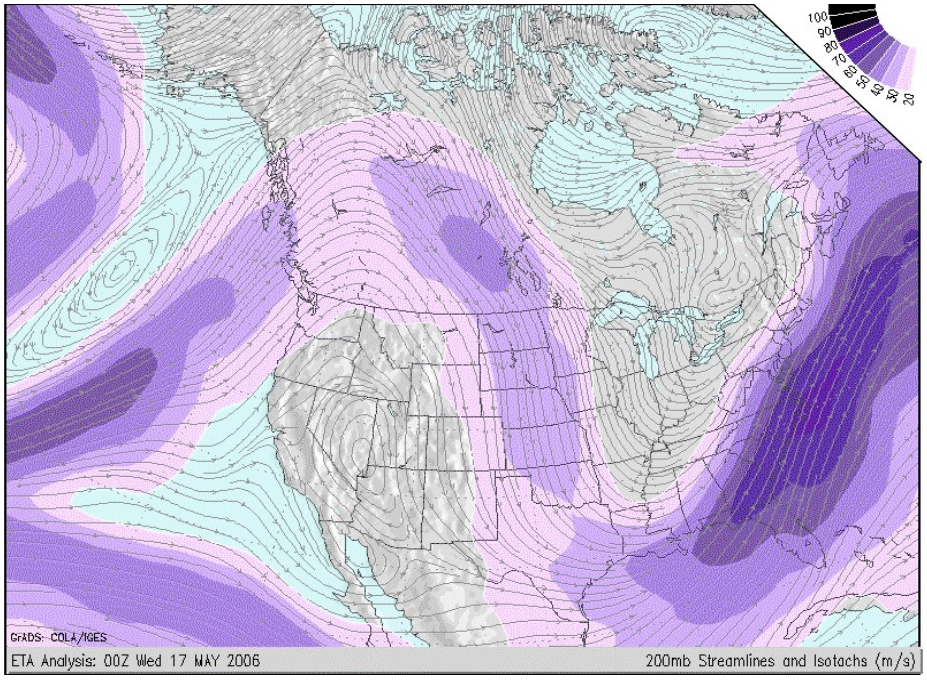

E:4 EC analysis 500mb

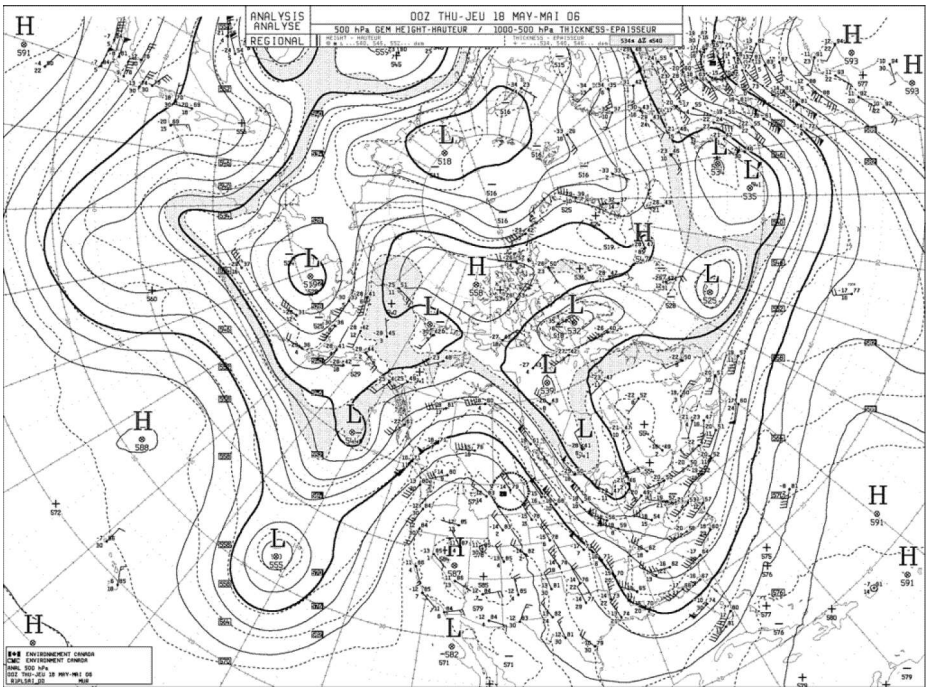

E:5 Satellite images for IR data, water vapour data and visible data.

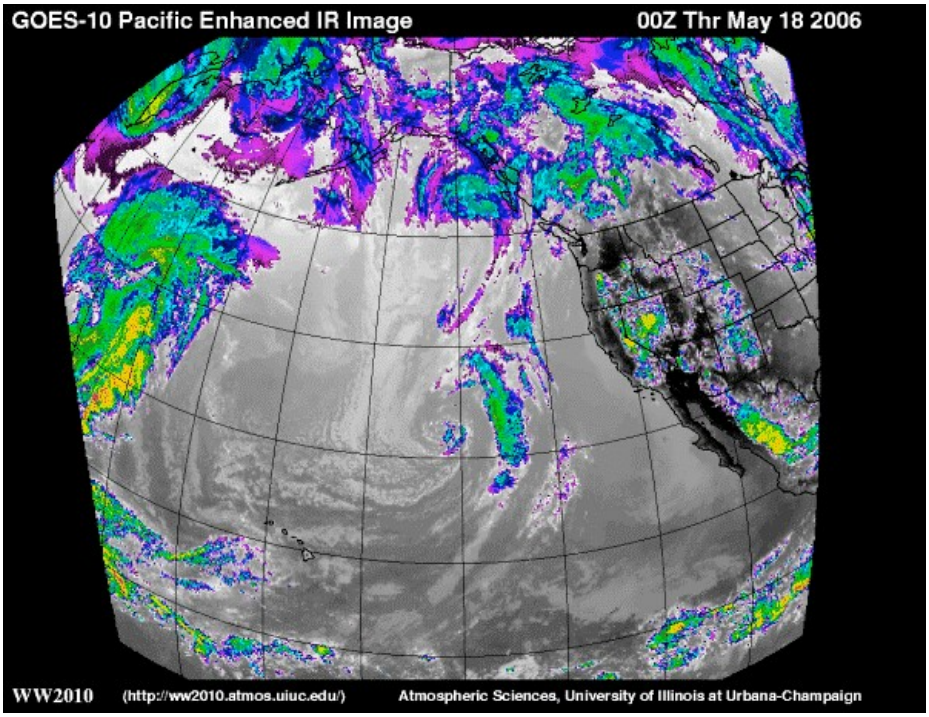

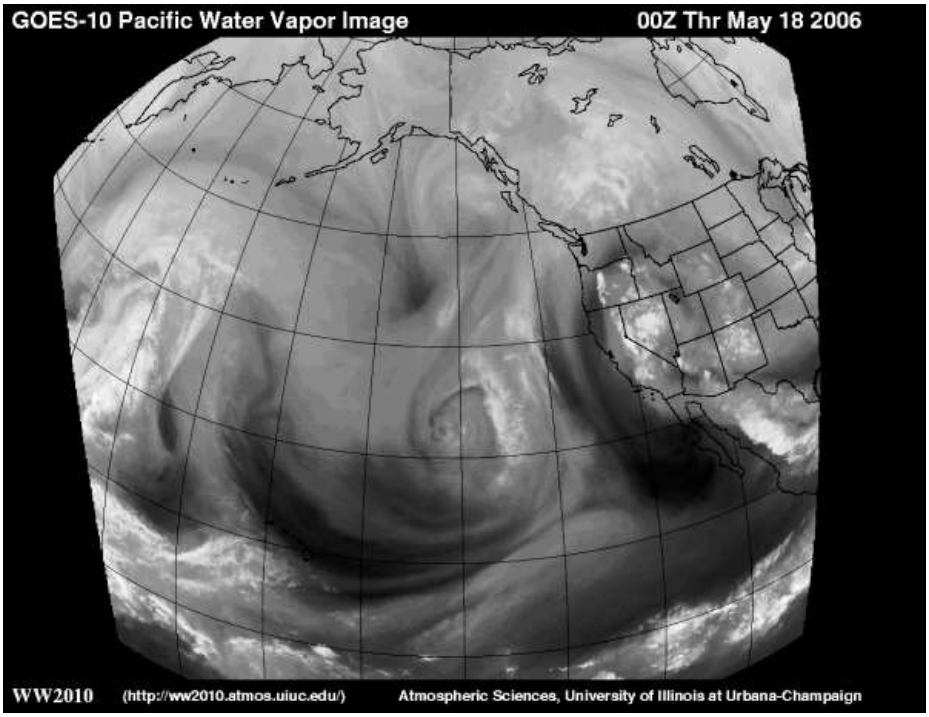

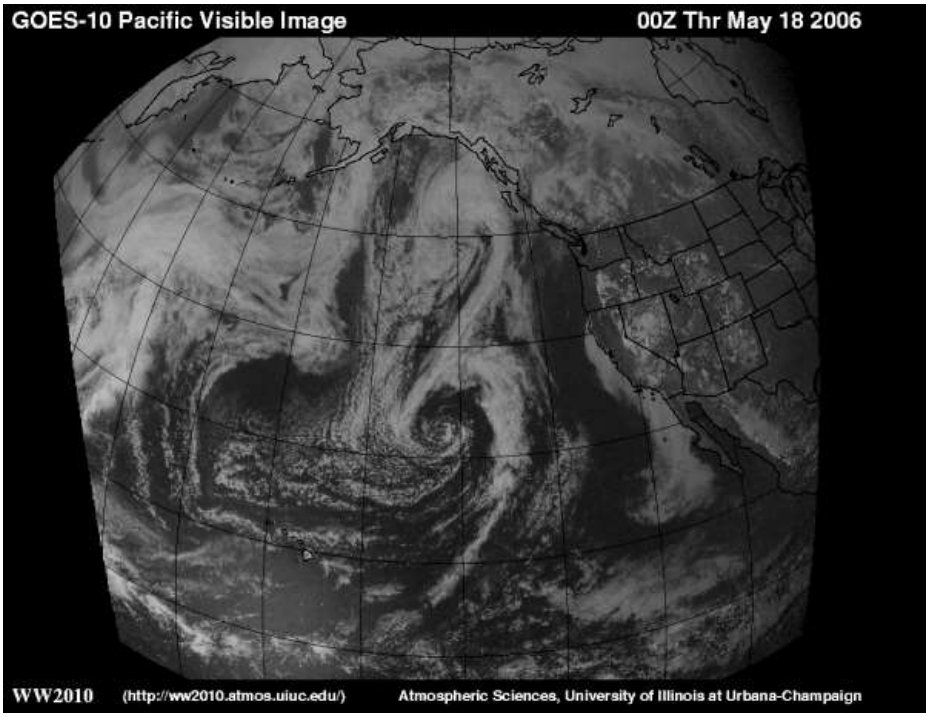

E:6 Surface analysis from NOAA, Environment Canada. Here Environment Canada.

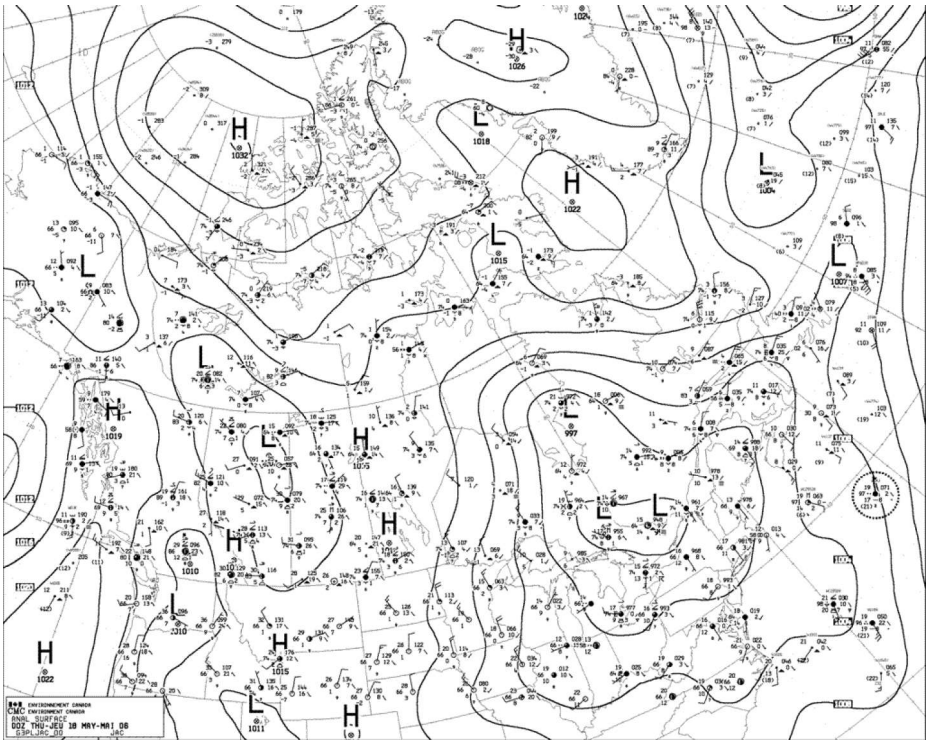

Appendix F: Temperature data

	Date	Tmax [C]	Tmin [C]
Vancouver airport	15/5	19,9	10,7
	16/5	27,1	14,0
	17/5	19,2	12,0
	18/5	18,9	11,6
Abbotsford	15/5	30,2	8,7
	16/5	28,4	11,9
	17/5	26,1	10,6
	18/5	25,7	9,4
Chilliwack	15/5	31,6	13,2
	16/5	29,8	17,6
	17/5	26,5	13,4
	18/5	26,7	12,5
Hope	15/5	32,8	11,9
	16/5	30,5	15,1
	17/5	26,8	14,4
	18/5	26,7	11,7

Source: Emergency Weather Net, UBC, Vancouver.

Appendix G: Acronyms and abbreviations

ACM	Asymmetric Convective Model
ARW	Advanced Research WRF
ASF	Advanced Software Framework
AQ	Air quality
AQM	Air quality model
BCON	Boundary Conditions processor
CB4	Carbon bond mechanism IV
CCME	Canadian Councils of Ministers of the Environment
CMAS	Community Modeling and Analysis
CMAQ	Community Multiscale Air Quality modeling system
CO	Carbon monoxide
CO_2	Carbon dioxide
CTM	Chemical Transport Model
CCTM	CMAQ Chemical Transport Model
EC	Environment Canada
EDGAR	Emissions database for Global Atmospheric Research
EMC	Environmental Modelling Center
EPA	Environmental Protection Agency
ETA	ETA (η) model, a numerical atmospheric model.
GMT	Greenwitch Mean Time
GVRD	Greater Vancouver regional District
ICON	Initial conditions processor
JPROC	Photolysis rates processor
LFV	Lower Fraser Valley
MC2	The Mesoscale Compressible Community model
MCIP	Meteorology-Chemistry Interface Processor
MM5	The PSU/NCAR Mesoscale model
NCAR	National Center for Atmospheric Research
NH_3	Ammonia
NMM	Nonhydrostatic Mesoscale Model
NOAA	National Oceanic and Atmospheric Administration
NO_2	Nitrogen Dioxide
NOx	Nitrogen Oxides
NWP	Numerical Weather Prediction
O_3	Ozone
PDT	Pacific Daylight Time
PM	Particulate Matter
$PM_{2,5}$	Particulate matter less than 2,5 m
PM_{10}	Particulate matter less than 10 m
PSU	Pennsylvania State University
RADM	Regional Acid Deposition Model
RPM	Regional Particulate model
S-O_3	Stratospheric Ozone
SMOKE	Sparse matrix operator kernel emissions
SO_2	Sulfur dioxide
T-O_3	Tropospheric Ozone
VOC	Volatile Organic Compound
WRF	Weather Research and Forecasting Model